

7N-63  
194173  
~~194173~~  
P-115

# TECHNICAL NOTE

## D-20

THE ANALYSIS AND DESIGN OF CONTINUOUS AND  
SAMPLED-DATA FEEDBACK CONTROL SYSTEMS  
WITH A SATURATION TYPE NONLINEARITY

By Stanley Francis Schmidt

Ames Research Center  
Moffett Field, Calif.

NATIONAL AERONAUTICS AND SPACE ADMINISTRATION  
WASHINGTON

August 1959

(NASA-TN-D-20) THE ANALYSIS AND DESIGN OF  
CONTINUOUS AND SAMPLED-DATA FEEDBACK CONTROL  
SYSTEMS WITH A SATURATION TYPE NONLINEARITY  
(NASA. Ames Research Center) 115 p

N89-70707

Unclas  
00/63 0194173

## TABLE OF CONTENTS

	<u>Page</u>
SUMMARY . . . . .	1
I. INTRODUCTION . . . . .	3
1.1 Discussion and Scope of the Problem . . . . .	3
1.2 History of Previous Work . . . . .	4
1.3 Description of the Problem . . . . .	5
II. METHODS FOR ANALYSIS AND DESIGN . . . . .	9
2.1 Introduction . . . . .	9
2.2 Root Locus . . . . .	9
2.3 Discussion . . . . .	12
2.4 Switch Time Method, Analysis . . . . .	13
2.5 Calculation of Response Times . . . . .	18
2.5.1 Linear region . . . . .	18
2.5.2 Saturated region . . . . .	19
2.6 The Determination of Nonlinear Functions to Improve the Step Response . . . . .	23
2.6.1 An optimum second-order system . . . . .	26
2.7 Limitations of the Switch Time Method . . . . .	28
2.8 Analysis and Design Methods for Sampled-Data Systems . .	32
2.8.1 Root locus . . . . .	32
2.8.2 Switch time method, analysis . . . . .	32
2.8.3 Calculation of response times . . . . .	37
2.8.4 Calculation of nonlinear functions . . . . .	37
2.8.5 Discussion . . . . .	39
III. DERIVATION OF THE OPTIMUM RESPONSE . . . . .	40
3.1 Introduction . . . . .	40
3.2 A Theorem on the Laplace Transform of a Truncated Time Signal . . . . .	40
3.3 A Method for Deriving the Optimum Response . . . . .	41
3.4 A Type 1 First-Order Plant . . . . .	43
3.5 A Type 1 Second-Order Plant . . . . .	44
3.6 A Type 1 Third-Order Plant . . . . .	50
3.6.1 Asymptotic solution for very large inputs . . . .	54
3.7 A Type 2 Second-Order Plant . . . . .	58
3.8 A Type 2 Third-Order Plant . . . . .	59
3.9 A Type 2 Fourth-Order Plant . . . . .	64
3.9.1 Asymptotic solution for a type 2 fourth-order plant . . . . .	67
3.10 A Type 3 Third-Order Plant . . . . .	68
IV. EXAMPLES OF SATURATED CONTROL SYSTEMS . . . . .	70
4.1 Introduction . . . . .	70
4.2 A Sampled-Data Bank-Angle Autopilot (Feedback Design) .	70
4.3 A Sampled-Data Bank-Angle Autopilot, $D(z)$ Design . . . .	80
4.4 A Continuous Normal Acceleration Autopilot . . . . .	86

	<u>Page</u>
V. CONCLUSIONS . . . . .	102
5.1 Summary of Results . . . . .	102
5.2 Suggestions for Further Research . . . . .	103
BIBLIOGRAPHY . . . . .	105

# LIST OF ILLUSTRATIONS

<u>Figure</u>		<u>Page</u>
1	Block diagram of systems to be considered . . . . .	4
2	Root loci of a type 1 system . . . . .	8
3	Root loci of a conditionally stable type 1 system . . . .	8
4	Root loci of a type 2 system . . . . .	9
5	Time step responses of a saturated type 2 system . . . .	9
6	Root loci of a conditionally stable type 2 system . . . .	10
7	Root loci of a type 3 system . . . . .	10
8	Block diagram of a saturated control system . . . . .	11
9	Step responses for a second-order system . . . . .	13
10	Block diagram of a saturated control system . . . . .	14
11	First reversal times of example system . . . . .	15
12	Calculation of response time of example system . . . . .	18
13	Sketch of response for example system . . . . .	19
14	Calculated and measured response times for example system	19
15	Block diagram of a relay control system . . . . .	20
16	Phase plane trajectories for a relay control system . . .	20
17	Nonlinear functions for example control system . . . . .	23
18	Root loci of a type 2 system . . . . .	27
19	Root loci of a type 1 system . . . . .	28
20	Block diagram of a type 1 system . . . . .	29
21	Block diagram of an example sampled-data system . . . . .	31
22	Plant input, $x(t)$ , for a step input, $R_0 u(t)$ . . . . .	32
23	Actual and optimum first reversal times for example system . . . . .	34
24	Step responses of example system . . . . .	34
25	Approximation to optimum first reversal curve for example system . . . . .	35
26	Nonlinear function for example system . . . . .	36
27	Step responses of modified system . . . . .	37
28	Optimum motion of the input, $x(t)$ , for a type 1 first- order plant . . . . .	41
29	Minimum response time for a type 1 first-order plant . .	42
30	Block diagram of a type 1 second-order plant . . . . .	42
31	Time histories for example system . . . . .	43
32	Optimum motion of the input, $x(t)$ , for a type 1 second- order plant . . . . .	44
33	Optimum first reversal time for a type 1 second-order plant . . . . .	47
34	Minimum response time for a type 1 second-order plant . .	48
35	Block diagram of a type 1 third-order plant . . . . .	49
36	Optimum motion of the input, $x(t)$ , for a type 1 third- order plant . . . . .	49
37	Optimum first reversal time for a type 1 third-order plant . . . . .	50

<u>Figure</u>		<u>Page</u>
38	Minimum response time for a type 1 third-order plant . .	51
39	Step responses of a second-order system . . . . .	53
40	Block diagram of a type 1 third-order plant . . . . .	54
41	Normalized data for asymptotic solutions . . . . .	55
42	Optimum switching times for a type 2 second-order plant .	56
43	Optimum motion of the plant input, $x(t)$ , for a type 2 third-order plant . . . . .	57
44	Optimum first reversal time for a type 2 third-order plant . . . . .	61
45	Minimum response time for a type 2 third-order plant . .	62
46	Optimum first reversal time for a type 2 fourth-order plant . . . . .	63
47	Minimum response time for a type 2 fourth-order plant . .	64
48	Block diagram of a type 2 fourth-order plant . . . . .	65
49	Optimum motion of the plant input, $x(t)$ , for a type 2 fourth-order plant . . . . .	65
50	Optimum switching times for a type 3 third-order plant .	67
51	Block diagram of a sampled-data bank angle autopilot; FB design . . . . .	69
52	Pole position loci as a function of the limiter gain; FB design . . . . .	71
53	First reversal times for a sampled-data bank-angle autopilot; FB design . . . . .	73
54	Step responses of a sampled-data bank-angle autopilot; FB design . . . . .	74
55	Calculated, measured, and minimum response times for the sampled-data bank-angle autopilot; FB design . . .	75
56	Staircase approximation to the optimum first reversal curve . . . . .	76
57	Nonlinear function used to modify the sampled-data bank- angle autopilot; FB design . . . . .	77
58	Step responses of the modified sampled-data bank-angle autopilot; FB design . . . . .	77
59	Block diagram of a sampled-data bank-angle autopilot; $D(z)$ design . . . . .	78
60	Pole position loci as a function of the limiter gain; $D(z)$ design . . . . .	80
61	First reversal times for a sampled-data bank-angle autopilot; $D(z)$ design . . . . .	81
62	Step responses of bank-angle autopilot; $D(z)$ design . . .	81
63	Calculated, measured, and minimum response times for the sampled-data bank-angle autopilot; $D(z)$ design . . . .	82
64	Nonlinear function used to modify the sampled-data bank- angle autopilot; $D(z)$ design . . . . .	83
65	Step responses of the modified sampled-data bank-angle autopilot; $D(z)$ design . . . . .	84

<u>Figure</u>		<u>Page</u>
66	Block diagram of a normal acceleration autopilot . . . .	85
67	Root loci of the normal acceleration autopilot as a function of the limiter gain . . . . .	87
68	First reversal times for the normal acceleration autopilot . . . . .	89
69	Step responses of the normal acceleration autopilot . . .	89
70	Nonlinear function used to modify the normal acceleration autopilot . . . . .	91
71	Step responses of the modified normal acceleration autopilot . . . . .	92
72	Loci of zero positions for variable $K_q$ and locus of complex pole position for $K_q = -0.328$ . . . . .	93
73	Locus of zero position for variable $K_l$ and locus of complex pole position for $K_l = -4.188$ . . . . .	95
74	Nonlinear function of error for normal acceleration autopilot . . . . .	96
75	Step responses of the modified normal acceleration autopilot . . . . .	96
76	$K_q$ versus $K_l$ for a constant damping ratio of the normal acceleration autopilot . . . . .	98
77	Nonlinear functions, $K_q(\epsilon)$ and $K_l(c)$ , for use in the normal acceleration autopilot . . . . .	99
78	Step responses of the modified normal acceleration autopilot . . . . .	99

# LIST OF TABLES

<u>Table</u>		<u>Page</u>
I	Plants considered in this investigation . . . . .	5
II	Optimum reversal times for a type 1 third-order plant . .	51
III	Optimum reversal times for a type 2 fourth-order plant .	64

NATIONAL AERONAUTICS AND SPACE ADMINISTRATION

---

TECHNICAL NOTE D-20

---

THE ANALYSIS AND DESIGN OF CONTINUOUS AND

SAMPLED-DATA FEEDBACK CONTROL SYSTEMS

WITH A SATURATION TYPE NONLINEARITY<sup>1</sup>

By Stanley Francis Schmidt

SUMMARY

The problem studied in this investigation is how to design and analyze feedback control systems in which a saturation type nonlinearity, or limiter, occurs on the input to the controlled system, or "plant." The plant is assumed to have one input and one output and to be describable by linear differential equations with constant coefficients. The scope of the investigation covers plants whose transfer functions are of first to fourth order.

As a result of the assumption of linearity and the fact that limiting has no effect for small signal inputs, the feedback control system can be designed by the use of conventional, linear feedback control theory for the small input signal range. The problem then becomes how one can analyze the response of the system for large signal inputs which cause saturation and how to design compensating nonlinear functions which will improve the response should the analysis show this to be necessary.

The root locus and the switch time methods are used in this investigation for solution of the problem. The application of the root locus method is conventional with the exception that the limiter is treated as a device whose equivalent gain decreases as its input increases. It is shown that a root locus graph with respect to the limiter gain gives a qualitative indication of the system response as a function of input amplitude. The switch time method is based on the use of step inputs for analysis and design purposes. It provides the control system designer with the following:

---

<sup>1</sup>This report was submitted to Stanford University in partial fulfillment of the requirements for the degree of Doctor of Philosophy in Electrical Engineering, June 1959.

- (1) A means for analysis of saturated control systems to determine the size of the step inputs which cause poor performance.
- (2) A means for quickly calculating the response time for large step inputs.
- (3) A means for synthesizing nonlinear functions which provide near optimum response for large step inputs.

The switch time method uses the optimum bang-bang solution for step inputs. It is shown that if the first reversal time after the application of the step is longer than the bang-bang solution, overshoot must exist. By forcing the first reversal time to be the optimum relay solution one obtains the method for synthesizing nonlinear functions which provide near optimum response for large inputs.

A number of optimum bang-bang first reversal times and minimum response times are derived and presented in normalized form.

The switch time and root locus methods are applied to several aircraft autopilot examples where the rate of control-surface motion is limited. Both sampled-data and continuous systems are presented. The results of simulation studies demonstrate the validity of the approach.

It is generally concluded that the combination of the switch time method along with certain root locus techniques offers a very powerful tool for analyzing and designing both sampled-data and continuous systems in which a saturation type nonlinearity is present.

## I. INTRODUCTION

### 1.1 Discussion and Scope of the Problem

A-310

The design of linear, continuous and sampled-data, feedback control systems has become a well advanced science in recent years. In most instances, control systems are designed by the use of a linear model. The actual system is then constructed and the difference between the desired response of the linear model and the response of the actual system is attributed to nonlinearities. Generally, one can subdivide the types of nonlinearities into classes which signify the manner in which they deteriorate the desired model response. For example, consider the two classes as (1) nonlinearities whose principal effect is on the nulling accuracies, and (2) nonlinearities whose principal effect is on the transient response. In the first class, one may place backlash, dead zones, hysteresis, quantizing errors, etc. In the second class, one can place saturation and nonlinearities which make the "plant"<sup>1</sup> transfer function change as a function of the magnitude of some plant variable (e.g., pitch-up of an aircraft where the pitching moment is a nonlinear function of the angle of attack). The classification can be made generally, since the nonlinearities of the first class produce bias errors and/or limit cycles whose amplitude must be kept small to be within the tolerable error region. If the plant is linear, which is one of the restrictions of this investigation, the effects of saturation can be fairly well isolated from the effects of many other nonlinearities. Since all systems must have saturation of one or more of the variables, it appears desirable to develop methods which are specially suited to analyze and design control systems with saturation.

The effects of saturation in a control system are to limit the velocity, acceleration, or higher derivatives with which an output can follow a given input. If the system is reasonably free of nonlinearities of the first class previously mentioned, linear methods may be used to design the system for a desired performance around zero error. Then, by means of the methods presented here, the effects of saturation on the particular system designed may be determined and appropriate compensating nonlinearities may be designed to insure adequate stability and transient response for large error conditions.

One of the significant features of saturation is that its presence in a control system permits an optimum system to be defined. This optimum system uses the maximum, or a smaller value of the saturated variable, in an optimum manner to reduce the error to zero in a minimum time. This

---

<sup>1</sup>The word "plant" refers to the controlled system. The plant transfer function could, for example, be the mathematical relationship between the output of an amplifier and a motor shaft position in a servo-position controller.

fact is used in this investigation for the derivation of minimum response times of saturated control systems for step inputs. A method is then presented in which the approximate response time of any given system which uses a linear controller can be obtained so that a comparison between the optimum and actual response can be made. These data allow the designer to determine if a larger controller is required and to what extent increasing the complexity of the control equations will decrease the response time.

This investigation considers plants whose transfer functions are of first to fourth order. Two examples, one second order and one third order, are used wherein the plant has a single zero in its transfer function. The other plants which are considered have only poles.

Two aircraft autopilot examples are designed for both sampled and continuous systems to demonstrate the design methods proposed; simulation results are presented for verification of the design philosophy.

## 1.2 History of Previous Work

Saturation in control systems has received considerable attention by many authors in recent years. Saturation is very closely related to relay or on-off control systems, since for large inputs the saturated variable takes on its maximum values (switching from one to the other) in a manner which is similar to the on-off control system. This means that much of the previous work related to on-off controllers can be used in studies of continuous-type saturated control systems. Not much has been accomplished until quite recently with regard to saturated sampled-data systems. Probably the most complete bibliography pertaining to both these subjects as well as other subjects dealing with control systems is the one being prepared by Higgins (ref. 1).<sup>2</sup> Previous work which is used in this investigation is listed in the Bibliography. One contribution which is used most directly can be found in a paper by Kalman (ref. 2). He showed that a sufficient condition for stability is that the roots of the characteristic equation with the nonlinearity replaced by a gain equal to its derivative remain in the left half plane. The abrupt changes in slope of a limiter are assumed to be formed by a segment of a circle with an arbitrarily small radius. This assumption permits the derivative to be defined at every point and, therefore, the gain of the limiter varies from some finite slope to zero in a continuous manner. A similar argument which shows a limiter can be treated as a gain which decreases as the input amplitude increases can be obtained by the use of describing-function analysis (see, e.g., ref. 3). As is shown by Kalman, one can draw a root locus as a function of limiter gain, which

---

<sup>2</sup>See the numbered references which appear in the Bibliography.

provides a qualitative indication of variation of system performance with input amplitude. This is used in developing some rules regarding systems in chapter II.

Bellman, Glicksberg, and Gross (ref. 4) proved that the minimum response time of a bang-bang controller was obtained by having the saturated variable go from one limit to the other with the number of reversal times being dependent on the order. This proof was restricted to systems containing distinct roots on the negative half of the real axis. Further discussion of optimum relay systems and application of the theorem of reference 4 is made in chapter III.

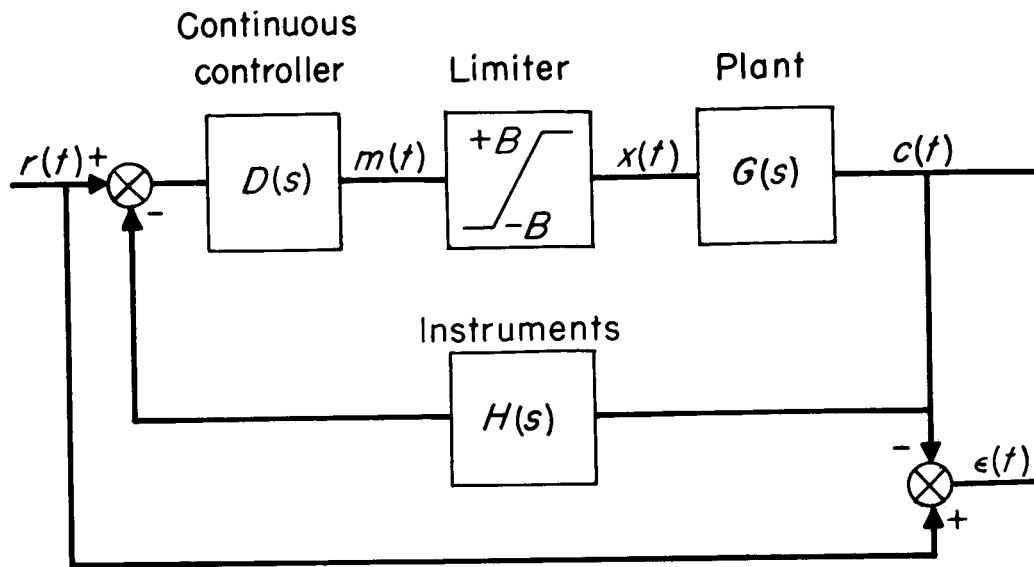
The author and Triplett (ref. 5) demonstrated one technique of designing nonlinearities for saturated control systems which makes use of the optimum relay solution. This technique is referred to as the switch time method and is derived in chapter II. One of the purposes of this investigation is to extend this switch time method to sampled-data systems. The extension is also explained in chapter II.

Standard design techniques are used for the design of the system in the linear region for continuous (ref. 3) as well as sampled-data (ref. 6) systems, with the exception that the sampled-data designs use the additional method described in a recent AIEE paper by the author (ref. 7) (also described in NASA MEMO 4-14-59A (ref. 8) by the author and Harper).

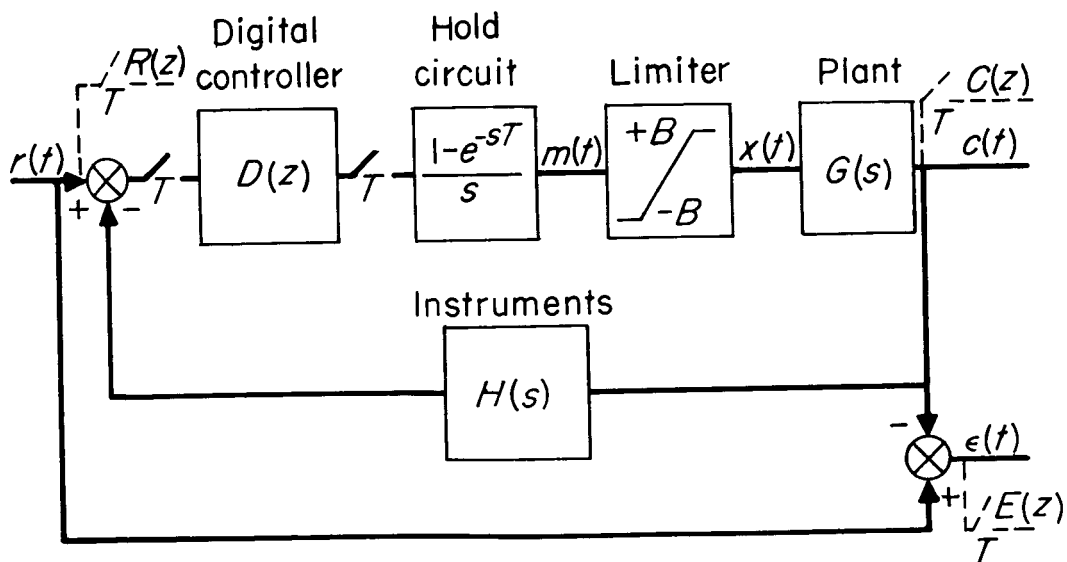
### 1.3 Description of the Problem

The problem is best understood with reference to the block diagrams shown in figures 1(a) and 1(b). Here,  $r(t)$  represents the input command signal and  $c(t)$  represents the output of the plant (controlled system). In general, one desires the error  $(r - c) = e(t)$  to be as small as possible for all inputs,  $r$ , the system will receive. A limiter is located on the input to the plant. Limiting in actual practice can come from a number of sources such as tube saturation in electronic systems, physical stops in mechanical systems, etc. This limiter causes the input to the plant,  $x$ , to be a bounded variable; that is,  $|x|$  cannot exceed  $B$  and (if one has the optimum system) will restore the error,  $e(t)$ , to zero in a minimum time.

In figure 1,  $D(s)$  represents the transfer function of an analog controller and  $H(s)$ , the transfer function of a feedback network. In the sampled-data system, a zero-order hold circuit is used to convert the pulse signal to a continuous signal;  $D(z)$  is the pulse transfer function of the digital controller.



(a) Continuous system.



(b) Sampled-data system.

Figure 1.- Block diagram of systems to be considered.

The plant transfer functions,  $G(s)$ , to be considered in this report are given in table I. The conventional definition according to "type,"<sup>3</sup> with the added specification of the order of the denominator of  $G(s)$ , is given in table I for the various plants. It is generally convenient to consider the various systems obtained by determining the lowest order output bounded derivative for  $x$  remaining at one of its bounded values for an infinite period of time. Since all the roots of the characteristic equation of the plants given in table I, other than those at the origin, are in the left half plane, one can state that all type 1 plants are "velocity limited," all type 2 plants are "acceleration limited," etc. This classification will be found useful in remembering some of the fundamental characteristics of saturated control systems which are derived later.

Table I.- Plants considered in this investigation

Case	$G(s)$	Type
1	$\frac{K}{s}$	1 - first order
2	$\frac{K(\tau_1 s + 1)}{s(\tau_2 s + 1)}$	1 - second order
3	$\frac{K}{s[(s^2/\omega_n^2) + (2\zeta s/\omega_n) + 1]}$	1 - third order
4	$\frac{K}{s^2}$	2 - second order
5	$\frac{K(\tau_1 s + 1)}{s^2(\tau_2 s + 1)}$	2 - third order
6	$\frac{K}{s^2[(s^2/\omega_n^2) + (2\zeta s/\omega_n) + 1]}$	2 - fourth order
7	$\frac{K}{s^3}$	3 - third order

<sup>3</sup>"Type" in this usage means the number of integrations of the plant or, in transfer function terms, it is the number of poles at the origin. In the usual definition of the word it refers to whether there is a zero error in the steady state to a step (type 1), zero error to a ramp (type 2), etc. In this investigation no integrations or cancellations of plant poles are permitted in the transfer function of the controllers  $D(s)$  or  $D(z)$ . Under these restrictions the conventional type definition and the usage of type on the plant transfer function are identical if  $H(s) = 1$ ; that is, a type 1 plant gives a type 1 system, etc.

The problem can be broken down into the following basic questions:

- (1) Given a control system as in figure 1(a) where  $D(s)$  and/or  $H(s)$  or figure 1(b) where  $D(z)$  and/or  $H(s)$  have been designed to give satisfactory performance in the unsaturated region,
  - (a) How can one predict the performance with large input transients?
  - (b) If this performance is unsatisfactory, what means can be used to improve it?
- (2) What is the optimum performance of a given plant for a step input? For example, what is the minimum response time as a function of the magnitude of the input?

Questions 1(a) and 1(b) are answered in chapter II. The examples in chapter IV demonstrate the method. Question 2 is answered in chapter III.

The author would like to express appreciation to Dr. G. F. Franklin of Stanford University for his technical advice during the course of this investigation. Appreciation is also expressed to both Dr. Franklin and Dr. Irmgard Flügge-Lotz of Stanford University for their helpful suggestions made during the preparation of this report.

## II. METHODS FOR ANALYSIS AND DESIGN

### 2.1 Introduction

Saturated control systems of the type shown in figures 1(a) and 1(b) have characteristics which are very much dependent on the input amplitude if the input is a step and on both the input amplitude and frequency if the input is a sine wave. Systems designed on a linear basis can become unstable or have a very long response time if excited into the nonlinear (saturated) region. It is the purpose of this chapter to review the various methods of treating saturation for continuous and sampled-data systems and to extend one method to sampled-data systems.

### 2.2 Root Locus

Describing function analysis (e.g., ref. 3) applied to a limiter gives the result that a limiter is equivalent to a gain reduction as a function of the input amplitude. Booton, Mathews, and Seifert (ref. 9) have also shown that for statistical inputs the effect of a limiter in a control system such as figure 1 can be treated approximately as an equivalent gain. If one assumes the limiter is equivalent to a gain which decreases as the input increases, then a root locus of the system drawn as a function of the limiter gain gives a qualitative picture of the system behavior as the input signal to the limiter changes amplitude. Kalman (ref. 2) states that if any nonlinear system is stable when linearized at every operating point, then the nonlinear system is stable. Thus, a root-locus plot of the pole positions as a function of the limiter gain can be used to give qualitative information as to what change in performance is to be expected.

The following rules<sup>1</sup> are developed by the root-locus method:

---

<sup>1</sup>This investigation is restricted to systems where any poles of  $D(s)$  or  $H(s)$  are heavily damped. This restriction is quite necessary in the method to be presented later for synthesizing nonlinear functions which provide near optimum response for large inputs. With reference to figure 1(a), one can see that large step inputs immediately saturate the limiter. This saturation tends to open up the loop, and thus poorly damped characteristics of  $H(s)$  or  $D(s)$  would cause the input to the limiter to become very oscillatory, possibly swinging the output of the limiter back and forth at a high frequency. This restriction is not too serious since, generally, lead or lag networks or other compensation networks with real poles are used for  $D(s)$  and reasonably well damped instruments are used for  $H(s)$ . From a practical standpoint, the methods presented here are almost always applicable.

Rule I. A type 1 system which is not conditionally stable<sup>2</sup> and which is designed for good performance for small inputs will always be stable for large inputs.

Proof:

Consider a root locus of a type 1 system as shown in figure 2 for a third-order example. If, for example, A, B, and C are the chosen pole positions for the operating gain of the system, then large inputs, which cause greater limiting action to take place, cause the poles to move back along the loci in reverse to the arrows. Note that the dominant mode of the system (the pole closest to the origin) represents a first-order lag which, as the gain reduces, becomes longer. This, then, allows the rule of thumb which is almost always true and is easily remembered, namely, "velocity limiting tends to stabilize the system."

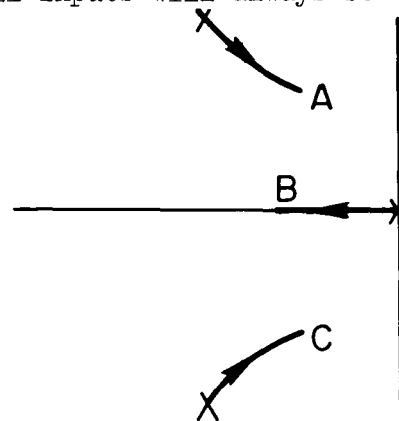


Figure 2.- Root loci of a type 1 system.

Corollary:

A type 1 system which is conditionally stable can be excited into a constant amplitude, constant frequency oscillation characteristic of a limit cycle.

Proof:

A conditionally stable type 1 system must by definition be unstable for low gains as well as high gains but stable for the operating point gain. The root loci of poles nearest the origin for a high order system can be of the form in figure 3.<sup>3</sup> If the gain is decreased from the operating point (by action of limiting), the characteristic poles of the system move in reverse direction to the arrows. An increase in the limiting action which causes the gain to decrease to point A

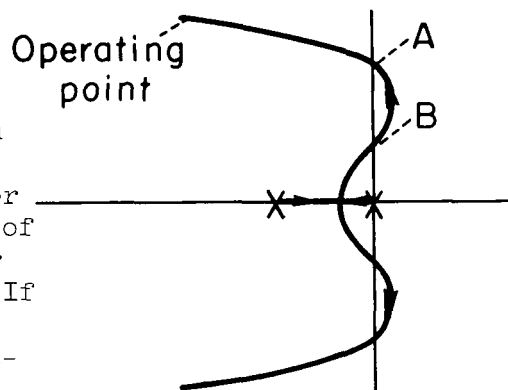


Figure 3.- Root loci of a conditionally stable type 1 system.

<sup>2</sup>A conditionally stable system is defined here as one in which either increasing or decreasing the limiter gain from the operating value results in the closed-loop poles moving into the right half plane.

<sup>3</sup>Conditionally stable designs can be obtained in high-order systems by any poles which cross into the right half plane and back to the left half plane as the limiter gain is varied from zero to the operating point. A similar argument to the one presented here shows the corollary to be true in these cases for systems of any type number.

results in an increasing amplitude decreasing frequency oscillation of the system, since points from A to B of the loci are in the right half plane. A further growth in the amplitude of oscillation, which would cause loci to move in the left half plane from point B results in a decrease in oscillation amplitude. Point B, therefore, is a stable limit cycle from which the system is unable to recover.<sup>4</sup> The system can be shocked into this limit cycle by large input transients such as steps which cause a large equivalent gain reduction of the limiter.

Rule II. A type 2 control system, which is designed to have good performance for small signals (linear region) and which is not a conditionally stable design, will have a transient performance which becomes increasingly poor as the size of the transient is increased (i.e., the equivalent gain is decreased).

Proof:

A root locus for a type 2 system for poles close to the origin will be as indicated in figure 4. As the gain is decreased (by limiting action) from the operating point A, the characteristic roots move to a position corresponding to decreased frequency and decreased damping. Thus, the response of the system to a large transient which gives a large amount of limiting will be characterized by a number of oscillations before the system comes to rest. Figure 5 illustrates the characteristic step response for several step input magnitudes. This, then allows a second rule of thumb, namely, "acceleration limiting tends to destabilize the system."

Corollary:

A conditionally stable type 2 system which is designed to be stable for small signal amplitudes may be excited (by a large transient) into an increasing amplitude, decreasing frequency, unstable mode.<sup>5</sup>

<sup>4</sup>Kalman (ref. 2) states that as points A and B move closer together (by other changes in system parameters) the limit cycle disappears before the locus is completely in the left half plane. This is not surprising because linear techniques certainly cannot explain all nonlinear phenomena. Since in control system design one generally tries to avoid both limit cycles and oscillatory transient responses this subject is not considered in this investigation.

<sup>5</sup>See footnote 3, chapter II, and refer to the corollary of Rule I for a proof that a constant amplitude limit cycle can exist in a high-order type 2 system.

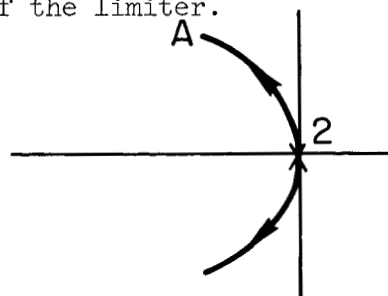


Figure 4.- Root loci of a type 2 system.

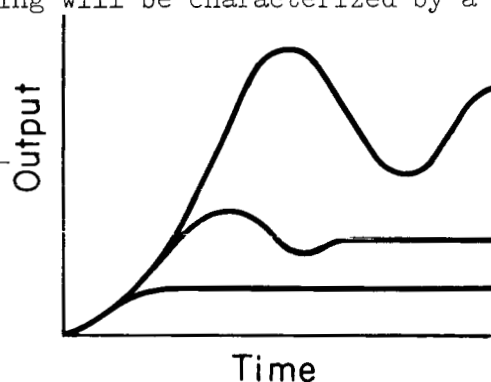


Figure 5.- Time step responses of a saturated type 2 system.

Proof:

A root locus for the poles closest to the origin of a type 2 conditionally stable system could be as indicated in figure 6. As the equivalent gain of the system is decreased by limiting action, the poles move in a reverse direction to the arrows. The response of the system becomes less and less damped as the input to the limiter grows (i.e., the greater the limiting action). If the system receives a transient which makes the equivalent gain less than that corresponding to point B, the response will diverge in a growing amplitude, decreasing frequency mode, since a further growth in the response gives greater limiting action which causes the poles to move closer to the origin in the right half plane.

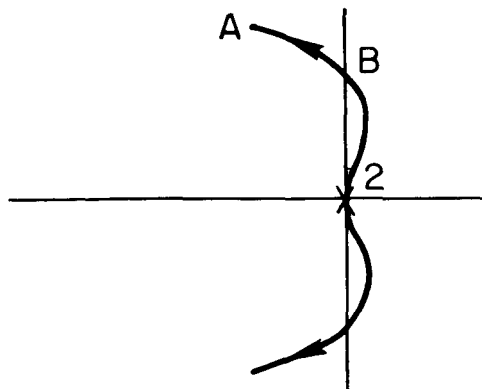


Figure 6.- Root loci of a conditionally stable type 2 system.

Rule III. A type 3 system which is designed for satisfactory performance for small signal levels can always be excited into a growing amplitude, decreasing frequency, unstable mode.<sup>6</sup>

Proof:

With reference to figure 7, it is seen that a type 3 system must always be conditionally stable. Therefore, a large input can cause limiting action to decrease the gain so that two poles are in the right half plane.

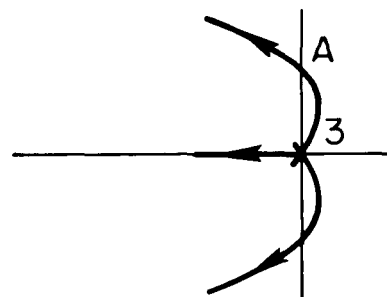


Figure 7.- Root loci of a type 3 system.

### 2.3 Discussion

The root-locus method gives considerable information on what kind of response to expect as a function of the size of the input. It can be used for saturated sampled-data systems by using root-locus plots in the  $z$  plane, examples of which are shown in chapter IV. The drawback of the root-locus method, however, is that no quantitative information is available, that is, there is no measure of the size of the input which causes a poor response. In order to gain quantitative information, it

<sup>6</sup>One should also note that a constant amplitude, constant frequency limit cycle can exist for high-order type 3 systems.

is necessary to resort to a different technique. One possibility might be the phase space; however, it is the opinion of the author that analysis of a system of third order or fourth order by visualizing trajectories in a phase space is very difficult. A second method suggested by Kalman (ref. 10) uses a transformation to a state space where the system can be approximated by a dominant second-order mode. The problem is then solved in a phase plane and the results are transformed back to the original state space. Although this method appears to have some merit, it is only approximate, and there may be a question of which is the dominant mode. With reference to the preceding root-locus presentations, one could state that a type 1 system usually has a first-order dominant mode, a type 2 system usually has a second order, and a type 3 system usually has a third order. This would mean that Kalman's method could not be used for a type 3 system. A third method was proposed by the author and Triplett (ref. 5) for the analysis and synthesis of an aircraft autopilot with control-surface rate limiting. Control-surface rate limiting is equivalent to saturation of the input to the plant, and, therefore, this method can be used for any saturated control system. The method will be referred to as the switch time method. It provides the control system designer with the following:

- (1) A means for the analysis of saturated control systems to determine the size of the step inputs which cause poor performance. This is described in section 2.4.
- (2) A means for quickly calculating the response time for large step inputs. This is described in section 2.5.2.
- (3) A means for synthesizing nonlinear functions which provide near optimum response for large inputs. This is described in section 2.6. Section 2.7 discusses some of the limitations and how root loci may be used in conjunction with the switch time method to overcome some of these limitations.
- (4) A direct extension of items (1), (2), and (3) to sampled-data systems. This extension is discussed in section 2.8.

## 2.4 Switch Time Method, Analysis

Consider the block diagram of a saturated control system shown in figure 8. If interest is restricted to step inputs, then the time

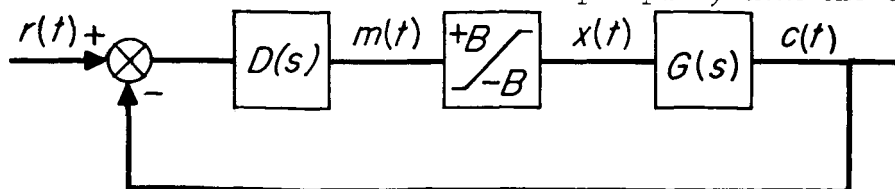


Figure 8.- Block diagram of a saturated control system.

response of the output,  $c(t)$ , can be computed completely, since the system can be treated by piecewise linear analysis. The system is linear for  $m(t)$  less than  $\pm B$ . For  $m(t)$  greater than  $\pm B$ , the response is simply the response of  $G(s)$  for an input step of magnitude  $\pm B$ , plus initial conditions. For almost all systems  $D(s)$  will be a network which has a high frequency response equal to a constant or at least, for a step into  $D(s)$  the output response,  $m(t)$ , will be very fast during the initial part of the transient. Therefore,  $m(t)$  for a step input,  $r(t)$ , will initially jump to a value dependent on the size of the input step. This value is usually easy to calculate from the high frequency response of  $D(s)$ . One can, therefore, calculate the size of the input step which first causes saturation. Below this amplitude the response is linear and is given by equation (1), if zero initial conditions are assumed.

$$c(t) = L^{-1} \left[ \frac{R_0}{s} \frac{G(s) D(s)}{1 + G(s) D(s)} \right] \quad (1)$$

( $L^{-1}[F(s)]$  reads the inverse Laplace transform of  $F(s)$ , similarly  $L[f(t)]$  reads the Laplace transform of  $f(t)$ .) For an input step,  $R_0$ , large enough to cause saturation, the response,  $c(t)$ , is given by equation (2) so long as  $|m(t)| > B$ .

$$c(t) = L^{-1} \left[ \pm \frac{B}{s} G(s) \right] \quad (2)$$

and  $m(t)$  is given by equation (3)

$$m(t) = L^{-1} \left\{ \frac{R_0}{s} - \left[ \pm \frac{B}{s} G(s) \right] \right\} [D(s)] \quad (3)$$

For  $R_0$  positive, the sign is taken as positive in equations (2) and (3), thus,  $|m(t)|$  given by equation (3) is generally a decreasing function of time. As a result a certain time, after the application of the step, has to pass before  $|m(t)|$  is less than  $B$ . Since  $m(t) = x(t)$  for  $|m(t)| \leq B$ , this is the value of time during which the input to the plant,  $x(t)$ , is at its maximum value. The value of this time is referred to as the first reversal time,  $T_1$ , and with reference to equation (3) it is seen to be a function of the step input magnitude,  $R_0$ . If a way can be found for relating the first reversal time to some characteristic of the output response, then  $T_1$ , as a function of input step magnitude, can be used as a criterion of design. This can be accomplished by defining an optimum  $T_1$  as the first reversal time after the application of the input step, which is such that if succeeding motions of the bounded variable are optimum, the error and its derivatives will be reduced to zero in a minimum time. Consider as an example the system shown in

figure 8 with  $G(s)$  equal to  $1/s^2$  and  $B$  equal to unity. For an input step,  $r(t) = R_0 u(t)$ , the problem is to determine the optimum motion of  $x$  so that  $e(t)$  is restored to zero in a minimum time. For this example, the bounded variable,  $x$ , equals  $\ddot{c}$ , the output acceleration, and it is a well known fact that in order for this system, with bounded acceleration, to start from rest at one point and come to rest at another in the minimum time, the system must accelerate at its maximum half of the time and decelerate the other half. The time histories of  $x$ ,  $\dot{c}$ , and  $c$  for an optimum step response are shown in figure 9(a). It is apparent from the time history of  $\dot{c}$  that this must be the optimum response since

$$\int_0^{T_m} (\dot{c}) dt \text{ is a maximum in the given time.}$$

An area integration of the triangular curve for  $\dot{c}(t)$  in figure 9(a) gives the desired relationship between  $R_0$ , the optimum first reversal time  $T_1$ , and the minimum response time,  $T_m$ .

$$R_0 = T_1^2 = \frac{T_m^2}{4} \quad (4)$$

If the first reversal time for this system is longer than the optimum defined in equation (4), the system must overshoot. This is caused by the fact that  $\ddot{c}$  or  $x$  is limited and it is impossible for the error  $(R_0 - c)$ ,  $\dot{c}$ , and  $x$  (or  $\ddot{c}$ ) to be zero simultaneously until some time greater than the minimum response time,  $T_m$ , of the optimum shown in figure 9(a). An example of such a motion is shown in figure 9(b). If the first reversal time is shorter than the optimum, the total response time will be longer than the optimum, since optimum use is not being made of the saturated variable.

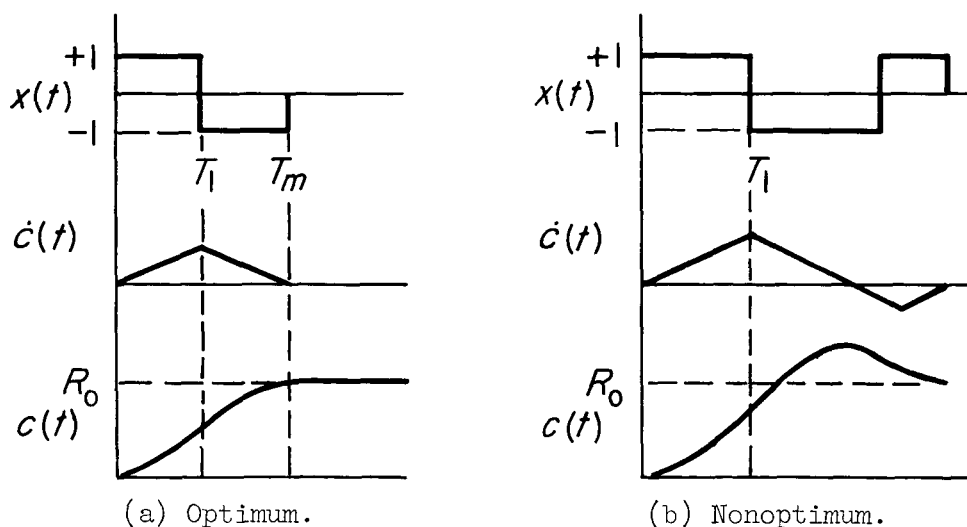


Figure 9.- Step responses for a second-order system.

Note that for both examples, the transition time for  $x$  to go from one limit to the other is assumed to be zero. This is only true for an infinite gain limiter or an ideal relay. This is one limitation in the application of the switch time method to finite gain situations. It is an approximation which only becomes exact for infinite gain limiters or infinite inputs. Applications of the analysis method, however, which are shown in succeeding sections illustrate very good results for most saturated control systems.

An application of the switching time analysis method to the example shown in figure 10 is now considered. Prior to applying the method, a linear design for small signals must be established. For this purpose

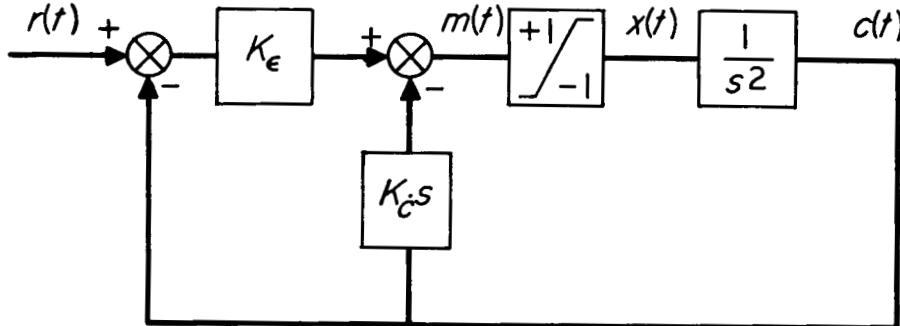


Figure 10.- Block diagram of a saturated control system.

it is assumed that the system gains,  $K_\epsilon$  and  $K_c s$ , are to be chosen so that the response from  $r$  to  $c$  in the linear region has a second-order denominator with a natural frequency,  $\omega_n$ , of 10 and damping ratio,  $\zeta$ , of 0.7. The desired transfer function is given in equation (5).

$$\frac{C(s)}{R(s)} = \frac{1}{(s^2/100) + 0.14s + 1} \quad (5)$$

The transfer function of figure 10 is

$$\frac{C(s)}{R(s)} = \frac{1}{(s^2/K_\epsilon) + (K_c s/K_\epsilon)s + 1} \quad (6)$$

Equating the unknown coefficients of equation (6) to equation (5) gives  $K_\epsilon = 100$ ,  $K_c = 14.0$ . From equation (3) and with reference to figure 10  $m(t)$ , for step inputs which saturate the limiter, is given by

$$m(t) = L^{-1} \left[ \left( \frac{R_0}{s} - \frac{1}{s^3} \right) K_\epsilon - \frac{K_c}{s^2} \right] = \left( R_0 - \frac{t^2}{2} \right) K_\epsilon - K_c t \quad (7)$$

Equation (7) is valid until  $m(t)$  is smaller than unity, the limit level. Note from figure 10 that for  $K_\epsilon = 100$ , saturation will occur for a step

input,  $R_0$ , greater than 0.01. For this system, then, one can set  $m(t)$  equal to unity in equation (7) and solve for  $T_1$ , the first time  $x$  will come off its limit.

$$T_1^2 + \frac{2}{K_c} K_c T_1 + \frac{2}{K_c} - 2R_0 = 0 \quad (8)$$

Solving equation (8) for  $T_1$  and recognizing that  $T_1$  must be positive gives (for  $K_c = 100$ ,  $K_c = 14$ )

$$T_1 = -0.14 + \sqrt{2R_0 - 0.0004} \quad (9)$$

Equation (9) is only valid for  $R_0$  greater than 0.01, since, as was previously mentioned, saturation does not occur for  $R_0$  less than this value.

It has been shown that the system must overshoot because of the limiting action if  $T_1$ , given by equation (9), becomes greater than the optimum given by equation (4). One can thus plot  $T_1$  versus  $R_0$  as obtained from equations (4) and (9) and compare the results. This comparison is shown in figure 11 where it is seen that if the input step magnitude,  $R_0$ , is greater than 0.12, overshoot as a result of limiting action must exist. Thus switch time analysis gives the size of the inputs at which overshoot caused by limiting must occur, and the root locus can be used to determine qualitatively what deterioration in response may be expected above this value.

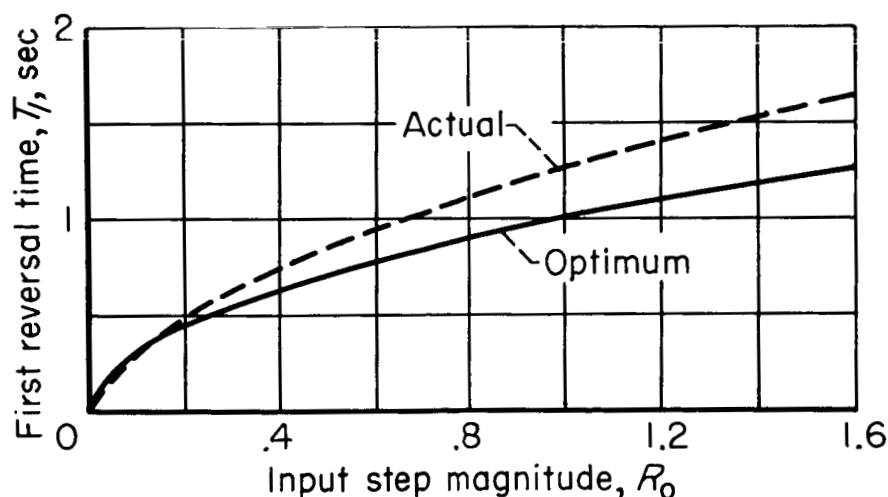


Figure 11.- First reversal times of example system.

## 2.5 Calculation of Response Times

As has been mentioned, saturation in a control system is one type of nonlinearity for which the output response can be calculated exactly, since the system can be treated linearly on a piecewise basis. It is the opinion of the author that these exact time history calculations are much too laborious for hand calculations except in the simplest cases and, if exact results are desired, one should use electronic computers. From this standpoint the method described here is approximate and is intended for use by those who desire to obtain quickly the approximate behavior of the output of a saturated control system when the input command is a step.

When step inputs are applied to a saturated control system the problem of the calculation of response times can be subdivided into three categories dependent on the size of the input. These categories are (1) small inputs where the system is linear, (2) medium size inputs where the time the system is saturated is a small percent of the total transient time,<sup>7</sup> and (3) large inputs where saturation occurs a large percentage of the total transient time. Of these three categories, an approximate calculation of the response time can be made for (1) and (3). The second category represents a transition region where the system response is slightly nonlinear and the response time is not much greater than that of the linear region. The proposed methods will be demonstrated using the example and coefficients previously computed for figure 10.

2.5.1 Linear region.— The transfer function relating C/R for figure 10 is given in equation (5). If one assumes that  $r(t)$  is a step of magnitude  $R_0$ , ( $r(t) = R_0 u(t)$ ), then the error time function,  $e(t)$ , can be written as (for  $\omega_n$  and  $\zeta$  of arbitrary value)

$$e(t) = L^{-1}[R(s) - C(s)] = L^{-1}\left\{\frac{R_0}{s}\left[1 - \frac{1}{(s^2/\omega_n^2) + (2\zeta s/\omega_n) + 1}\right]\right\} \quad (10)$$

$$= R_0 \left[ \frac{e^{-\zeta\omega_n t}}{\sqrt{1-\zeta^2}} \sin\left(\omega_n \sqrt{1-\zeta^2} t - \tan^{-1} \frac{\sqrt{1-\zeta^2}}{-\zeta}\right) \right] \quad (11)$$

The error time function for this second-order example is seen to be a damped sine wave whose amplitude is proportional to the magnitude of the input,  $R_0$ . In general, the error time function for a step input to any satisfactory linear feedback control system is composed of exponential

---

<sup>7</sup>Transient time is defined as the time from the initial application of the step until the error is smaller than some number, and remains smaller than this number indefinitely. If the transient time is infinite, this, by definition, means the system is either unstable or the response has a constant amplitude oscillation.

decays and/or damped sinusoids whose magnitudes are proportional to the magnitude of the input step. It is thus clear that the time required to reduce the error to zero is infinite. This leads to a difficulty in defining the response time of a linear system. There are two reasonable ways to define a useful response time. First, response time can be defined as the transient time (see footnote 7, chapter II); second, the response time can be defined as the time required after the application of the step for the error to be reduced (and stay below) a given percentage of the input step magnitude. The second method is generally referred to as the settling time (ref. 11). The first method has the advantage in many instances of being a criterion which has practical meaning to the control designer and shows a linear system to have a response time which increases with the magnitude of the transient disturbance. The method has the disadvantage that it is very complicated to calculate the response time. The second method has the strong advantage of simplicity, and for this reason it will be used in this investigation. The disadvantage of the second method is in trying to use it in nonlinear problems where the characteristics of the step response change significantly with the size of the input. In this case the method loses its simplicity and one should probably use the first method.

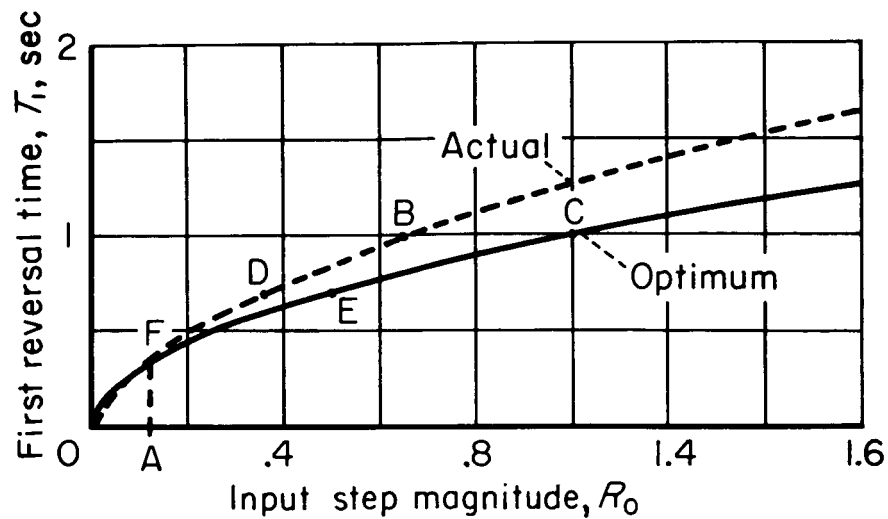
For the second-order example with  $\omega_n = 10$  and  $\zeta = 0.7$  and using only the exponential of equation (11) with the assumption that the response time is the time when the envelope of the error time response curve is less than 10 percent of its initial value, one obtains

$$e^{7T_r} = 10 \quad (12)$$

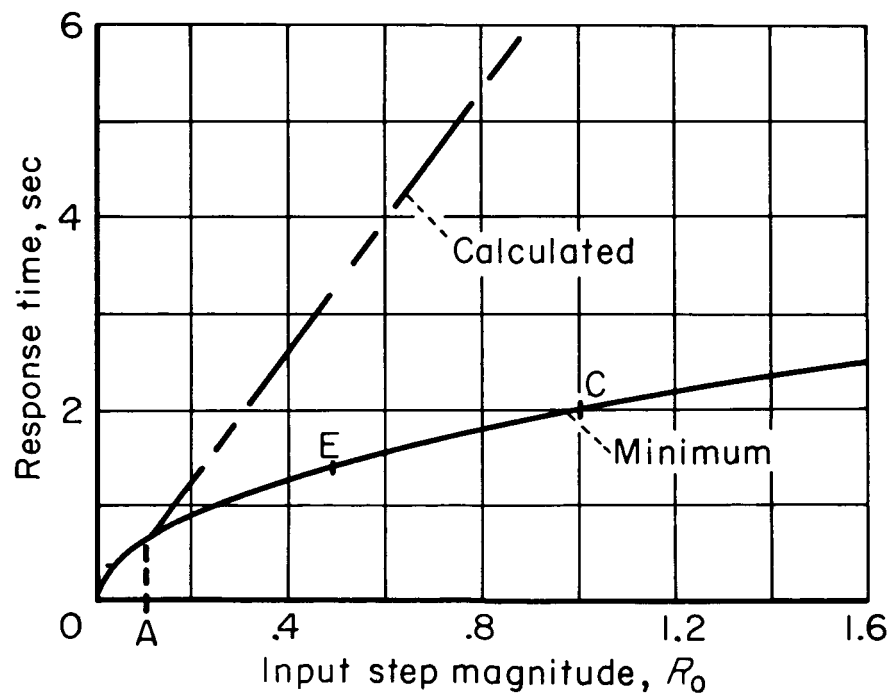
or the response time

$$T_r = \frac{\ln 10}{7} = 0.33 \text{ sec} \quad (13)$$

2.5.2 Saturated region.— If the input is in the saturated region a large percentage of the transient time, then it seems reasonable that a good criterion for the response time would be the response time of the relay or bang-bang solution. A method of accomplishing this is best described using the previous second-order example. In order to calculate the response time, one needs the actual first reversal time, the optimum first reversal time, and the minimum response time as functions of the input step. The first two were computed for this example in section 2.4 with results given in figure 11. The minimum response time is given as a function of the step magnitude in equation (4). The three results are shown in figure 12. For inputs less than point A ( $R_0 = 0.12$ ), we shall assume the response time is equal to the minimum until one reaches the intersection point of the computed linear response time and the minimum response time curves. This is a reasonable approximation, although the response time of the linear system and the minimum response



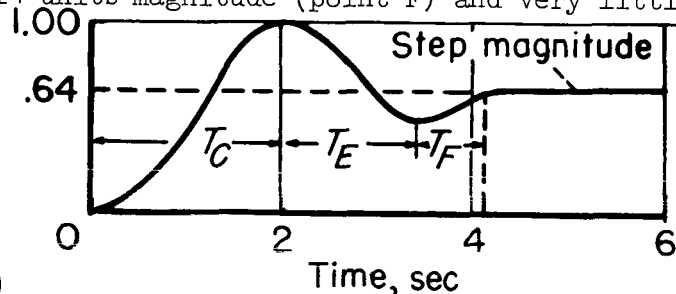
(a) First reversal time.



(b) Response time.

Figure 12.- Calculation of response time of example system.

time have different definitions. The response times for inputs greater than A are calculated in the following manner. Assume the input is equal to 0.64, for example. One first proceeds to point B which is the first reversal time for the system for this size step. The first reversal time is greater than the optimum so the system must overshoot. If succeeding motions of the system were optimum, the system would overshoot to a value given by point C (arriving there with all derivatives zero). The time required to arrive at this point is given by the minimum curve for an input of 1.0 in figure 12(b). Calling this time  $T_C$  and reading its value from the curve gives  $T_C = 2$  seconds. The system starts from point C with only the error having a value, so it is equivalent to a step of magnitude equal to the difference between C and B which is 0.36 units. From this one proceeds to point D, the first reversal time for a step of 0.36 units. From here one proceeds to point E and reads  $T_E$  from figure 12(b),  $T_E = 1.4$  seconds. The difference between point E and D then gives a step of 0.14 units magnitude (point F) and very little overshoot for this input is predicted. Reading response time for this magnitude input from figure 12(b) gives  $T_F = 0.7$  second. The calculated response time for a 0.64 unit step is thus



$$T_R = T_C + T_E + T_F = 4.1 \text{ sec} \quad (14)$$

This is one of the points on the calculated curve shown in figure 12(b). The time response of the system is sketched in figure 13. One proceeds in a similar manner to calculate response times for inputs of other sizes.

The method outlined above for predicting the response time for large inputs is approximate in many cases and needs some clarification with regard to when it is exact and what its accuracy is in general. With regard to accuracy, the response time of the example system was measured from analog computer results, and the calculated and measured curves are shown in figure 14.

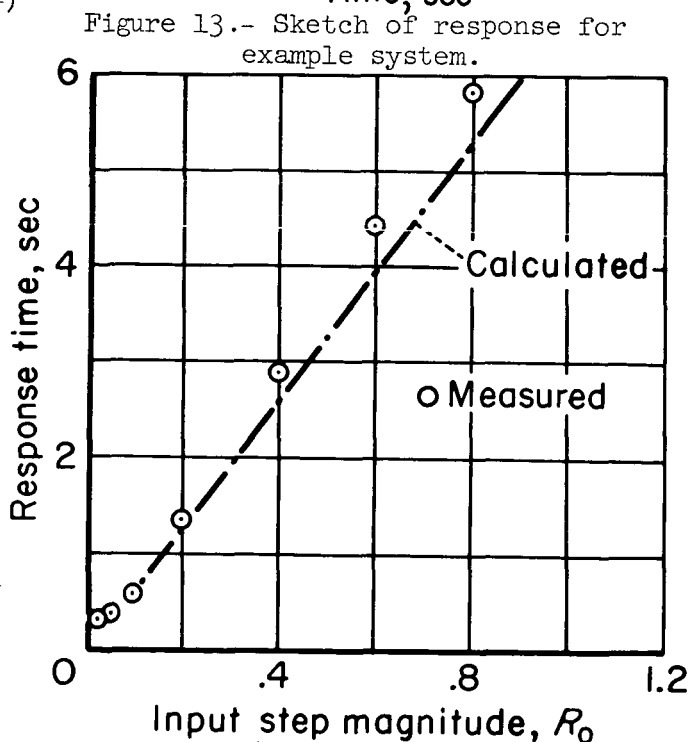


Figure 14.- Calculated and measured response times for example system.

The measured curves were obtained by measuring the time required for the error to reduce and remain below 0.01 units for inputs greater than 0.1 units. Data for step inputs with amplitudes less than 0.10 units were obtained from the definition of response time as the time for the error to be reduced and remain below 10 percent of the input step magnitude. The measured and calculated results are seen to be in close agreement.

The method is exact when an ideal relay is used in place of the limiter and the plant transfer functions are either first or second order. The validity of this statement for the first-order system should be obvious. For the second-order case it can be shown by means of the phase plane. Consider the system shown in figure 15. Step inputs to

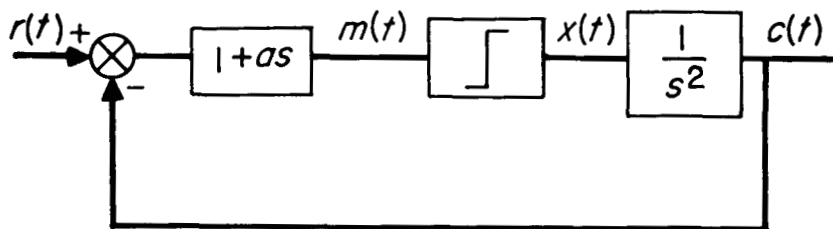


Figure 15.- Block diagram of a relay control system.

this system are equivalent to initial conditions on  $c$ ; therefore, we can use either  $c$  and  $\dot{c}$  as phase space variables or  $\epsilon$  and  $\dot{\epsilon}$ , since the trajectories are identical except for sign. The trajectories are parts of parabolas (see, e.g., ref. 10); a typical trajectory for one input is shown in figure 16. The time for the trajectory to go from A to B is obtained by taking  $|A|+|B|$  as the input step magnitude and using the minimum curve in figure 12(b).<sup>8</sup> Similarly, the time required to go from B to C is obtained by taking  $|B|+|C|$  as the input magnitude and using the minimum curve of figure 12(b), etc. The total time is obtained by summing all the individual times and adding the time required to go to the origin from the end point where Flügge-Lotz and Lindberg (ref. 12) have shown the system follows the switching equation. The switching equation is linear and first order in this example, and the response time can be readily estimated. What is done then for higher order systems is to approximate them by a second-order relay-type system. The accuracy of the calculation depends on the degree to which this approximation is valid.

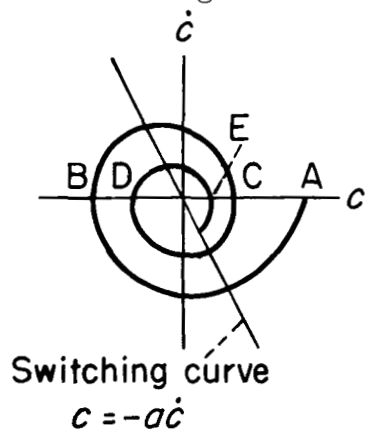


Figure 16.- Phase plane trajectories for a relay control system.

<sup>8</sup>This statement can be verified by reviewing section 2.4 where the minimum curve was derived.

The sampled-data results presented in chapter IV for third-order systems show the method gives a good idea of the deterioration of the response with the size of the input. This, of course, is all that is intended for the method, and, thus, it satisfies the original purpose for which it was developed. The advantage of the method is its simplicity. The curves used for calculation have additional use in the determination of nonlinear functions which, when introduced in the system, give almost optimum response. The subject of the determination of nonlinear functions to improve poor responses is considered next.

## 2.6 The Determination of Nonlinear Functions to Improve the Step Response

The proposed method for the design of nonlinearities to improve the step response is based on the idea of forcing the first reversal or switching time to be equal to the first reversal time of the optimum bang-bang system. This objective is achieved by introducing a nonlinear function into the error channel (for example, making the error gain a function of the error) or into the output derivative channel (for example, making the output velocity feedback a nonlinear function of the output velocity).

This method was first reported in reference 5. In this previous report both a type 2 third-order and a type 2 fourth-order plant were designed with considerable success, although the limitations of the method and the theory behind the derivation were not very well understood at the time. In this section the method will first be explained. It will then be shown that for second-order optimum bang-bang systems, it gives precisely the same result as the phase plane.

The method is best described by working an example. The example chosen is the simple second-order system shown in figure 10 whose actual and optimum first reversal times are plotted in figure 12(a). The design will result in a nonlinear function in place of either  $K_e$  or  $K_c$ . As was previously mentioned, if the step input is greater than 0.12 units, the system must overshoot. We shall thus use the gains  $K_e = 100$  and  $K_c = 14$  until we arrive at a condition which would have overshoot. Above this condition  $K_e$  and/or  $K_c$  will be made nonlinear to prevent the overshoot.

Equation (7) gives  $m(t)$  as a function of  $R_0$ ,  $t$ ,  $K_e$ , and  $K_c$ . This equation is valid until the first reversal time,  $T_1$ . Since the optimum first reversal curve (fig. 12(a)) gives  $R_0$  as a function of  $T_1$  and the value of  $m(T_1)$  is equal to 1, equation (7) can be solved for  $K_e$  or  $K_c$  at  $T_1$ . These gains can be plotted as functions of error or output

rate in order to determine a function of a single variable<sup>9</sup> (i.e.,  $K_\epsilon(\epsilon)$  or  $K_{\dot{c}}(\dot{c})$ ). When either one or the other is introduced into the system in place of the constants, it will give the desired first reversal time for a zero overshoot output response.<sup>10</sup> Note that what we are actually doing is taking the optimum relay solution at one time (the first reversal time) and designing nonlinear functions which force the bounded variable of the actual system to reverse at the same time for the same input as the optimum relay system.

At the first reversal time,  $T_1$ , (for large inputs which cause  $x$  to be saturated)

$$\epsilon(T_1) = R_0(T_1) - L^{-1} \left[ \frac{BG(s)}{s} \right] = R_0(T_1) - \frac{T_1^2}{2} \quad (15)$$

$R_0(T_1)$  is obtained from figure 12(a), that is, it is the optimum relay solution. The output velocity,  $\dot{c}$ , at the reversal time,  $T_1$ , is

$$\dot{c}(T_1) = L^{-1} [BG(s)] = T_1 \quad (16)$$

One can solve equation (7) for  $K_\epsilon$  to give

$$K_\epsilon(\epsilon) = \frac{m(T_1) - K_{\dot{c}}T_1}{R_0(T_1) - (T_1^2/2)} \quad (17)$$

If  $K_{\dot{c}}$  is assumed to be a constant ( $K_{\dot{c}} = 14$ ) and  $m(T_1) = 1$ , we can obtain  $K_\epsilon(\epsilon)$  (from eq. (17)) and  $\epsilon(T_1)$  (from eq. (15)); the nonlinear function of a single variable which when introduced in place of the constant gain  $K_\epsilon$  on figure 10 will give the optimum first reversal time.<sup>11</sup>

<sup>9</sup>One need not find only functions of single variables. For example one could obtain  $K_{\dot{c}}(\epsilon)$ . However, in the installation a multiplier would be required which is undesirable. These functions of more than one variable have not been studied, since to be realized they require a more complex system.

<sup>10</sup>One need not design for zero overshoot. The optimum first reversal curve may be shifted upward to give any desired overshoot the designer requires. Although this modification is recognized, it has not been studied in this investigation.

<sup>11</sup>Note again that the transition time, that is, the time for  $m(t)$  to go from one limit to another is assumed zero. Since this assumption can never be valid except for an ideal relay, it is preferable to make  $m(T_1) = 0$  in equation (7). This gives  $K_\epsilon(\epsilon)$  a slightly lower value than equation (17) which improves the approximation.

Similarly one can solve equation (7) for  $K_{\dot{c}}(\dot{c})$  which is given in equation (18)

$$K_{\dot{c}}(\dot{c}) = \frac{K_{\epsilon}\epsilon(T_1) - m(T_1)}{\dot{c}(T_1)} = \frac{K_{\epsilon}[R_0(T_1) - (T_1^2/2)] - 1}{T_1} \quad (18)$$

and use equation (16) to obtain the nonlinear function of a single variable. In equation (18),  $K_{\epsilon}$  is assumed constant ( $K_{\epsilon} = 100$ ). Note again that it is probably better to make  $m(T_1) = 0$  in equation (18).

The results of the equations (17) and (18) are plotted in figures 17(a) and 17(b). The dotted portions of the solutions are eliminated, since we desire the system to be linear in this region of error or output rate.

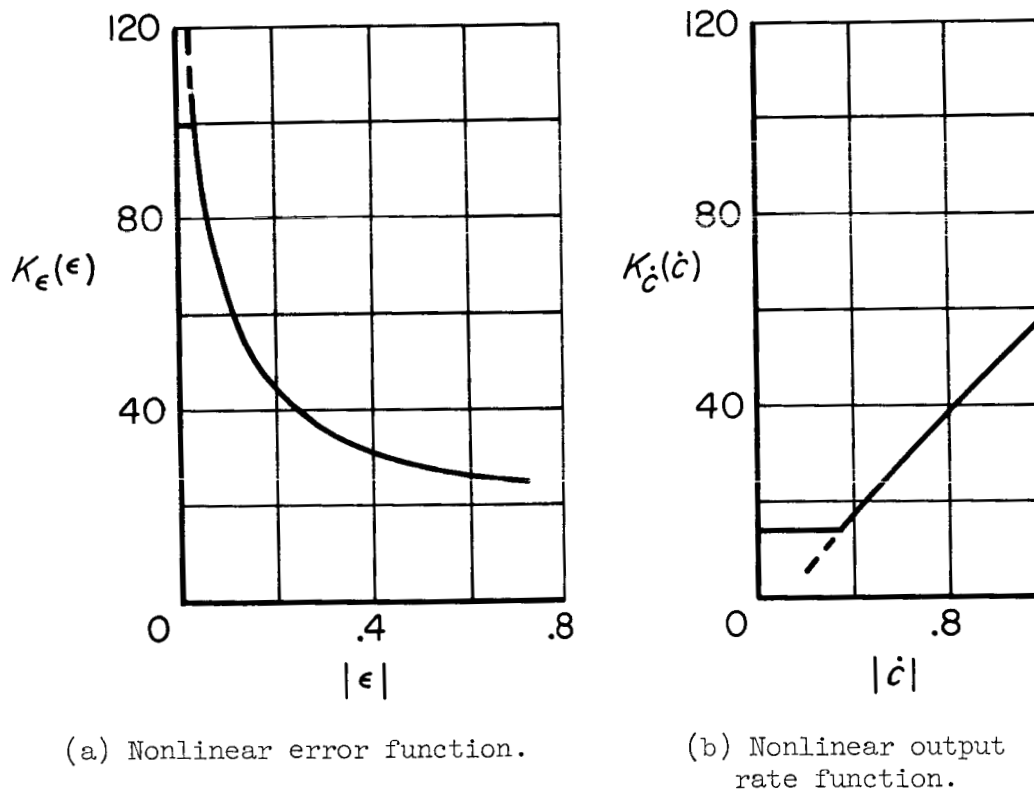


Figure 17.- Nonlinear functions for example control system.

If one desires to generate these nonlinear functions by means of a function generator, the input-output curve of the function generator can be obtained by plotting  $\epsilon$  vs.  $K_{\epsilon}(\epsilon)\epsilon$  or  $\dot{c}$  vs.  $K_{\dot{c}}(\dot{c})\dot{c}$ .

The results of simulation studies have shown either one of these systems (nonlinear error function or nonlinear output rate function) to have desirable (i.e., almost optimum) characteristics for large inputs.

For the general case one can give the following steps for computing nonlinear functions:

- (1) Determine for the given  $G(s)$  or an approximate  $G(s)$  the actual and the optimum first reversal times as a function of the input size,  $R_0$ .
- (2) Determine the switching equation for the input to the limiter in general equation form. For large inputs all the quantities will be known as functions of time.
- (3) For inputs where the actual first reversal time is longer than the optimum time, determine  $R_0(T_1)$  from the optimum curve. This will be read from curves in chapter III for complicated cases.
- (4) Solve the switching equation of step 2 for the desired nonlinear function (e.g.,  $K_\epsilon(\epsilon)$ ). All quantities in this equation can be computed at the switching time,  $T_1$ , except  $R_0$ ;  $R_0(T_1)$  is determined according to step 3.<sup>12</sup>

2.6.1 An optimum second-order system.— This section shows that using the switch time method for an on-off second-order system results in the same optimum system, that is, the same switching equation as the phase plane method. This result along with the discussion on limitations in the next section should give the user some confidence in when to expect good results from this method.

Consider the on-off system of figure 15. The input,  $m(t)$ , to the infinite gain limiter (or ideal relay) is given by equation (19).

$$m(t) = \epsilon(t) + a\dot{\epsilon}(t) \quad (19)$$

The output of the limiter is

$$x(t) = \text{sgn } m(t) \quad (20)$$

---

<sup>12</sup>These functions which are derived are symmetrical with respect to the origin. This symmetry is a result of the assumption that the limiter is symmetrical, that is, its maximum values (positive or negative) are identical. Although the switch time method could be extended to cover cases where the maximum values were not the same, it has not been done in this investigation.

Since we are only concerned with the sign of  $m(t)$ , we set  $m(T_1) = 0$  in equation (19) to obtain the switching equation

$$\epsilon(T_1) = -a\dot{\epsilon}(T_1) \quad (21)$$

If we want the optimum step response,  $\epsilon(T_1)$  is given by equation (15) and  $R_0(T_1)$  is taken as  $|R_0(T_1)| = T_1^2$ . Thus

$$\epsilon(T_1) = \frac{T_1^2}{2} \operatorname{sgn} R_0 \quad (22)$$

and from equation (16) with reference to figure 15

$$\dot{\epsilon}(T_1) = -\dot{c}(T_1) = -T_1 \operatorname{sgn} R_0 \quad (23)$$

Using equations (22) and (23) in equation (21) and solving for  $a$  gives

$$a = \frac{T_1}{2} \quad (24)$$

From equation (23)

$$\frac{T_1}{2} = -\frac{\dot{\epsilon}(T_1)}{2 \operatorname{sgn} R_0} \quad (25)$$

Since  $\dot{\epsilon}$  is negative for  $R_0$  positive and vice versa, equation (25) can be simplified to

$$a = \frac{T_1}{2} = \frac{|\dot{\epsilon}(T_1)|}{2} \quad (26)$$

Substituting this result in equation (19) and recognizing it must be true for all times gives the optimum first reversal curve

$$\epsilon(t) + \frac{|\dot{\epsilon}(t)|}{2} \dot{\epsilon}(t) = 0 \quad (27)$$

Equation (27) gives the optimum system which is the exact result of previous work (see, e.g., ref. 10).

## 2.7 Limitations of the Switch Time Method

Section 2.6 demonstrated a method of computing functions of a single variable in order to obtain near optimum response for large step inputs. It was also demonstrated that the method, when applied to one second-order plant ( $G(s) = 1/s^2$ ), gives the same optimum switching equation as has been derived by the phase plane. It can be shown that the method will also give the optimum switching curve for a plant transfer function  $G(s) = K/s(\tau s + 1)$ , that is, for a type 1 second-order plant. What remains to be considered are the following questions:

- (1) In what general cases can one always expect good results?  
This question could be rephrased as, "When is a single non-linear function adequate to insure good response to large steps?"
- (2) In what special cases can one use a function of a single variable and what additional technique is required to determine simple functions of two variables (e.g.,  $K_\epsilon(\epsilon)\epsilon + K_c(\dot{c})\dot{c}$ ) which will give good step response to a broader class of systems?

Question number 1 can be answered in general by the following statement: "The method will always give good results if there is not more than one zero in the expression  $G(s) H(s) D(s)$  and the system has 'adequate stability'<sup>13</sup> in the linear region." Arguments which make this statement plausible will be made in two steps; first, we shall investigate the restriction of no zeros in the expression  $G(s) H(s) D(s)$  and, second, the restriction of only one zero.

The characteristic equation of the closed-loop transfer function of figure 1(a) is given by equation (28), where  $K_L$  is the gain of the limiter.

$$1 + K_L G(s) H(s) D(s) = 0 \quad (28)$$

If there are no zeros in the expression  $G(s) H(s) D(s)$ , then immediately one can rule out type 2 or type 3 plants, since they could not have adequate stability. This can be verified by sketching root loci for any type 2 or type 3 plants under the restriction of no zeros in  $G(s) H(s) D(s)$ . Thus, only type 1 plants need to be considered.<sup>14</sup> A type 1 plant must of necessity be "dominant" first order for large inputs

<sup>13</sup>If all poles of the linear closed-loop transfer function have a damping ratio greater than 0.5, the system is defined as adequately stable. The number, 0.5, is relatively arbitrary and probably best determined by the experience of the control designer.

<sup>14</sup>Type 0 plants are not considered in this investigation.

(see rule I, section 2.2). The additional restrictions of adequate stability for the linear region and no zeros in  $G(s) H(s) D(s)$  also rule out conditionally stable systems. As a matter of fact, it appears to be impossible for the damping of any complex poles to decrease appreciably as the limiter gain is decreased without the system becoming dominant first order.

A second argument is that if  $G(s) D(s) H(s)$  contains no zeros, we might as well let  $H(s) = 1$  and  $D(s) = K_1$ , the gain constant. With reference to figure 1(a) it can be seen that the  $x$ , the saturating quantity, is only a function of the error. Thus, there is no reversal of the sign of  $x$  required to obtain satisfactory response for step inputs in the linear region. This system, therefore, requires no braking force in the linear region. Since it is velocity limited (see section 2.2), saturation essentially "slows down the motion" which reduces the necessity of braking even more in the saturated region than in the linear region. Thus, it is difficult to reason why any reversal of the sign of  $x$  should be required in the saturated region.

The root-locus argument appears to be the best, and the reader should sketch the root loci for a few plants to satisfy himself of the plausibility of the argument. One can conclude that under the restriction of no zeros, no nonlinear function will be required for adequate stability for large inputs.

Consider now the case with one zero in  $G(s) H(s) D(s)$ . For this example we can immediately rule out type 3 plants, as they cannot have adequate stability under this restriction. Furthermore, one can also rule out conditionally stable systems. This can easily be verified by sketching a Nyquist diagram for type 1 or type 2 plants under the restriction of adequate stability and one zero in  $G(s) D(s) H(s)$ . Finally, the worst case we can have, under these restrictions, is a type 2 plant, and the only conceivable root loci meeting the requirements of adequate stability are shown in figure 18. The root loci here are for a fifth-order system; however, the loci in the vicinity of the origin (the dominant mode) will be approximately the same regardless of the order. From figure 18 it can be seen that the response will become less damped as the magnitude of the input is increased (see rule II, section 2.2). It also seems reasonable that if the zero is shifted closer toward the origin as the gain of the limiter decreases, then one could keep the poles nearest the origin from ever becoming lightly damped. We can make the zero position shift closer toward the origin as a function of the error. As a matter of

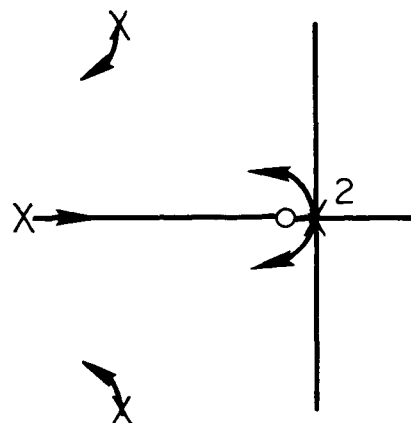


Figure 18.- Root loci of a type 2 system.

fact the method described in section 2.6 does just this if we choose  $K_\epsilon$  to be a nonlinear function of  $\epsilon$ . For a simple zero, the switching equation, that is, the equation determining the sign of  $x$  (fig. 1), can be written, for step inputs, as  $K_\epsilon \epsilon(t) + K_\epsilon \dot{\epsilon}(t)$ . If  $K_\epsilon$  decreases with  $\epsilon(t)$ , this causes the zero of the incremental model of the system to shift toward the origin. The method, if carried through for any type 2 plant, will show that  $K_\epsilon$  must be a decreasing function of  $\epsilon$  if the first reversal time is to be maintained optimum.

Question 2 is now considered. It cannot be answered precisely, although root-locus arguments give the following answer: "A function of a single variable is sufficient in those examples where a change in a single variable can shift the zeros, as a function of limiter gain, in such a manner that all poles stay in a well-damped region of the  $s$  plane as the limiter gain is decreased." The problem with this statement is, of course, that one cannot adequately define the equivalent gain of the limiter. At least two previous examples (ref. 5) and several examples in chapter IV show that only the error gain need be made a nonlinear function of the error if step inputs are considered. Thus, it shall be assumed that making the zero positions change with error is equivalent (for step inputs) to making the zeros change as a function of the equivalent limiter gain.

To illustrate generally how one can get at least an approximate idea of whether a single function of error is sufficient, consider the following type 1 third-order system with  $G(s) H(s) D(s)$  having two zeros. The root loci for the linear design is sketched in figure 19. The points A represent the pole positions for one open loop, or equivalent limiter gain of the system. It is seen that this system is not dominant first order, unless the equivalent gain of the limiter is considerably less than that corresponding to the points A (letting the real pole move close to the origin). Thus, one could well expect that the transient response will change quite markedly with the size of the step input, becoming increasingly bad for a certain range of inputs. This result is hypothesized, since the damping at point A of the complex poles is very low.

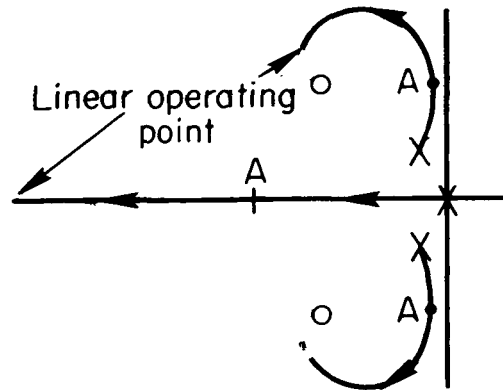


Figure 19.- Root loci of a type 1 system.

A block diagram for this system can be as shown in figure 20.<sup>15</sup>

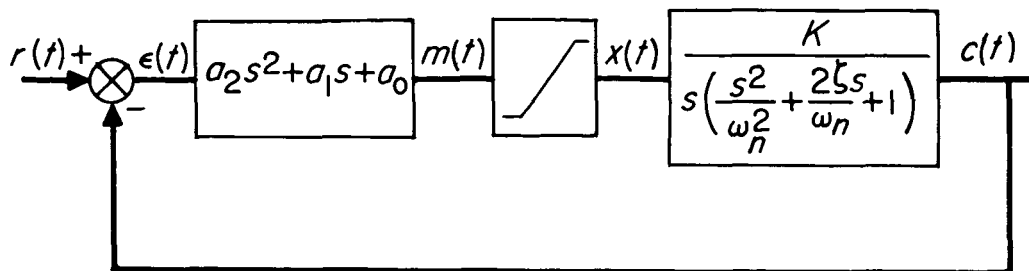


Figure 20.- Block diagram of a type 1 system.

The zero positions are given by equation (29).

$$s = - \frac{a_1 \pm \sqrt{a_1^2 - 4a_0a_2}}{2a_2} = - \frac{a_1}{2a_2} \pm i \sqrt{\frac{a_0}{a_2} - \frac{a_1^2}{4a_2^2}} \quad (29)$$

From equation (29) it can be seen that decreasing  $a_0$  alone causes the zeros of figure 19 to move in a direction of constant real part and decreasing imaginary part. This, from root-locus reasoning, would appear to be helpful. Similarly decreasing  $a_1$  would cause the real parts to decrease while the imaginary part increases. This does not appear to be desirable. Increasing  $a_2$  causes both real and imaginary parts to change, and it is necessary to investigate the loci as  $a_2$  changes to see whether beneficial results should be expected. The variation of  $a_0$  with  $e(t)$  is the simplest from a construction standpoint, and a design based on a nonlinear function of  $e$  should be investigated first by designing the nonlinearity and then by means of simulation. If simulation studies show that neither variations of  $a_2$  with error nor  $a_0$  with error give satisfactory results, then one must change two of the  $a$ 's of figure 20 with error so that the loci of zero positions move along a path which keeps the closed-loop poles in a well-damped region of the  $s$  plane. Such a path might be one which keeps the damping ratio of the zeros constant.

In summarizing this section on limitations one can state that the method, when used in conjunction with root locus and simulation, appears, at least for step inputs, to be primarily limited by the ingenuity of the designer. Its true drawbacks are that for successful results in arbitrary order cases a large number of trial designs may have to be simulated before a satisfactory design can be obtained.

<sup>15</sup>For step inputs, output rate and output acceleration feedbacks for this system give identical results as zeros in the error channel.

## 2.8 Analysis and Design Methods for Sampled-Data Systems

The material presented thus far can almost be used for sampled-data systems with the single substitution of the  $z$  plane wherever the  $s$  plane has been used. There are, however, certain modifications necessary. It is believed that these modifications are best described by taking up the subjects presented in this chapter for continuous systems and showing the modifications which are required for their application to sampled-data systems.

2.8.1 Root locus.— The rules presented for continuous systems can be used for sampled-data systems with the following modifications:

- (1) The stability boundary in the  $z$  plane is the unit circle.
- (2) All poles of the plant should be in the principal strip<sup>16</sup> of the  $s$  plane for the transformation  $z = e^{sT}$ .
- (3) The poles of the digital computer pulse transfer function are well damped. Point 3 is introduced here for reasons identical to those which are discussed in section 2.2 (footnote 1); that is, the poles must be well damped to prevent the output of the limiter from being switched from one extreme to another when the loop is essentially "opened up" by limiter action.
- (4) Since

$$z = e^{sT} = 1 + sT + \frac{(sT)^2}{2!} + \dots \quad (30)$$

mapping in the vicinity of the origin ( $sT \ll 1$ ) in the  $s$  plane transforms into mapping in the  $z$  plane around  $z = 1$ .

2.8.2 Switch time method, analysis.— The technique to be applied here is almost identical to that for the continuous system. In order to give the reader some confidence in the technique as well as to introduce the small differences in approach, an example will be worked out in detail. The principal difference in approach is simply that we are now dealing with a sampled-data system; thus, the output of the digital computer can change only at discrete times.

---

<sup>16</sup>Principal strip means that the imaginary part of any complex poles should be less than one half the sampling frequency, that is,  $\omega_n \sqrt{1 - \zeta^2} < \pi/T$ . The implications of or necessity for this restriction seem up to now not to be well understood. It is imposed so that there is a one to one correspondence between positions of poles in the  $s$  plane and positions of poles in the  $z$  plane.

Consider the block diagram of the system shown in figure 21.

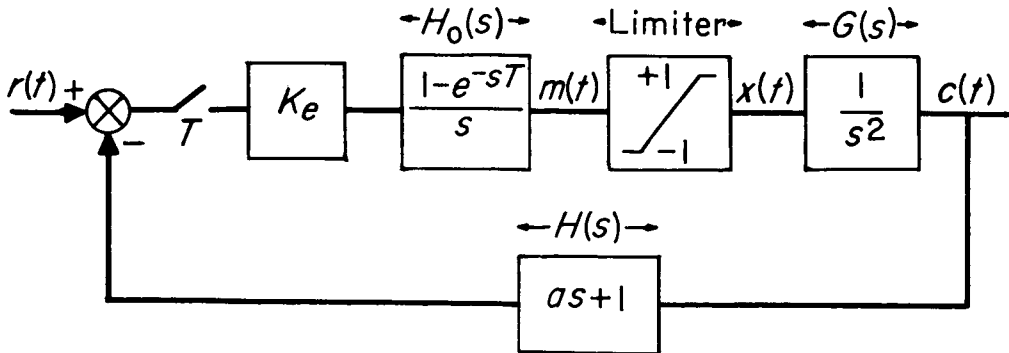


Figure 21.- Block diagram of an example sampled-data system.

Let us assume that  $T = 1$  and that a "finite settling time" design<sup>17</sup> is desired for the linear region. To obtain such a design one writes the characteristic equation of the closed-loop pulse transfer function in general terms of the available parameters; the characteristic equation in terms of  $a$  and  $K_e$  is

$$\left. \begin{aligned} 1 + K_e Z[H_0(s) G(s) H(s)] &= 0 \\ 1 + K_e Z\left(\frac{1 - e^{-sT}}{s} \frac{as + 1}{s^2}\right) &= 0 \\ 1 + K_e \left\{ \frac{[a + (1/2)]z^{-1} - [a - (1/2)]z^{-2}}{(1 - z^{-1})^2} \right\} &= 0 \end{aligned} \right\} \quad (31)$$

(The symbol  $Z[F(s)]$  reads the  $Z$  transform of  $F(s)$ . The  $Z$  transform of a function can be obtained by expanding the Laplace transform in partial fraction expansions and looking up individual terms in tables (ref. 6).) The roots of equation (31) must all occur at  $z = 0$  to give a finite settling time design. Thus, the resultant equation in terms of  $z$  is

$$z^2 - 2z + 1 + K_e \left[ \left(a + \frac{1}{2}\right)z - \left(a - \frac{1}{2}\right) \right] = 0 \quad (32)$$

<sup>17</sup>A finite settling time design can always be obtained using output feedback derivatives provided that a sufficient number (order of the system minus one) are used and a zero-order hold exists in the system. It can likewise be obtained using a  $D(z)$  (fig. 1(b)) with  $H(s) = 1$ . The  $D(z)$  pulse transfer function for this example, however, has a very lightly damped pole. This type example, that is, where  $D(z)$  has a lightly damped pole cannot be treated by the methods used here.

Since we only allow  $z = 0$  then

$$\left. \begin{aligned} -2 + K_e \left( a + \frac{1}{2} \right) &= 0 \\ 1 - \left( a - \frac{1}{2} \right) &= 0 \end{aligned} \right\} \quad (33)$$

or

$$\left. \begin{aligned} a &= \frac{3}{2} \\ K_e &= 1 \end{aligned} \right\} \quad (34)$$

Of interest also is the pulse transfer function  $C(z)/R(z)$

$$\frac{C(z)}{R(z)} = \frac{K_e Z [H_0(s) G(s)]}{1 + K_e Z [H_0(s) G(s) H(s)]} = \frac{1}{2} z^{-1} + \frac{1}{2} z^{-2} \quad (35)$$

The unit pulse response given by equation (35) shows the output to be zero at the end of the third sampling instant which simply proves a finite settling time design has been achieved. Without saturation being present (for small step inputs) the output will be at the desired value of the step input in two sampling instants. This can be seen by writing  $C(z)$  for a step input  $R(z)$  and expanding the result in a power series of  $z^{-n}$ .

It is also desirable to consider the output of the limiter,  $x(t)$ , for a step input  $R_0 u(t)$

$$Z \left[ \frac{X(s)}{R(s)} \right] = \frac{Z [K_e H_0(s)]}{1 + Z [K_e H_0(s) G(s) H(s)]} = (1 - z^{-1})^2 \quad (36)$$

For  $r(t) = R_0 u(t)$  then  $R(z) = R_0 / (1 - z^{-1})$ ; thus for a step of  $R_0$  magnitude

$$X(z) = R_0 (1 - z^{-1}) \quad (37)$$

As one can recognize from equation (37), for a step input,  $R_0$ ,  $x(t)$  has a wave form as shown in figure 22. Since  $x = \ddot{c}$ , this motion agrees with what we know about controlling second-order plants with limited acceleration;

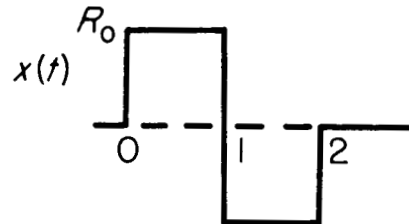


Figure 22.- Plant input,  $x(t)$ , for a step input,  $R_0 u(t)$ .

namely, that to move from one point to another one applies acceleration half the time and deceleration the other half. It can be recognized that if  $R_0$  is greater than one unit, saturation must take place, and then a greater number of sampling instants will be required in order that the error be reduced to zero. This is the principal difference in the way we shall treat sampled-data systems over continuous systems, that is, the first reversal time can only vary in discrete increments of  $T$  seconds (1 second for this example).

The curve for the first reversal time as a function of the input will now be derived. For inputs smaller than 1 unit it will be 1 second. For inputs greater than 1 unit saturation takes place, effectively "opening the loop" and allowing one to write the equation for  $M(z)$  in a power series expression in terms of  $z^{-1}$ . With reference to figure 21 letting  $K_e = 1$ ,  $a = 3/2$ , and  $x(t) = u(t)$  gives

$$\left. \begin{aligned} M(z) &= \frac{R_0}{1 - z^{-1}} - Z\left(\frac{1}{s^3} + \frac{1.5}{s^2}\right) \\ &= R_0 \sum_{n=0}^{\infty} z^{-n} - \sum_{n=0}^{\infty} \left[ \frac{(nT)^2}{2!} + 1.5nT \right] z^{-n} \\ &= \sum_{n=0}^{\infty} \left[ R_0 - \frac{(nT)^2}{2!} - 1.5nT \right] z^{-n} \end{aligned} \right\} \quad (38)$$

Equation (38) is written in infinite series form to allow one to pick out the sampling instant and the size of the step input when  $m(t)$  reverses from +1 to -1. For this example  $T$  is unity, so it is quite easy to derive a curve of  $T_1$  versus  $R_0$  from equation (38). For example, for  $n = 2$  we have the equation

$$-1 \geq R_0 - 2 - 3 \quad \text{or} \quad R_0 \leq 4 \quad (39)$$

Similarly for  $n = 3$

$$-1 \geq R_0 - \frac{9}{2} - \frac{9}{2} \quad \text{or} \quad R_0 \leq 8 \quad (40)$$

There is a range of inputs at a given value of  $n$  in which  $m(nT)$  is larger than -1 but less than +1. This range will be dotted on the switch time curve. Thus, for a first reversal time of  $n = 3$  one obtains the range of  $R_0$  as  $6 < R_0 < 8$ , with a dotted line connecting the points  $T_1 = 2$ ,  $R_0 = 4$  and  $T_1 = 3$ ,  $R_0 = 6$ .

The first reversal time of this system is shown with the optimum (for a continuous system, eq. (4)) in figure 23.

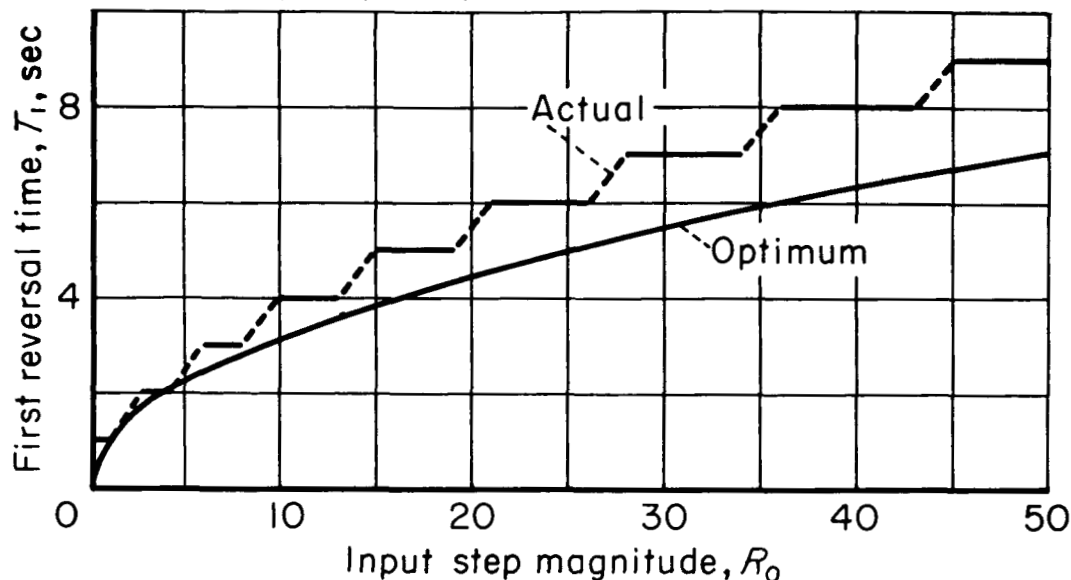


Figure 23.- Actual and optimum first reversal times for example system.

Now the same hypothesis is true for sampled-data systems as was true for continuous systems, that is, if the first reversal time,  $T_1$ , is greater than the optimum, then overshoot must exist if the bounded variable is saturated (see section 2.4). With reference to figure 22 it can be seen for  $R_0$  less than unity, the sampled-data system is linear, and, therefore, the first reversal time can be longer than the optimum for the range of inputs  $0 < R_0 < 1$ . For inputs greater than unity, reference to figure 23 shows that serious overshoot should not be expected for inputs less than approximately 5. This hypothesis is confirmed by the step responses for this system presented in figure 24.

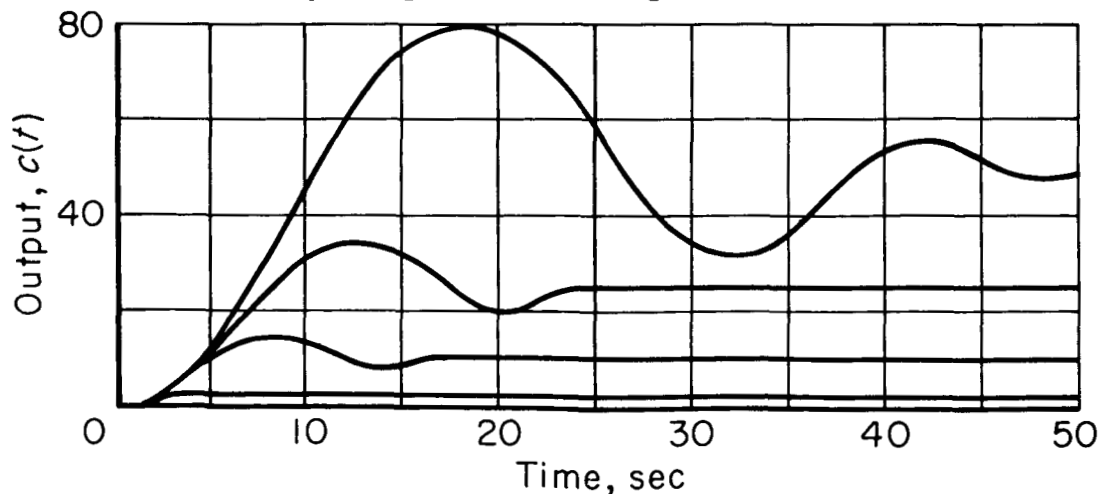


Figure 24.- Step responses of example system.

By comparing figures 24 and 23 one can see that the switch time curves can be used for sampled-data systems as well as for continuous systems. For example, for an input of 10 units the first reversal curve shows that the output should overshoot to 16 units. In other words, the actual reversal time for an input of 10 units is equal to the optimum reversal time for an input of 16 units. To obtain this number, one reads the abscissa of the optimum curve for the ordinate corresponding to an input of 10 units for the actual curve. The simulator results show the overshoot to be very close to 16 units for this input. Likewise, the overshoot of the response gets larger as the size of the input is increased as the switch time analysis method demonstrates.

2.8.3 Calculation of response times.— The method for calculation of the response times follows that previously described for continuous systems. Due to the fact that the system is sampled, the approximations make the calculated results less accurate than for the continuous case. Two examples are shown in chapter IV to allow the reader to obtain an idea of the accuracy of this method.

2.8.4 Calculation of nonlinear functions.— Figure 23 showed that the example system must overshoot. The simulator results of figure 24 demonstrate this overshoot and the poor response of the system for large step inputs. It is thus assumed that one should design compensating, nonlinear functions. We shall now investigate how this can be accomplished. The method is identical to that described in section 2.6 except that reversal of the saturated variable can take place only at discrete increments of time. This constraint forces one to take an approximation to the optimum first reversal curve. This approximation is shown in figure 25. This is only one approximation which could be used. One

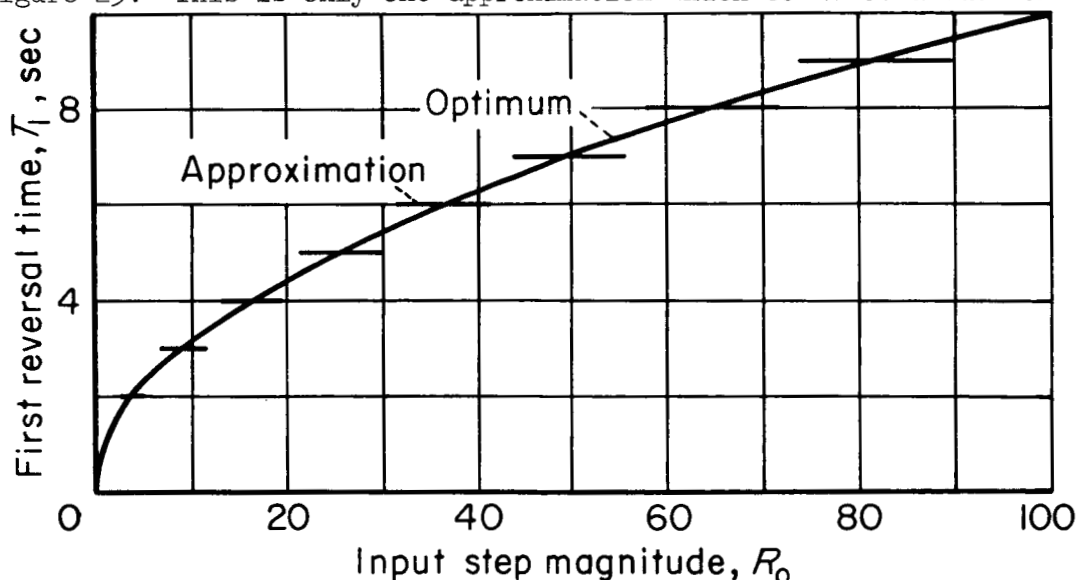


Figure 25.— Approximation to optimum first reversal curve for example system.

could design for overshoot or undershoot by shifting the staircase shaped curve upward or downward, respectively. The approximation taken here allows both a small amount of overshoot as well as undershoot, distributed in a manner which should give near optimum response for the sampled-data system.

If one assumes the approximation shown in figure 25 is satisfactory, then the problem is to determine a nonlinear function which will give this first reversal curve. First one writes the equation for the input to the limiter for step inputs large enough to cause saturation. For this example the  $Z$  transform equation is (with reference to fig. 21)

$$\sum_{n=0}^{\infty} m(nT)z^{-n} = \sum_{n=0}^{\infty} \{K_e[R_0 - c(nT)] - K_e a \dot{c}(nT)\} z^{-n} \quad (41)$$

In this equation every quantity is known up to the first reversal time. For example,  $c(nT) = (nT)^2/2!$ ;  $\dot{c}(nT) = nT$ ;  $R_0(nT)$  is obtained from figure 25 ( $R_0$  is the maximum value obtained for any sampling time); and  $m(nT) = -1$ . Thus, we must generate a nonlinear function so that this equation is satisfied for all values of  $nT$ . For the example here it will be assumed that the nonlinear function  $K\dot{c}(\dot{c})$  is desired. Thus, assume that  $K_e = 1$  and  $a = 3/2$  (in the linear region), rewrite equation (41) and solve for  $a\dot{c}(nT)$  to obtain

$$a\dot{c}(nT) = R_0 - \frac{(nT)^2}{2!} + 1 = f[\dot{c}(t)] \quad (42)$$

One point on the curve of  $f[\dot{c}(t)]$  is for  $n = 3$  and  $R_0 = 11.5$ . These values substituted in equation (42) give  $f[\dot{c}(t)] = 8$  for  $\dot{c}(t) = 3$ . The desired curve obtained by taking all values of  $n$  in the range of interest is shown in figure 26. This is half of a symmetrical curve with respect to the origin for reasons mentioned in footnote 12, chapter II.

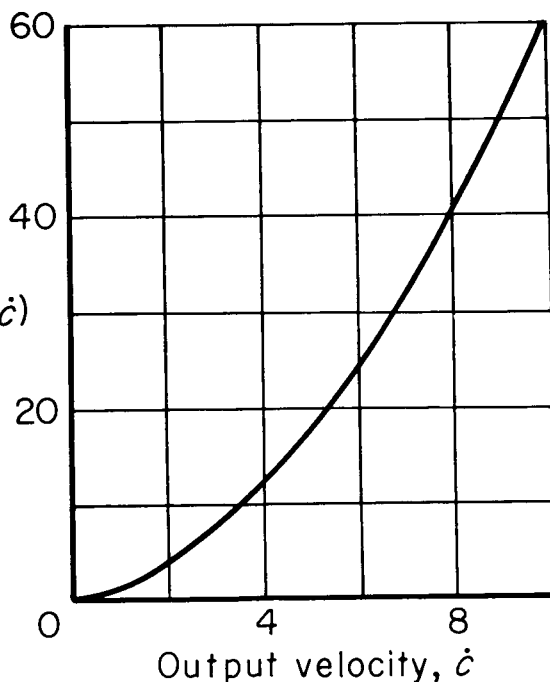


Figure 26.- Nonlinear function for example system.

The benefits gained by introducing the designed nonlinearity into the system can be observed by comparing the previous results for a linear controller shown in figure 24 with the step responses shown in figure 27 which are for the nonlinear controller.

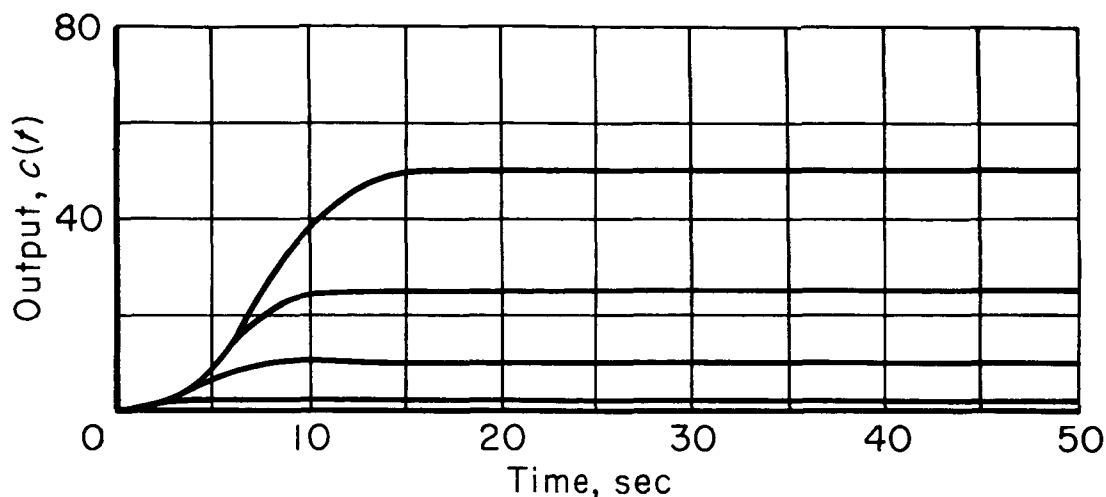


Figure 27.- Step responses of modified system.

2.8.5 Discussion.- The example worked out in this section shows that the switch time method gives good results when applied to sampled-data systems. There are, of course, more approximations involved than in the continuous case.

The limitations of the method appear to be the same as in the case of continuous systems. In this case also one can probably combine root-locus techniques in the  $z$  plane with the switch time method to give reasonably powerful tools for the treatment of systems of any order.

The best success will probably be attained when the sampling frequency is high compared to the dominant modes of the continuous system from which the sampled-data system is derived (see ref. 8). One is then treating an almost continuous system, and, consequently, methods based on continuous system design practices will give very nearly the same results as their continuous system counterpart.

### III. DERIVATION OF THE OPTIMUM RESPONSE

#### 3.1 Introduction

The previous chapter demonstrated that the switch time method is quite useful for the analysis of linear controllers which control a plant whose input is limited. The method also has been shown to provide a synthesis technique for determining nonlinear controllers which provide near optimum response when large step inputs are applied to the feedback control system. The application of both the proposed analysis and synthesis methods requires so-called optimum curves which give the first reversal time of the saturated quantity and the minimum response time of the system as a function of the input step magnitude. It is the purpose of this chapter to derive these optimum curves for the plants given in table I in normalized form so they may be used for any saturated control system, provided the "linear" design meets the restrictions imposed in chapter II.

In order to derive the optimum response curves, it is convenient to use the concept of an entire function.<sup>1</sup> A theorem is given in the following section and then succeeding sections are devoted to using it to derive the optimum response curves.

#### 3.2 A Theorem on the Laplace Transform of a Truncated Time Signal

**Theorem:** If a Laplace transformable function of time,  $f(t)$ , is truncated (i.e.,  $f_T(t) = 0$  for  $a > t > b$  where  $f_T(t)$  is the truncated time signal), then the Laplace transform of  $f_T(t)$ ,  $L[f_T(t)]$  is an entire function.

**Proof:** A complete proof of this theorem is available by applying theorems 95-98 of Titchmarsh (ref. 14). The only characteristic of the entire function that will be needed here is that it has no poles; that is,  $F_T(s)$  is bounded in the finite portion of the  $s$  plane. We shall prove this one characteristic about  $F_T(s)$  because the proof is short and will give the reader confidence in the application made later.

$$L[f_T(t)] = F_T(s) = \int_0^{\infty} f_T(t)e^{-st}dt = \int_a^b f_T(t)e^{-st}dt \quad (43)$$

---

<sup>1</sup>An entire function is regular in the entire finite  $s$  plane (see ref. 13, for example).

The limits on the integral may be changed since  $f_T(t) = 0$  for  $a > t > b$ . It is assumed that  $a$  and  $b$  are both positive numbers. One now expands the exponential in an infinite series giving

$$F_T(s) = \sum_{n=0}^{\infty} \frac{(-s)^n}{n!} \int_a^b f_T(t) t^n dt \quad (44)$$

Assume that  $f_T(t) \leq M$  where  $M$  is some finite number. Then,

$$|F_T(s)| \leq M \sum_{n=0}^{\infty} \frac{(-s)^n}{n!} \int_a^b t^n dt = M \sum_{n=0}^{\infty} \frac{(-s)^n}{n!} \left( \frac{b^{n+1} - a^{n+1}}{n+1} \right) \quad (45)$$

By multiplying inside the summation sign by  $-s$  and outside by  $1/-s$ , one obtains

$$|F_T(s)| \leq \frac{M}{-s} \left[ \sum_{n=0}^{\infty} \frac{(-bs)^{n+1}}{(n+1)!} - \sum_{n=0}^{\infty} \frac{(-as)^{n+1}}{(n+1)!} \right] \quad (46)$$

The right-hand side of equation (46) can be expressed in closed form, giving

$$|F_T(s)| \leq -\frac{M}{s} \left[ (e^{-bs} - 1) - (e^{-as} - 1) \right] = -M \left( \frac{e^{-bs} - e^{-as}}{s} \right) \quad (47)$$

Since the function of  $s$  given in equation (47) is finite in the finite portion of the  $s$  plane,  $F_T(s)$  is bounded.

### 3.3 A Method for Deriving the Optimum Response

The theorem of section 3.2 can be used to advantage in deriving the optimum response if further information regarding the shape of  $x(t)$ , the bounded variable, is attainable. Consider figure 1 for  $r(t) = R_0 u(t)$  and zero initial conditions. Then

$$L[\epsilon(t)] = E(s) = \frac{R_0}{s} - X(s) G(s) \quad (48)$$

A necessary but not a sufficient condition if we are to attain the optimum is that  $E(s)$  must be an entire function because  $\epsilon(t) = 0$  for  $t < 0$  and we desire  $\epsilon(t) = 0$  for  $t > T_m$ . In other words, the desired  $\epsilon(t)$  is a truncated time signal. In order to meet the

sufficiency condition one must know the optimum shape of  $x(t)$  in general terms of unknown reversal times. One then derives  $X(s)$  and determines the relationship between these unknown reversal times and  $R_0$  by forcing equation (48) to be an entire function.

The general shape of  $x(t)$  for the minimum response time can be found by either (1) inspection, or (2) by use of a theorem proved by Bellman, Glicksberg, and Gross (ref. 4) for the conditions for which it applies. The theorem applied to this problem states that in order to have a minimum response time to an input step  $x(t)$  should be at its maximum value plus or minus throughout the response, the maximum number of reversals being equal to  $n-1$  where  $n$  is the order of the system. The proof, however, is only for  $G(s)$  having real, distinct, and negative roots. It is shown later that if one confines his interest to plants having only poles in the left half plane or at  $s = 0$  and is interested only in responses to step inputs, the theorem gives a sufficient number of reversals of  $x(t)$  in order to restore the error and its derivatives to zero in a finite time, that is, to allow  $E(s)$  given by equation (48) to be an entire function. As will be demonstrated, the response time obtained by using this number of reversals may not be the minimum for plants with lightly damped complex poles. It will also be shown here that if zeros exist in  $G(s)$  then one does not want the bounded variable,  $x(t)$ , to be at its maximum throughout the entire response, that is, until the time when all the states of the system are restored to zero or a constant.

The steps involved in obtaining the optimum responses are summarized below.

(1) Determine  $x(t)$  in terms of the unknown switch times for the optimum response. This function will be the limit level times a sum of delayed steps for  $G(s)$  having only poles. The delay times will be written as undetermined coefficients.

(2) Determine  $X(s)$  from  $x(t)$ .

(3) Use the fact that the error transform must be an entire function to obtain algebraic or transcendental equations relating  $R_0$  and the unknowns of  $x(t)$ .

(4) Solve the equations of step (3) to obtain the optimum first reversal time and the minimum response time as functions of the input step magnitude  $R_0$ .

## 3.4 A Type 1 First-Order Plant

For this example,  $G(s) = K/s$ . Considering figure 1, we see that  $x = \dot{c}/K$ . Thus, in order for  $c$  to move from zero to  $R_0$ , in the minimum time, one simply uses the maximum value of  $x(t)$ , which provides the maximum value of the output velocity,  $\dot{c}(t)$ , until  $c = R_0$  and then restores  $x$  to zero. The motion of  $x$  is shown in figure 28. This example is so simple that the answer relating  $T_m$  and  $R_0$  can be written by inspection of figure 28; however, we will go through the steps of section 3.3 to familiarize the reader with the technique. The steps are as follows:

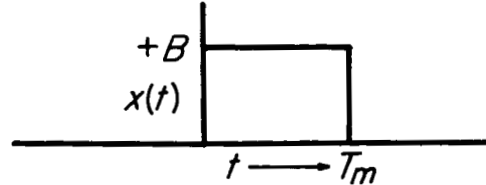


Figure 28.- Optimum motion of the input,  $x(t)$ , for a type 1 first-order plant.

$$x(t) = B[u(t) - u(t-T_m)] \quad (49)$$

$$X(s) = B \left( \frac{1-e^{-sT_m}}{s} \right) \quad (50)$$

$$E(s) = \frac{R_0}{s} - BK \left( \frac{1-e^{-sT_m}}{s^2} \right) \quad (51)$$

Since  $E(s)$  must be an entire function, then

$$E(s) \Big|_{s=0} = \text{some finite number}$$

thus

$$\frac{R_0 s - BK \left( 1 - e^{-sT_m} \right)}{s^2} \Big|_{s=0} = \frac{0}{0} \quad (52)$$

Differentiating the numerator and the denominator with respect to  $s$  gives

$$\left. \frac{R_0 - BK \left( T_m e^{-sT_m} \right)}{2s} \right|_{s=0} = \frac{R_0 - BKT_m}{0} \quad (53)$$

Differentiating additional times provides no more information. In order that equation (52) be entire then, the numerator of equation (53) must be equal to zero or

$$R_0 = BKT_m \quad (54)$$

Equation (54) can readily be solved for  $T_m$  and the curve showing  $R_0/KB$  vs.  $T_m$  can be plotted. This result is given in figure 29. For this simple example  $T_m$  is both the minimum response time and optimum first reversal time,  $T_1$ .

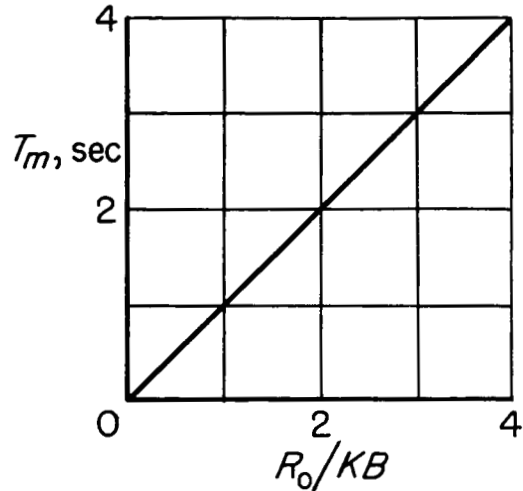


Figure 29.- Minimum response time for a type 1 first-order plant.

### 3.5 A Type 1 Second-Order Plant

For this example,  $G(s) = K(\tau_1 s + 1)/s(\tau_2 s + 1)$  and we have allowed a zero to exist in the plant transfer function. The problem is to determine the optimum motion of  $x(t)$  in order to reduce  $\epsilon(t)$  to zero in a minimum time. The solution to this problem can be found most conveniently by expanding  $G(s)$  by the partial fraction expansion and constructing a block diagram in terms of the components as shown in figure 30.

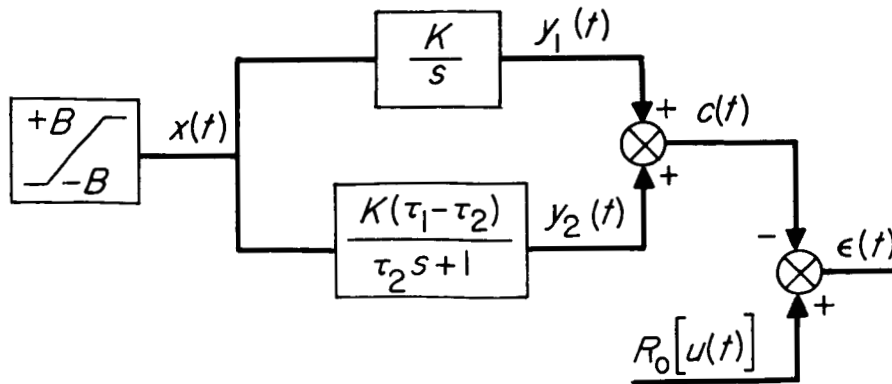


Figure 30.- Block diagram of a type 1 second-order plant.

It should be obvious from inspection of figure 30, that if  $x = +B$  and  $y_1(0) = y_2(0) = 0$ , then  $y_2(t)$  either aids ( $\tau_1 > \tau_2$ ) or hinders ( $\tau_1 < \tau_2$ )  $c(t)$  in reaching  $R_0$  in the minimum time. Regardless of whether  $y_2(t)$  aids or hinders, any positive value of  $\tau_1$  will allow  $c(t)$  to reach  $R_0$  in a shorter time than if  $\tau_1 = 0$ . Thus, a zero (in the left half plane) can speed up the response if one can find a motion of  $x(t)$  which will allow  $c(t)$  to remain at  $R_0$  while  $y_1(t)$  and  $y_2(t)$  change. This motion of  $x(t)$  can most conveniently be determined by solving for the  $x(t)$  which causes  $c(t)$  to jump to a constant and remain there.

For  $c(t)$  to jump to a constant value,  $C_0$ , then

$$X(s) G(s) = \frac{C_0}{s} \quad (55)$$

or

$$X(s) = \frac{C_0}{s} \left[ \frac{1}{G(s)} \right] = \frac{C_0}{K} \left( \frac{\tau_2 s + 1}{\tau_1 s + 1} \right) \quad (56)$$

and

$$x(t) = L^{-1}[X(s)] = \frac{C_0}{K} \frac{\tau_2}{\tau_1} \delta(t) + \frac{C_0}{K} \frac{(\tau_1 - \tau_2)}{\tau_1^2} e^{-t/\tau_1} \quad (57)$$

The  $\delta$  function simply puts an initial condition on  $y_1(t)$  and  $y_2(t)$  of figure 30 and from then on,  $y_1(t)$  and  $y_2(t)$  vary as  $c(t)$  remains constant. The motions are shown in figure 31.

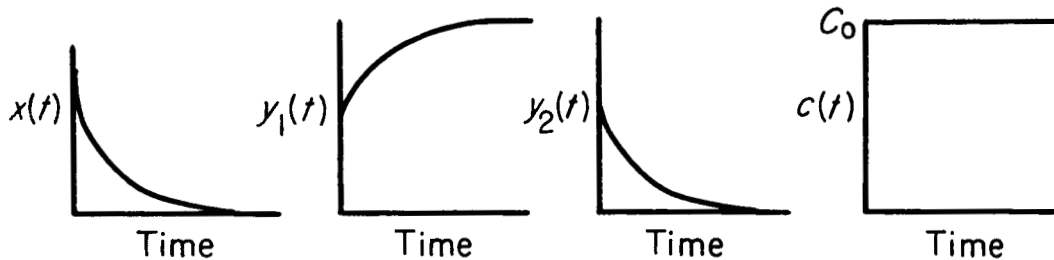


Figure 31.- Time histories for example system.

If  $x(t)$  is bounded,  $\delta$  functions cannot be permitted. However, if the maximum value of  $x(t)$  is applied,  $y_1(t)$  and  $y_2(t)$  will arrive at values in a finite time which will give  $y_1(t) + y_2(t) = c(t) = R_0$ . If  $x(t)$  is forced to have the decaying exponential motion of figure 31,  $y_1(t)$  and  $y_2(t)$  can change while  $c(t)$  remains at  $R_0$ . The optimum motion of  $x(t)$  will change as the ratio of  $\tau_2/\tau_1$  changes as well as when the size of the input changes. A little physical reasoning, however, should make it clear that  $x(t)$  can only be one of the two forms shown in figure 32. Figure 32(a) is in general terms and so long as  $|b| < B$ , the responses will be valid. With  $b = 0$ , the results

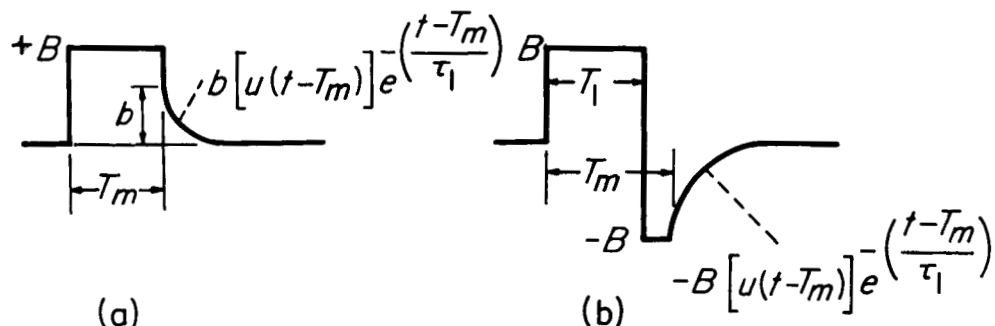


Figure 32.- Optimum motion of the input,  $x(t)$ , for a type 1 second-order plant.

correspond to the condition for  $\tau_2 = \tau_1$ , which reduces the plant to the first-order case;  $b$  will be positive for  $\tau_1 > \tau_2$  and negative for  $\tau_1 < \tau_2$ . If  $\tau_1$  is considerably smaller than  $\tau_2$ ,  $b$  will gradually increase in the negative direction as the size of the input step is increased until  $b = -B$ , then the solution of figure 32(b) is used for larger inputs. Figure 32(b) is in general terms and for  $\tau_1 = 0$ , it gives the bang-bang solution expected for a second-order system with no zeros.

One thus proceeds to write the Laplace transform of the  $x(t)$  motions shown in figure 32 and then, by forcing  $E(s)$  to be an entire function, finds the relationships between  $R_0$  and the undetermined coefficients  $b$ ,  $T_m$ , and  $T_1$ .

Considering  $x(t)$  as shown in figure 32(a)

$$x(t) = B \left[ u(t) - u(t-T_m) + \frac{b}{B} u(t-T_m) e^{-\left(\frac{t-T_m}{\tau_1}\right)} \right] \quad (58)$$

$$X(s) = B \left( \frac{1-e^{-sT_m}}{s} + \frac{b}{B} \frac{e^{-sT_m}}{s + \frac{1}{\tau_1}} \right) \quad (59)$$

$$E(s) = \frac{R_0}{s} - B \left[ \frac{\left(1 - e^{-sT_m}\right) \left(s + \frac{1}{\tau_1}\right) + \left(\frac{b}{B}\right) s e^{-sT_m}}{s \left(s + \frac{1}{\tau_1}\right)} \right] \left[ \frac{K(\tau_1 s + 1)}{s(\tau_2 s + 1)} \right] \quad (60)$$

$$= \frac{R_0 s(\tau_2 s + 1) - BK \left[ \left(1 - e^{-sT_m}\right) (\tau_1 s + 1) + \frac{b\tau_1 s}{B} e^{-sT_m} \right]}{s^2(\tau_2 s + 1)}$$

There are two potential singularities of  $E(s)$  indicated in equation (60), a second-order one at  $s = 0$ , and a first-order one at  $s = -1/\tau_2$ . At both these potential singularities,  $E(s)$  must be finite in order to be entire. Thus evaluating  $E(s)$  first at  $s = -1/\tau_2$  gives

$$E(s) \Big|_{s = -1/\tau_2} = \frac{BK \left[ \left(1 - e^{T_m/\tau_2}\right) \left(1 - \frac{\tau_1}{\tau_2}\right) - \left(\frac{b\tau_1}{B\tau_2}\right) e^{T_m/\tau_2} \right]}{0} \neq \infty \quad (61)$$

The numerator of equation (61) must therefore be zero, giving

$$\left(1 - e^{T_m/\tau_2}\right) \left(1 - \frac{\tau_1}{\tau_2}\right) - \left(\frac{b\tau_1}{B\tau_2}\right) e^{T_m/\tau_2} = 0 \quad (62)$$

Differentiating the numerator and the denominator of equation (60) will show  $E(s)$  is finite at  $s = -1/\tau_2$  if equation (62) is satisfied.

One next finds the relationship required to force  $E(s)$  to be finite at  $s = 0$ .

$$E(s) \Big|_{s=0} = \frac{0}{0} \quad (63)$$

Evaluating the 0/0 by differentiating the numerator and denominator of equation (60) with respect to  $s$  gives

$$E(s) \Big|_{s=0} = \frac{R_0 - BK \left( T_m + \frac{b\tau_1}{B} \right)}{0} \quad (64)$$

And again, since  $E(s)$  must be entire

$$\frac{R_0}{BK} = T_m + \frac{b\tau_1}{B} \quad (65)$$

Rewriting equation (62), solved for  $b/B$ , gives

$$\frac{b}{B} = \left(1 - e^{-T_m/\tau_2}\right) \left(1 - \frac{\tau_2}{\tau_1}\right) \quad (66)$$

The desired solution is obtained by solving equations (65) and (66) under the constraint that  $|b/B| \leq 1$ . Thus, it can be seen from equation (66) that if  $\tau_2/\tau_1 \leq 2$ , the solution is always valid. For  $\tau_2/\tau_1 > 2$ , the solution is valid for  $T_m$  less than or equal to the value that gives  $|b/B| = 1$  in equation (66). For larger values of  $T_m$ , one must use the form of  $x(t)$  given by figure 32(b) which is now considered.

With reference to figure 32(b)

$$x(t) = B \left[ u(t) - 2u(t-T_1) + u(t-T_m) - u(t-T_m)e^{-\left(\frac{t-T_m}{\tau_1}\right)} \right] \quad (67)$$

$$X(s) = B \left( \frac{1-2e^{-sT_1}+e^{-sT_m}}{s} - \frac{\tau_1 e^{-sT_m}}{\tau_1 s+1} \right) \quad (68)$$

$$E(s) = \frac{R_0}{s} - BK \left\{ \frac{\left(1-2e^{-sT_1}+e^{-sT_m}\right) (\tau_1 s+1) - \tau_1 s e^{-sT_m}}{s^2(\tau_2 s+1)} \right. \\ \left. = \frac{R_0 s(\tau_2 s+1) - BK \left[ \left(1-2e^{-sT_1}+e^{-sT_m}\right) (\tau_1 s+1) - \tau_1 s e^{-sT_m} \right]}{s^2(\tau_2 s+1)} \right\} \quad (69)$$

Forcing  $E(s)$  to be an entire function in the same manner as was done previously gives

$$2T_1 - T_m - \tau_1 = \frac{R_0}{KB} \quad (70)$$

$$\left(1 - 2e^{T_1/\tau_2} + e^{T_m/\tau_2}\right) \left(1 - \frac{\tau_1}{\tau_2}\right) + \left(\frac{\tau_1}{\tau_2}\right) e^{T_m/\tau_2} = 0 \quad (71)$$

Equation (71) can be solved for  $T_1$  in terms of  $T_m$  or vice versa. The results are

$$\frac{T_1}{\tau_2} = \ln \left[ \frac{1}{2} + \frac{e^{T_m/\tau_2}}{2 \left(1 - \frac{\tau_1}{\tau_2}\right)} \right] \quad (72)$$

$$\frac{T_m}{\tau_2} = \ln \left[ 2e^{T_1/\tau_2} \left(1 - \frac{\tau_1}{\tau_2}\right) - \left(1 - \frac{\tau_1}{\tau_2}\right) \right] \quad (73)$$

The solutions of (70) and (71) are only valid for  $|b/B|$  of equation (66) greater than unity.

The solutions for this plant were computed by means of equations (65), (66), (70), and (71). As can be recognized from the equations, it is convenient to normalize with respect to  $\tau_2$  and plot results for various values of the ratio  $\tau_1/\tau_2$ . These results are presented in figures 33 and 34. One should note again in using these results that  $T_1 = T_m$  for small values of  $R_0/KB\tau_2$  so long as  $\tau_1$  has any value whatsoever.

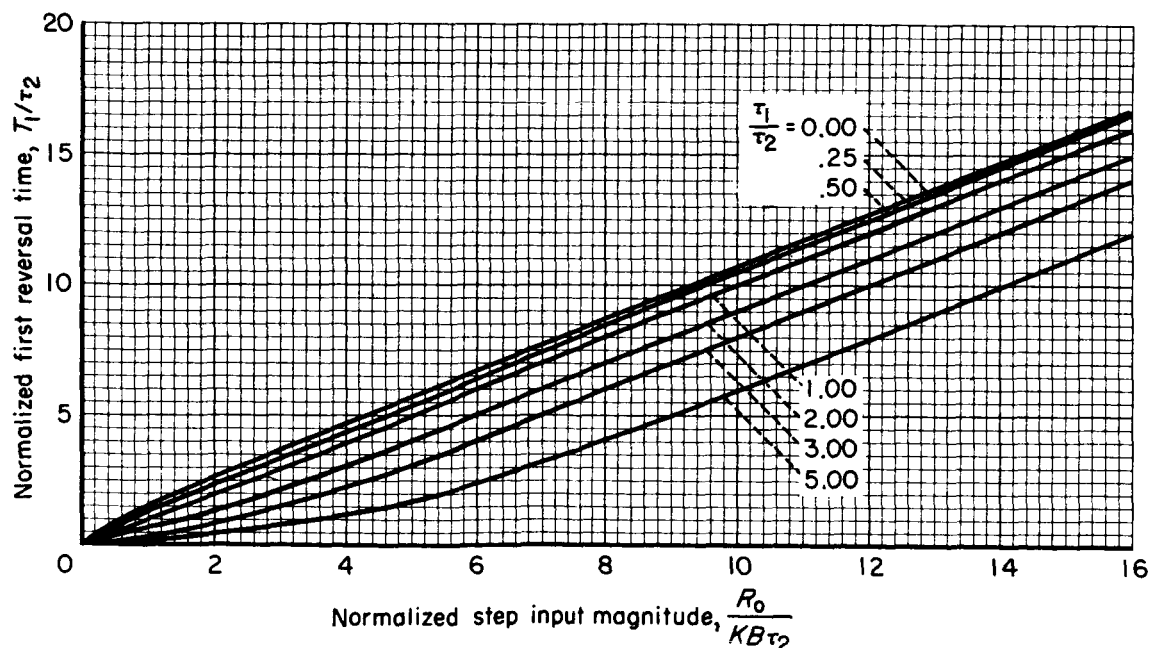


Figure 33.- Optimum first reversal time for a type 1 second-order plant.

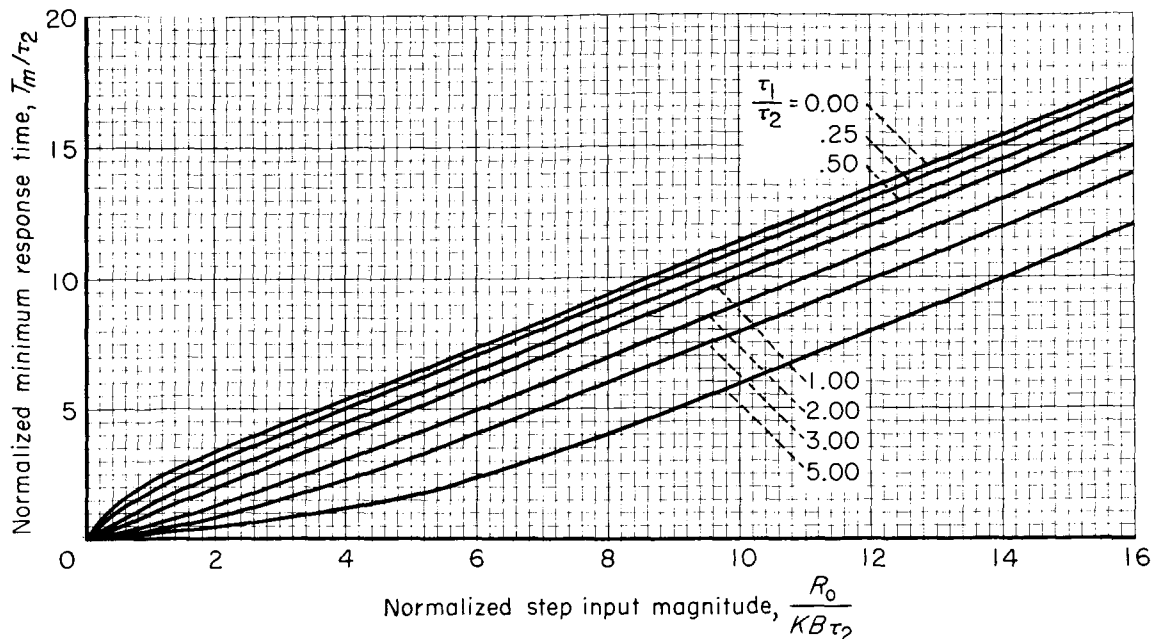


Figure 34.- Minimum response time for a type 1 second-order plant.

A considerable improvement in minimum response time can be achieved if the zero is much closer to the origin than the pole.

### 3.6 A Type 1 Third-Order Plant

The plant transfer function for this example is

$$G(s) = \frac{K}{s \left( \frac{s^2}{\omega_n^2} + \frac{2\zeta s}{\omega_n} + 1 \right)}$$

The optimum motion of  $x(t)$  in order for  $\epsilon(t)$  to be reduced to zero in a minimum time with  $r(t) = R_0 u(t)$  and zero initial conditions must be found first. If  $\zeta$  is greater than 1, a simple intuitive argument suffices to show that  $x(t)$  should be at its maximum all the time and that the number of reversals is two. This argument is facilitated by considering the block diagram of figure 35.

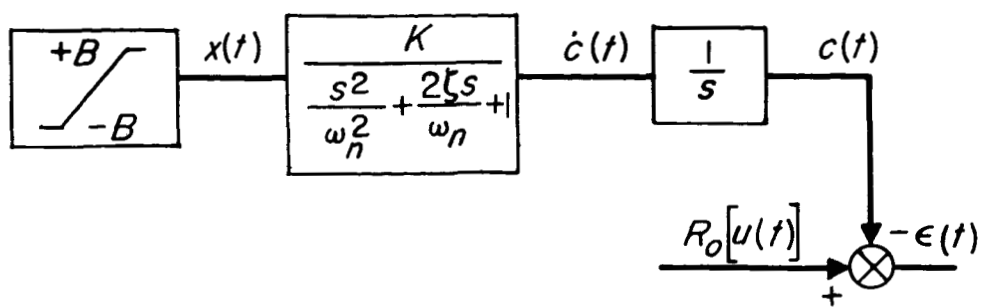


Figure 35.- Block diagram of a type 1 third-order plant.

The problem is to force  $c(t)$  to move to a value of  $R_0$  and arrive there with  $\dot{c} = \ddot{c} = 0$ . To have the minimum response time we desire

$\int_0^{T_m} \dot{c} \, dt$  to be a maximum with the constraint that

$$\dot{c}(T_m) = 0 = \ddot{c}(T_m) = \dot{c}(0) = \ddot{c}(0)$$

To force  $\dot{c}(t)$  to obtain a maximum value it seems obvious that  $x$  should have its maximum value initially and hold that value as long as permissible, since for  $x = B$ ,  $\dot{c}$  asymptotically approaches  $+KB$ . We may then use the theorem of reference 4 on  $\dot{c}$  since we want it to be restored from initial conditions to zero in a minimum time. This says then that the optimum motion of  $x(t)$  should be as shown in figure 36. If  $\zeta$  is less than 1, intuition still tells us that this is a reasonable motion of  $x$ . Experiments were conducted with an analog computer which verified that two reversals are sufficient and furthermore indicated the motion pictured in figure 36 appeared to be optimum except perhaps for low values of  $\zeta$ . We shall assume that this represents the optimum motion for all values of  $\zeta$  which are positive and proceed to find the relationships between  $R_0$ ,  $\zeta$ ,  $\omega_n$ ,  $T_1$ , and  $T_m$  in the same manner used previously.

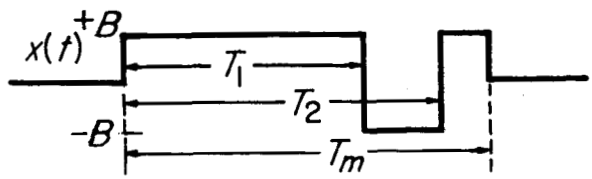


Figure 36.- Optimum motion of the input,  $x(t)$ , for a type 1 third-order plant.

$$x(t) = B[u(t) - 2u(t-T_1) + 2u(t-T_2) - u(t-T_m)] \tag{74}$$

Solving for the  $L[x(t)]$ , using equation (48) to obtain  $E(s)$ , and forcing  $E(s)$  to be an entire function gives the following equations:

A-310

$$1 - 2e^{\omega_n \left( \zeta \pm \sqrt{\zeta^2 - 1} \right) T_1} + 2e^{\omega_n \left( \zeta \pm \sqrt{\zeta^2 - 1} \right) T_2} - e^{\omega_n \left( \zeta \pm \sqrt{\zeta^2 - 1} \right) T_m} = 0 \quad (75)$$

$$2T_1 - 2T_2 + T_m = \frac{R_0}{KB} \quad (76)$$

Note that there are two equations given in (75), one for the positive sign and one for the negative; thus, for any fixed value of  $R_0/KB$ , there are three equations for three unknowns. These equations are best normalized by plotting  $\omega_n T_1$  and  $\omega_n T_m$  vs.  $(R_0/KB)\omega_n$  for various values of  $\zeta$ .

The solution of equations (75) and (76) can only be obtained by some iterative process. This was accomplished here by setting up an iterative procedure on a digital computer. The results of the calculations are shown in figures 37 and 38.

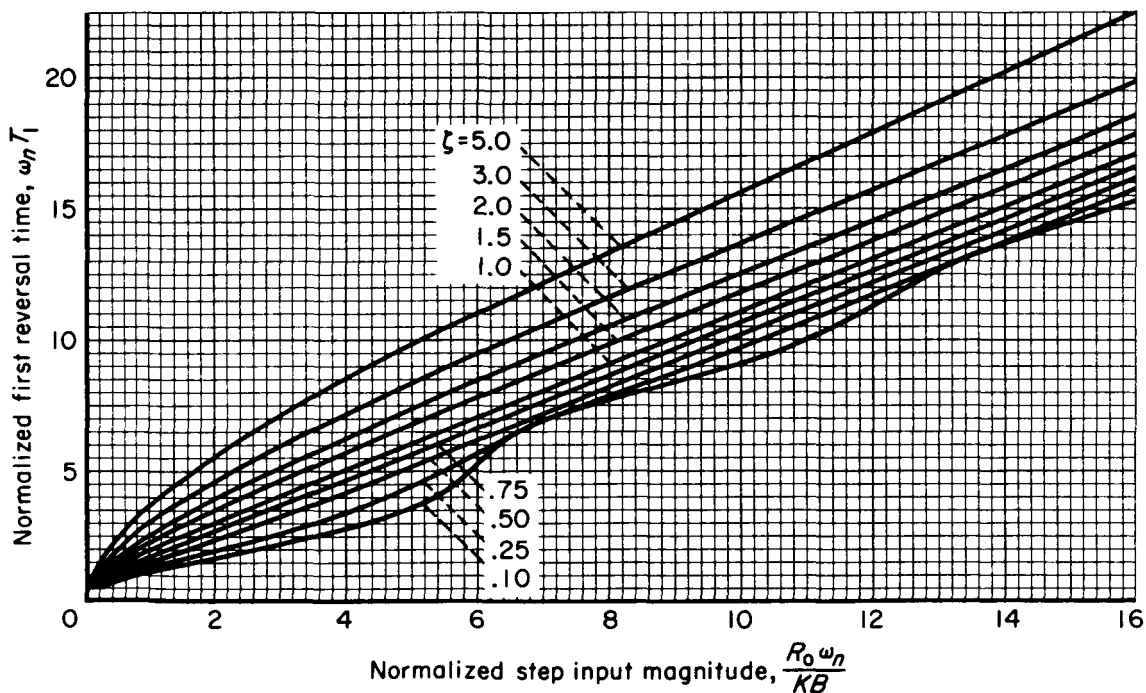


Figure 37.- Optimum first reversal time for a type 1 third-order plant.

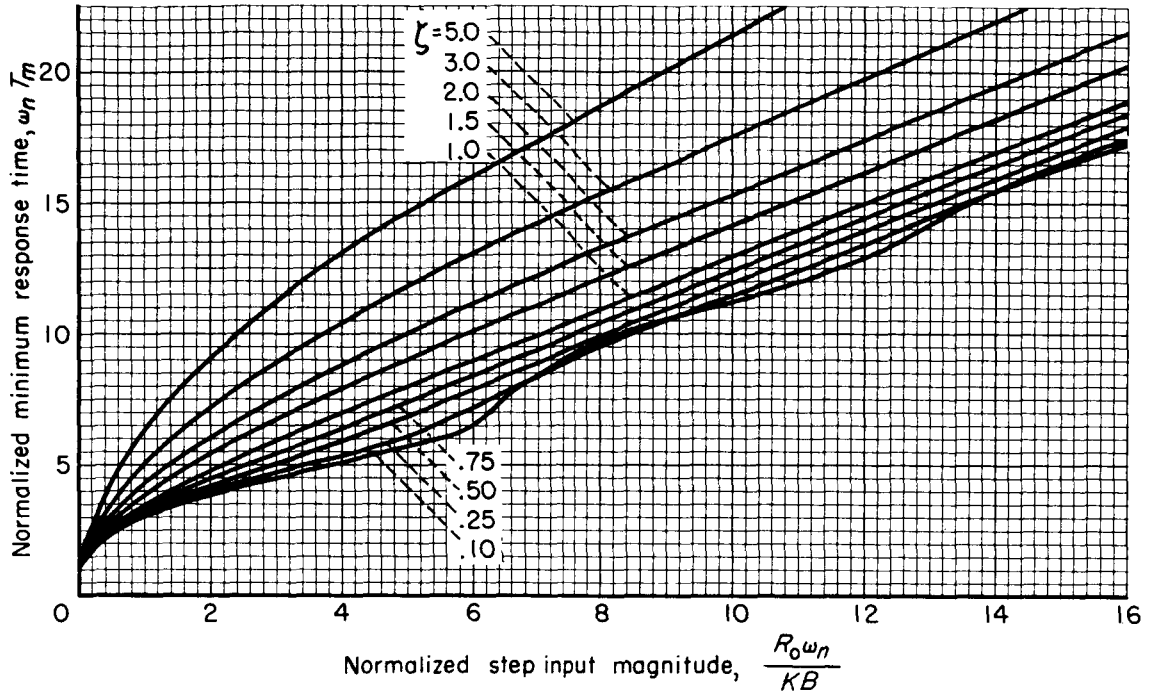


Figure 38.- Minimum response time for a type 1 third-order plant.

Included also in table II are the points of the curves near the origin where, because of the scale chosen, it is difficult to read the curves to any degree of accuracy.

Table II.- Optimum reversal times for a type 1 third-order plant

$\omega_n T_1$	$\omega_n T_m$	$\frac{R_0}{KB} \omega_n$	$\zeta$	$\omega_n T_1$	$\omega_n T_m$	$\frac{R_0}{KB} \omega_n$	$\zeta$
0.5	1.742	0.1719	0.1	0.5	1.328	0.06379	1.5
1.0	2.895	.8148		1.0	2.217	.2544	
1.5	3.717	1.704		1.5	2.973	.5252	
.5	1.661	.1475	.25	.5	1.262	.05509	2.0
1.0	2.726	.6662		1.0	2.156	.2014	
1.5	3.484	1.370		1.5	2.946	.4209	
.5	1.556	.1186	.50	.5	1.196	.03078	3.0
1.0	2.536	.5080		1.0	2.094	.1423	
1.5	3.256	1.035		1.5	2.926	.3113	
.5	1.477	.09866	.75	.5	1.130	.009403	5.0
1.0	2.411	.4086		1.0	2.038	.1014	
1.5	3.127	.8325		1.5	2.930	.2102	
1.049	2.401	.3718	1.00				
2.098	3.800	1.192					

As can be noted from figures 37 and 38, the first reversal time and minimum response time decrease for decreasing values of  $\zeta$ . However, for  $\zeta = 0.1$  the curves become quite oscillatory and for certain ranges of step input the optimum times are larger for  $\zeta = 0.1$  than for  $\zeta = 0.25$ . This suggests that for low values of  $\zeta$  a larger number of reversals of the bounded variable may be necessary to obtain the minimum response time for certain ranges of the step input magnitude. For a different treatise on this third-order plant transfer function see Flügge-Lotz and Ishikawa (ref. 15).

3.6.1 Asymptotic solution for very large inputs.- The data presented in figures 37 and 38 were obtained by an iterative procedure on a digital computer. To extend this data to larger values one would need to use this same iterative procedure again unless a short cut is possible. It is the purpose here then to derive the asymptotic solution of equations (75) and (76) which is valid for large inputs. This asymptotic solution is sufficiently accurate for inputs in excess of those values shown in figures 37 and 38 to allow it to be used should an extension of the curves be necessary.

For large inputs one can see from previous arguments that large values of  $T_1$  of figure 36 will be required. As was mentioned with reference to figure 35,  $\dot{c}$  is bounded. As a matter of fact, when  $x$  is equal to  $+B$  and so long as  $\zeta > 0$ ,  $\dot{c}$  will gradually approach  $KB$  and  $\ddot{c}$  will approach zero. With reference to figure 36 it can be recognized that  $T_m - T_1$  and  $T_2 - T_1$  will approach constants as  $T_1 \rightarrow \infty$ .<sup>2</sup> The time required for  $\dot{c}$  to reach its steady-state value (or at least within a few percent of it) can be obtained from the step responses for a second-order system given in figure 39. For example, when  $\zeta = 0.9$ ,  $\dot{c}$  will reach its steady-state value (for all practical purposes) if the first reversal time,  $T_1$ , is greater than  $2\pi/\omega_n$ , that is,  $T_1 > 2\pi/\omega_n$ .

In this example for large inputs  $T_m - T_1$  and  $T_2 - T_1$  approach constants which are a function of the damping ratio and natural frequency. Multiplying equation (76) by  $\omega_n$  and rewriting it in terms of  $T_m - T_1$ ,  $T_2 - T_1$ , and  $T_1$  gives

$$\frac{R_0}{KB} \omega_n = \omega_n T_1 - \omega_n 2(T_2 - T_1) + (T_m - T_1) \omega_n \quad (77)$$

$$= \omega_n T_1 - 2T_1^* + T_2^* \quad (78)$$

<sup>2</sup>See reference 15 for a good visualization of this statement.

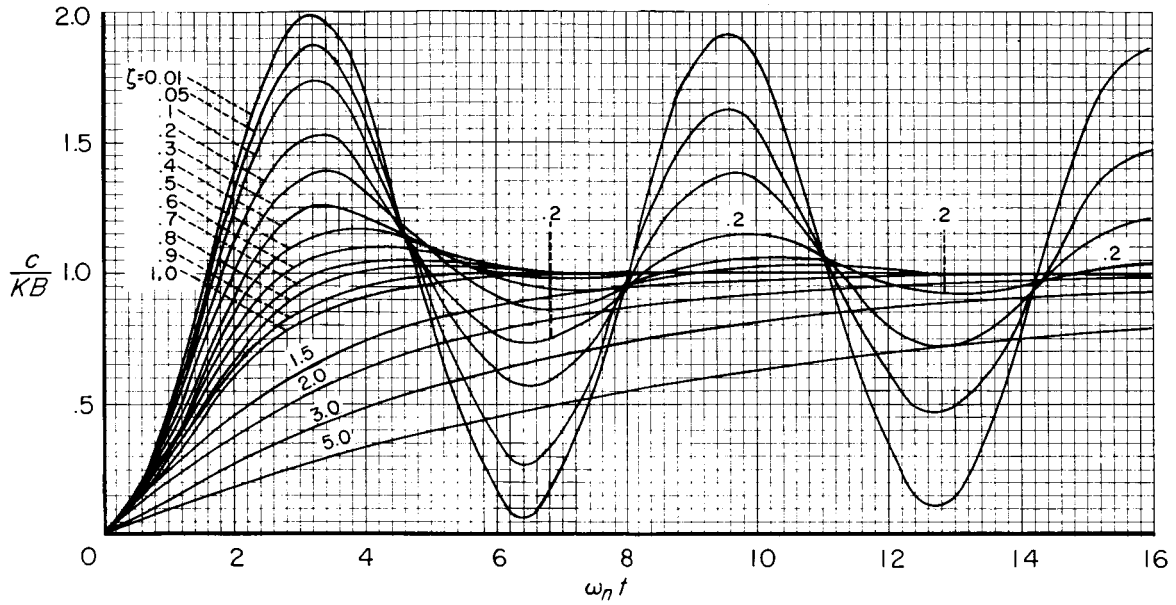


Figure 39.- Step responses of a second-order system.

where  $T_1^* = (T_2 - T_1)\omega_n$  and  $T_2^* = (T_m - T_1)\omega_n$ . To solve for  $T_1^*$  and  $T_2^*$  it is convenient to use a partial fraction expansion of the original system and define state variables  $y_1(t)$ ,  $y_2(t)$ , and  $y_3(t)$  as shown in figure 40.

$$G(s) = \frac{K}{s \left( \frac{s^2}{\omega_n^2} + \frac{2\zeta s}{\omega_n} + 1 \right)} = \frac{K}{s} + \frac{\frac{-K}{\omega_n^2} s}{\frac{s^2}{\omega_n^2} + \frac{2\zeta s}{\omega_n} + 1} + \frac{-K \left( \frac{2\zeta}{\omega_n} \right)}{\frac{s^2}{\omega_n^2} + \frac{2\zeta s}{\omega_n} + 1} \quad (79)$$

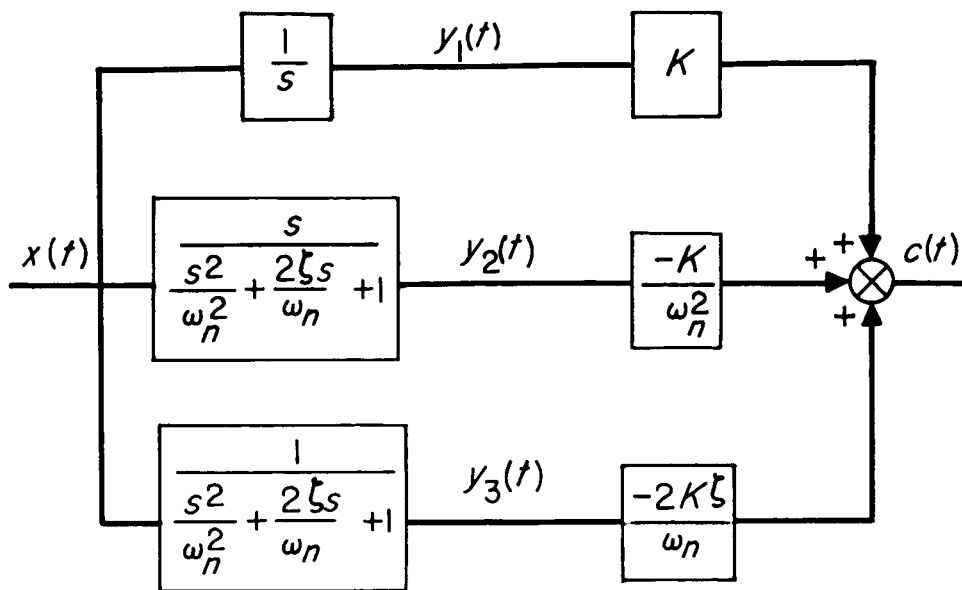


Figure 40.- Block diagram of a type 1 third-order plant.

From figure 40 it can be recognized that if  $T_1$  is large enough, then  $y_2(t) = 0$  at  $T_1$  and must also be zero at  $T_m$ . We can re-define the time axis in terms of  $t - T_1$  and let

$$t - T_1 = t^*$$

$$T_2 - T_1 = t_1^*$$

$$T_m - T_1 = t_2^*$$

Then deriving  $x(t^*)$  and  $L[x(t^*)]$  one can now force  $L[y_2(t^*)]$  to be an entire function since  $y_2(t^*)$  is truncated in the range  $0 < t^* \leq t_2^*$

$$L[y_2(t^*)] = \frac{-2 + 2e^{-st_1^*} - e^{-st_2^*}}{\frac{s^2}{\omega_n^2} + \frac{2\zeta s}{\omega_n} + 1} \quad (80)$$

In terms of the normalized times,  $T_1^* = \omega_n t_1^*$  and  $T_2^* = \omega_n t_2^*$ , the fact that equation (80) must be an entire function gives

$$-2 + 2e^{\left(\zeta \pm \sqrt{\zeta^2 - 1}\right) T_1^*} - e^{\left(\zeta \pm \sqrt{\zeta^2 - 1}\right) T_2^*} = 0 \quad (81)$$

These two equations (81) were solved by trial and error methods for  $T_1^*$  and  $T_2^*$  as a function of  $\zeta$  and the results are plotted in figure 41. One should note that the initial assumptions are invalid for  $\zeta = 0$  and that for  $\zeta = 1$  one must differentiate equation (80) with respect to  $x$  to solve for the transcendental equations. This differentiation is necessary because the two poles of the transfer function are not distinct for  $\zeta = 1$ .

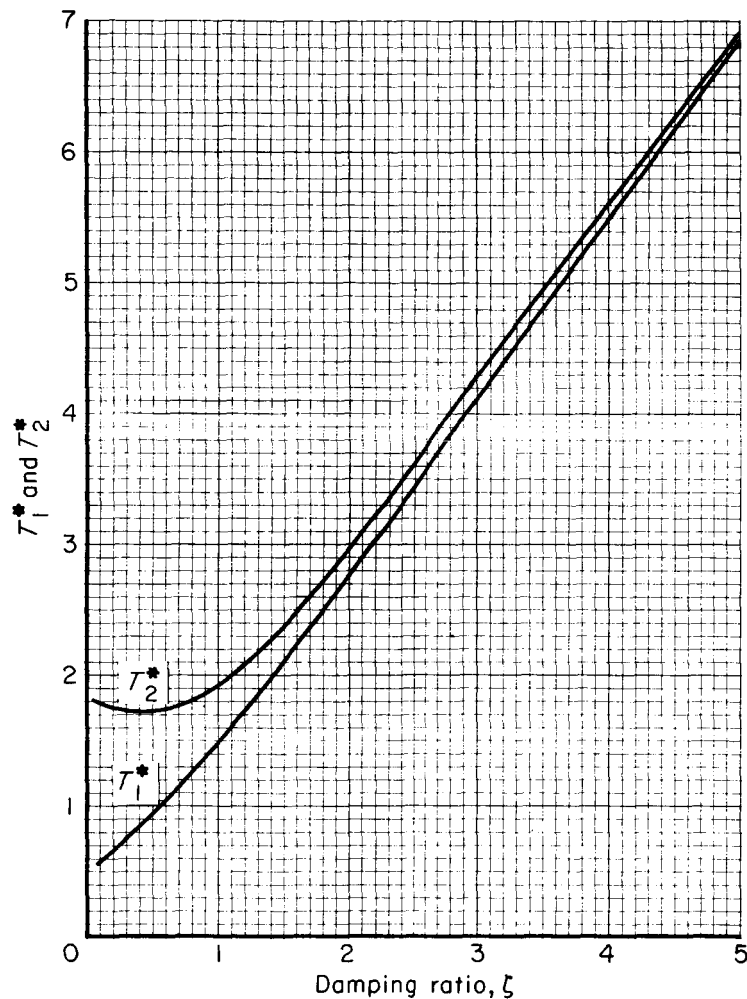


Figure 41.- Normalized data for asymptotic solutions.

One can thus use the results of figure 41 placed in equation (78) to find  $R_0$  vs.  $T_1$  for values of  $R_0$  greater than those given previously.

Since  $\omega_n T_m = \omega_n [T_1 + (T_2^*/\omega_n)]$ , the equation relating  $T_m$  and  $R_o$  is (from eq. (78))

$$\frac{R_o}{KB} \omega_n = \omega_n T_m - 2T_1^* \quad (82)$$

### 3.7 A Type 2 Second-Order Plant

For this example  $G(s) = K/s^2$ . The optimum response curves were derived in chapter II by a simple area integration. One can also obtain them using the entire function concept. Only the results given by equations (83) and (84) and in figure 42 are presented.

$$T_1 = \sqrt{\frac{R_o}{KB}} \quad (83)$$

$$T_m = 2 \sqrt{\frac{R_o}{KB}} \quad (84)$$

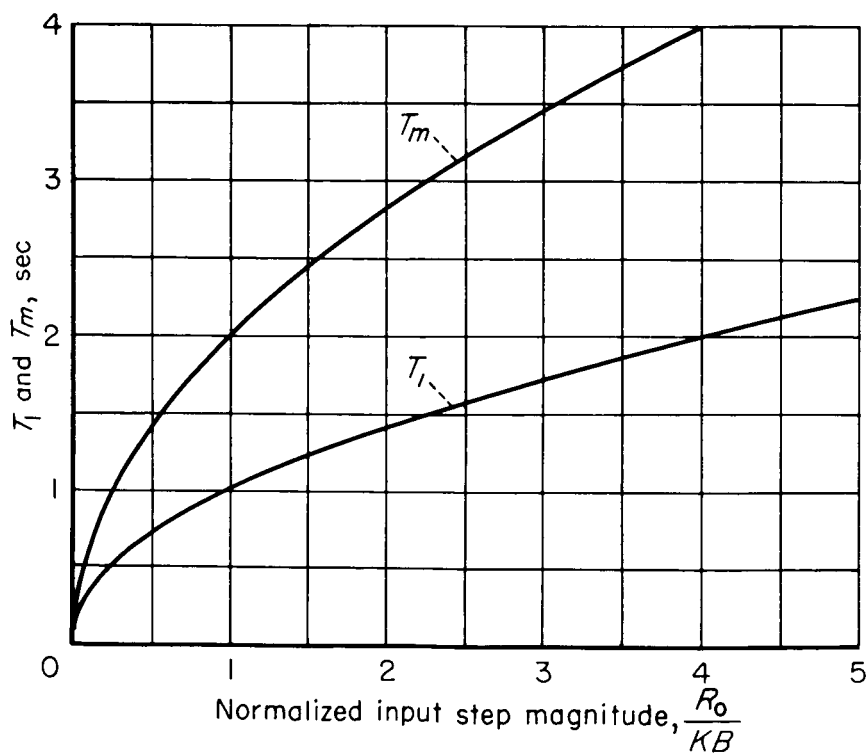


Figure 42.- Optimum switching times for a type 2 second-order plant.

## 3.8 A Type 2 Third-Order Plant

For this example  $G(s) = K(\tau_1 s + 1)/s^2(\tau_2 s + 1)$ . One can determine the optimum motions of  $x(t)$  by arguments similar to those of section 3.5. The two possible motions of  $x(t)$  are shown in figure 43.

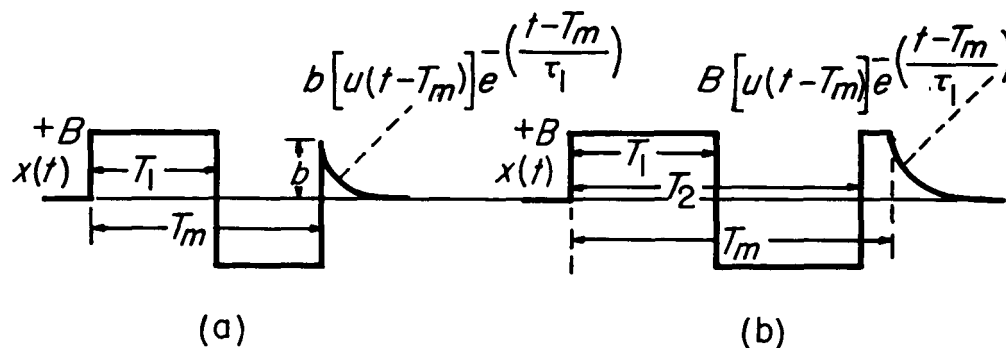


Figure 43.- Optimum motion of the plant input,  $x(t)$ , for a type 2 third-order plant.

The solutions using  $x(t)$  of the form shown in figure 43(a) will be valid so long as  $|b/B| \leq 1$ . For  $b = 0$  the solution will correspond to  $\tau_1 = \tau_2$  which is given in section 3.7. If  $|b/B| > 1$  in this solution, then the results are invalid and one must use the solution obtained for  $x(t)$  of the form shown in figure 43(b).

If  $x(t)$  is as shown in figure 43(a) then

$$x(t) = B \left[ u(t) - 2u(t-T_1) + u(t-T_m) + \frac{b}{B} u(t-T_m) e^{-\left(\frac{t-T_m}{\tau_1}\right)} \right] \quad (85)$$

$$X(s) = B \left[ \frac{1-2e^{-sT_1}+e^{-sT_m}}{s} + \frac{b\tau_1 e^{-sT_m}}{B(\tau_1 s+1)} \right] \quad (86)$$

and  $E(s) = (R_0/s) - X(s) G(s)$  which for this example, after some manipulation, becomes

$$E(s) = \frac{R_0 s^2(\tau_2 s+1) - BK \left[ \left(1-2e^{-sT_1}+e^{-sT_m}\right) (\tau_1 s+1) + (b/B)\tau_1 s e^{-sT_m} \right]}{s^3(\tau_2 s+1)} \quad (87)$$

Since  $E(s)$  must be entire,  $E(s)\big|_{s=0}$  and  $E(s)\big|_{s=-1/\tau_2}$  must be finite. Equations (88), (89), and (90) give the relationship between the parameters which force  $E(s)$  to be an entire function.

$$\left(1 - 2e^{T_1/\tau_2} + e^{T_m/\tau_2}\right) \left(1 - \frac{\tau_1}{\tau_2}\right) - \frac{b}{B} \frac{\tau_1}{\tau_2} e^{T_m/\tau_2} = 0 \quad (88)$$

$$2T_1 - T_m + \frac{b}{B} \tau_1 = 0 \quad (89)$$

$$2\tau_1(2T_1 - T_m) - 2T_1^2 + T_m^2 - 2 \frac{b}{B} \tau_1 T_m = \frac{2R_0}{KB} \quad (90)$$

These equations in their present form are not usable. One can through mathematical manipulations obtain a form suitable for calculation. From equation (88)

$$\frac{b}{B} = \left[ e^{-T_m/\tau_2} - 2e^{(T_1 - T_m)/\tau_2} \right] \left( \frac{\tau_2}{\tau_1} - 1 \right) \quad (91)$$

Solving for  $b/B$  in equation (89) and putting the result in equation (91) gives

$$2T_1 - T_m = \left[ e^{-T_m/\tau_2} - 2e^{(T_1 - T_m)/\tau_2} \right] (\tau_1 - \tau_2) \quad (92)$$

let

$$2T_1 - T_m = t^* \quad (93)$$

then

$$t^* = \left[ e^{(t^* - 2T_1)/\tau_2} - 2e^{(t^* - T_1)/\tau_2} \right] (\tau_1 - \tau_2) + (\tau_1 - \tau_2) \quad (94)$$

One now adds and subtracts a term to allow for the completion of the square

$$t^* = e^{t^*/\tau_2} \left( e^{-2T_1/\tau_2} - 2e^{-T_1/\tau_2} \right) (\tau_1 - \tau_2) + (\tau_1 - \tau_2) \left( 1 - e^{t^*/\tau_2} \right) \quad (95)$$

and changes terms around to give

$$\left(e^{-T_1/\tau_2} - 1\right)^2 = \frac{t^* + (\tau_2 - \tau_1) \left(1 - e^{t^*/\tau_2}\right)}{e^{t^*/\tau_2} (\tau_1 - \tau_2)} \quad (96)$$

or

$$e^{-T_1/\tau_2} = 1 - \sqrt{\frac{\frac{t^*}{\tau_2} + \left(1 - \frac{\tau_1}{\tau_2}\right) \left(1 - e^{t^*/\tau_2}\right)}{e^{t^*/\tau_2} \left(\frac{\tau_1}{\tau_2} - 1\right)}} \quad (97)$$

The negative sign must be used since for positive  $T_1$  the left-hand side of equation (97) is less than unity. Finally

$$\frac{T_1}{\tau_2} = -\ln \left[ 1 - \sqrt{\frac{\frac{t^*}{\tau_2} + \left(1 - \frac{\tau_1}{\tau_2}\right) \left(1 - e^{t^*/\tau_2}\right)}{e^{t^*/\tau_2} \left(\frac{\tau_1}{\tau_2} - 1\right)}} \right] \quad (98)$$

Now reviewing the definition of  $t^*$  (eq. (93)) and comparing with equation (89) shows  $t^* = -(b/B)\tau_1$  or normalizing with respect to  $\tau_2$

$$\frac{t^*}{\tau_2} = -\frac{b}{B} \frac{\tau_1}{\tau_2} \quad (99)$$

Since  $|b/B| \leq 1$ , one can use equation (99) to determine the maximum value of  $t^*/\tau_2$  permissible for any given ratio of  $\tau_1/\tau_2$ . A little further thought and study of figure 43(a) allows one to determine the sign of  $t^*$  as follows:

If  $\tau_1 = \tau_2$ ,  $t^* = 0$  since  $b/B$  must be zero.

If  $\tau_1 > \tau_2$ ,  $b/B$  must be negative  $\therefore t^*$  is positive.

If  $\tau_1 < \tau_2$ ,  $b/B$  must be positive  $\therefore t^*$  is negative.

Equation (90) can be normalized by dividing by  $\tau_2^2$  giving

$$\frac{2R_0}{KB\tau_2^2} = \frac{2\tau_1}{\tau_2} \left( \frac{2T_1}{\tau_2} - \frac{T_m}{\tau_2} \right) - 2 \left( \frac{T_1}{\tau_2} \right)^2 + \left( \frac{T_m}{\tau_2} \right)^2 - 2 \frac{b}{B} \frac{\tau_1}{\tau_2} \frac{T_m}{\tau_2} \quad (100)$$

One can thus compute curves relating normalized  $T_1$  and  $T_m$  versus the normalized input magnitude,  $R_0$ , for various values of the ratio  $\tau_1/\tau_2$ . The procedure is to determine the range of permissible values and the sign of  $t^*/\tau_2$ . Then one sets up a table for  $t^*/\tau_2$  in this range and uses equation (98) to obtain  $T_1/\tau_2$ ;  $T_m/\tau_2$  can be obtained from equation (93). These values are then used in equation (100) to find the normalized  $R_0$ .

Equation (91) shows that so long as  $\tau_2/\tau_1 \leq 2$  then  $|b/B| \leq 1$ . For values of  $\tau_2/\tau_1$  greater than 2 one can use the above solution until  $|b/B| = 1$ , and then one must use the solution for the  $x(t)$  motion given in figure 43(b). This motion is now considered.

If  $x(t)$  is as shown in figure 43(b) then

$$x(t) = B \left[ u(t) - 2u(t-T_1) + 2u(t-T_2) - u(t-T_m) + u(t-T_m)e^{-\left(\frac{t-T_m}{\tau_1}\right)} \right] \quad (101)$$

$$X(s) = B \left( \frac{1-2e^{-sT_1}+2e^{-sT_2}-e^{-sT_m}}{s} + \frac{\tau_1 e^{-sT_m}}{\tau_1 s+1} \right) \quad (102)$$

and  $E(s)$ , after some manipulation, is given by

$$E(s) = \frac{R_0 s^2 (\tau_2 s+1) - KB \left[ \left( 1-2e^{-sT_1}+2e^{-sT_2}-e^{-sT_m} \right) (\tau_1 s+1) + \tau_1 s e^{-sT_m} \right]}{s^3 (\tau_2 s+1)} \quad (103)$$

The relationships between the quantities which make  $E(s)$  an entire function are

$$\frac{2T_1}{\tau_2} - \frac{2T_2}{\tau_2} + \frac{T_m}{\tau_2} + \frac{\tau_1}{\tau_2} = 0 \quad (104)$$

$$-2 \left( \frac{T_1}{\tau_2} \right)^2 + 2 \left( \frac{T_2}{\tau_2} \right)^2 - 2 \left( \frac{\tau_1}{\tau_2} \right)^2 - \left( \frac{T_m}{\tau_2} \right)^2 - 2 \frac{\tau_1}{\tau_2} \frac{T_m}{\tau_2} = \frac{2R_0}{KB\tau_2^2} \quad (105)$$

$$\left(1 - 2e^{T_1/\tau_2} + 2e^{T_2/\tau_2}\right) \left(1 - \frac{\tau_1}{\tau_2}\right) - e^{T_m/\tau_2} = 0 \quad (106)$$

One can eliminate  $T_m$  from equations (104) and (106) and after certain manipulations obtain the following:

$$\frac{T_2}{\tau_2} = \left(\frac{2T_1}{\tau_2} + \frac{\tau_1}{\tau_2}\right) + \ln \left[ \left(1 - \frac{\tau_1}{\tau_2}\right) + \sqrt{\left(1 - \frac{\tau_1}{\tau_2}\right)^2 + \left(1 - 2e^{\frac{T_1}{\tau_2}}\right) \left(1 - \frac{\tau_1}{\tau_2}\right) e^{-\left(\frac{2T_1}{\tau_2} + \frac{\tau_1}{\tau_2}\right)}} \right] \quad (107)$$

One computes the results by first assuming  $T_1/\tau_2$  and then solving equation (107) for  $T_2/\tau_2$ . One then uses equation (104) to obtain  $T_m/\tau_2$  and equation (105) to obtain  $R_0/KB\tau_2^2$ . One should note again that these results are only for  $\tau_2/\tau_1 > 2$  and represent only part of the solution. They must be pieced together with the previous solution given by equations (93), (98), (99), and (100).

The optimum first reversal time,  $T_1$ , and minimum response time,  $T_m$ , versus the input step magnitude,  $R_0$ , are given in normalized form in figures 44 and 45. As can be noted from figure 45, a considerable reduction in response time is possible if the zero is closer to the origin than to the pole, that is, if  $\tau_1/\tau_2 > 1$ .

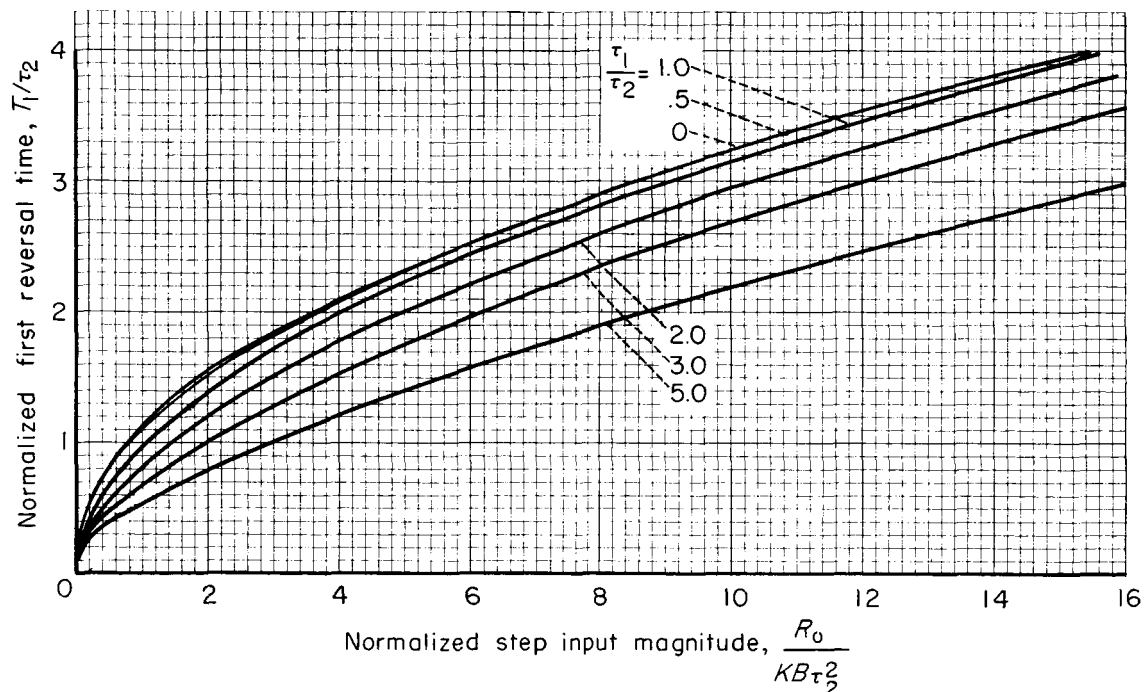


Figure 44.- Optimum first reversal time for a type 2 third-order plant.

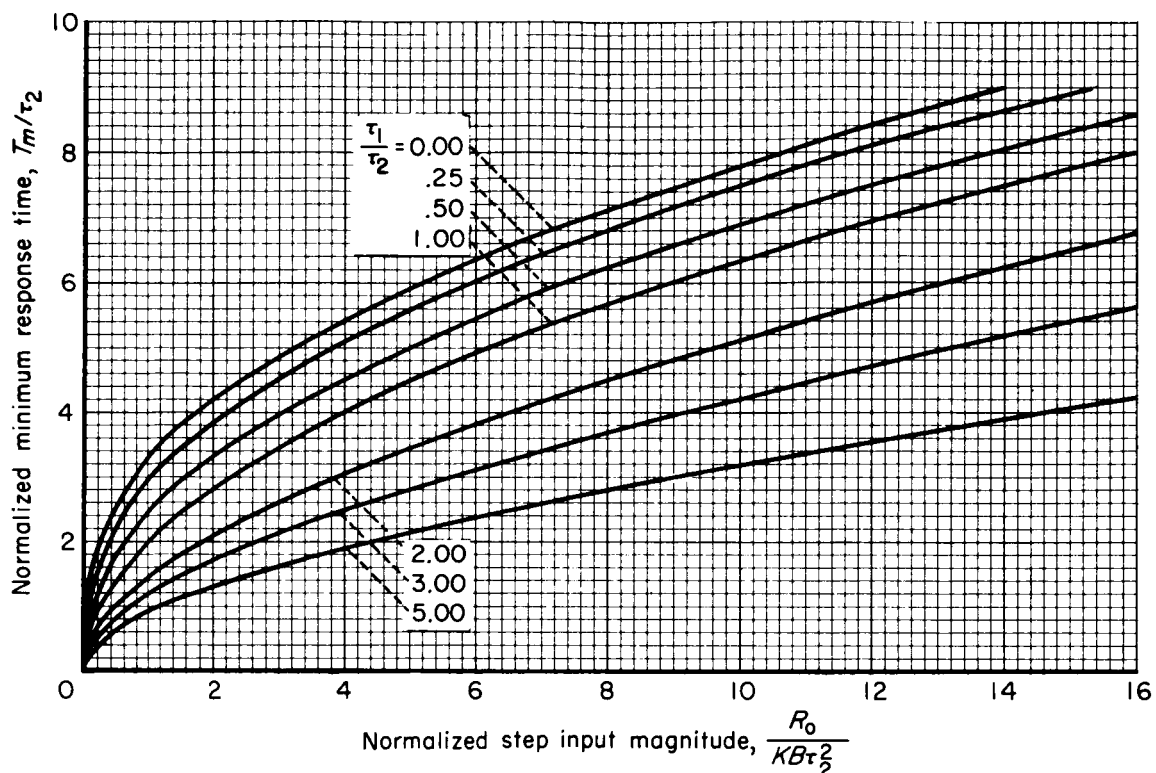


Figure 45.- Minimum response time for a type 2 third-order plant.

### 3.9 A Type 2 Fourth-Order Plant

For this example

$$G(s) = \frac{K}{s^2 \left( \frac{s^2}{\omega_n^2} + \frac{2\zeta s}{\omega_n} + 1 \right)}$$

According to the theorem of reference 4 and arguments following lines presented previously (see sec. 3.6)  $x(t)$  will have three reversals. The general motion is given by

$$x(t) = B[u(t) - 2u(t-T_1) + 2u(t-T_2) - 2u(t-T_3) + u(t-T_m)] \quad (108)$$

The same procedure can be followed through as was done in previous examples, and in order that  $E(s)$  be entire, the following equations must be satisfied

$$1 - 2e^{\omega_n \left( \zeta \pm \sqrt{\zeta^2 - 1} \right) T_1} + 2e^{\omega_n \left( \zeta \pm \sqrt{\zeta^2 - 1} \right) T_2} - 2e^{\omega_n \left( \zeta \pm \sqrt{\zeta^2 - 1} \right) T_3} + e^{\omega_n \left( \zeta \pm \sqrt{\zeta^2 - 1} \right) T_m} = 0 \quad (109)$$

$$2T_1 - 2T_2 + 2T_3 - T_m = 0 \quad (110)$$

$$-2T_1^2 + 2T_2^2 - 2T_3^2 + T_m^2 = \frac{2R_0}{KB} \quad (111)$$

As was the case for the type 1 third-order plant (section 3.6) an iterative procedure must be used to solve these equations. The equations are best normalized by obtaining solutions for  $\omega_n T_1$  and  $\omega_n T_m$  as functions of  $R_0 \omega_n^2 / KB$  for various values of the damping ratio  $\zeta$ . The solution as obtained by a digital computer is plotted in figures 46 and 47. Table III also gives some of the values near the origins where the curves are difficult to read with any accuracy.

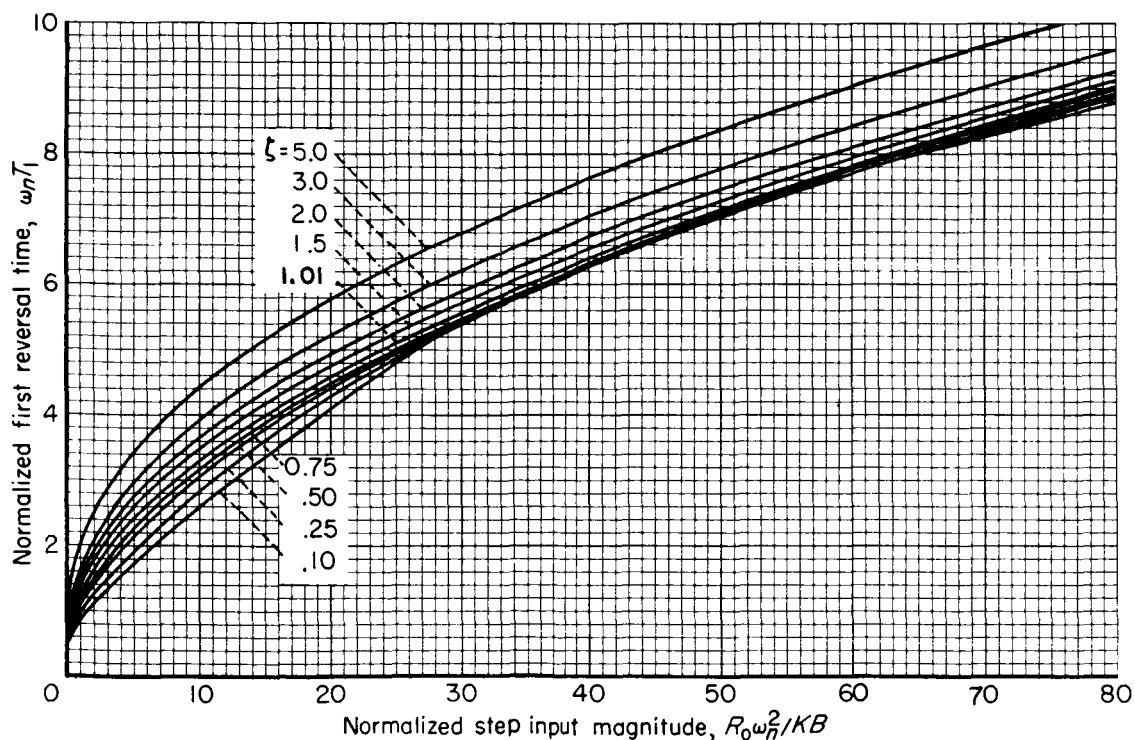


Figure 46.- Optimum first reversal time for a type 2 fourth-order plant.

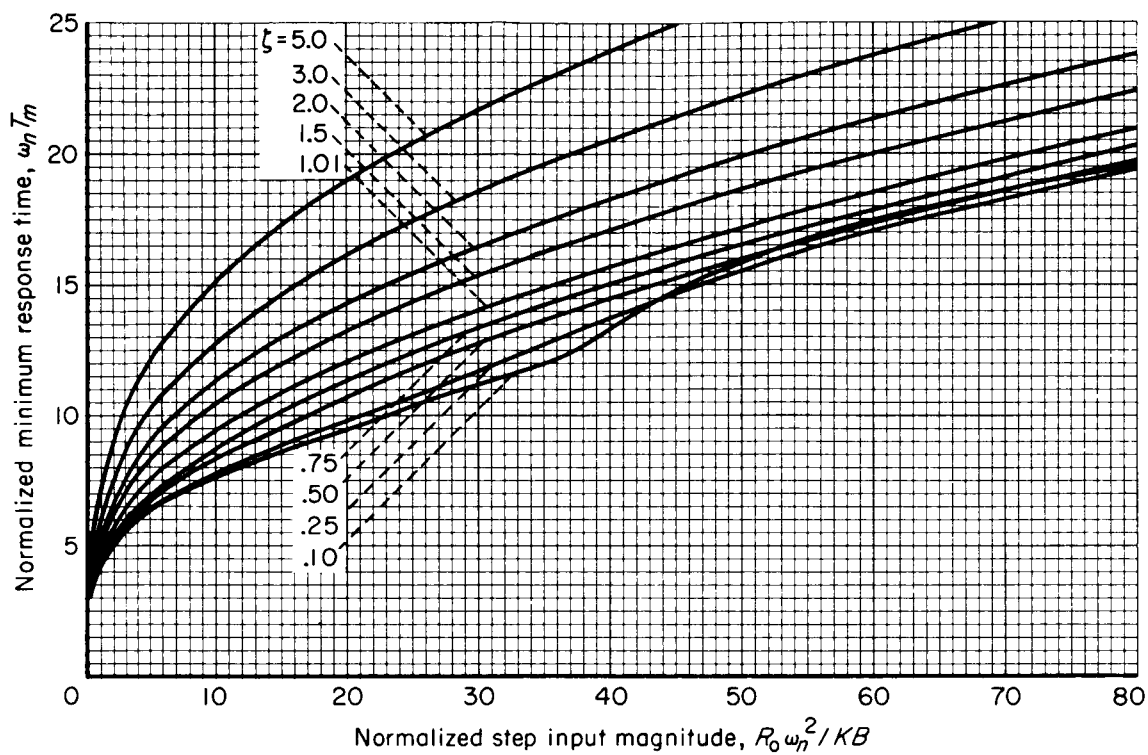


Figure 47.- Minimum response time for a type 2 fourth-order plant.

Table III.- Optimum reversal times for a type 2 fourth-order plant

$\omega_n T_1$	$\omega_n T_m$	$R_o \frac{\omega_n^2}{KB}$	$\zeta$	$\omega_n T_1$	$\omega_n T_m$	$R_o \frac{\omega_n^2}{KB}$	$\zeta$
0.5	2.931	0.2050	0.1	0.5	2.355	0.0606	1.5
1.0	4.724	1.504		1.0	4.022	.4570	
1.5	5.891	3.764		1.5	5.487	1.325	
				2.0	6.836	2.714	
.5	2.802	.1702	.25	.5	2.285	.0443	2.0
1.0	4.512	1.209		1.0	3.986	.3690	
1.5	5.660	3.057		1.5	5.526	1.1165	
				2.0	6.990	2.315	
.5	2.660	.1319	.50	.5	2.252	.0022	3.0
1.0	4.285	.9122		1.0	4.014	.2248	
1.5	5.475	2.369		1.5	5.656	.8066	
2.0	6.454	4.382		2.0	7.252	1.746	
.5	2.569	.1024	.75				5.0
1.0	4.211	.7183		1.5	5.880	.3702	
1.5	5.371	2.002		2.0	7.550	1.101	
2.0	6.381	3.812		2.5	9.240	2.054	
.5	2.425	.0923	1.01				
1.0	4.073	.6130					
1.5	5.426	1.6816					
2.0	6.639	3.303					

As was the case for the type 1 third-order example, the data presented in figures 46 and 47 indicate that a larger number of reversals may be required in order to obtain the optimum response for low values of  $\zeta$ . This is hypothesized since the minimum response time and first reversal time for  $\zeta = 0.1$  is larger than for  $\zeta = 0.25$  for certain ranges of input step magnitude.

An asymptotic solution for large inputs is also possible for this example in quite the same manner as was done for the type 1, third-order problem. This solution is now considered.

3.9.1 Asymptotic solution for a type 2 fourth-order plant.- The fourth-order plant can be visualized as shown in figure 48. From this

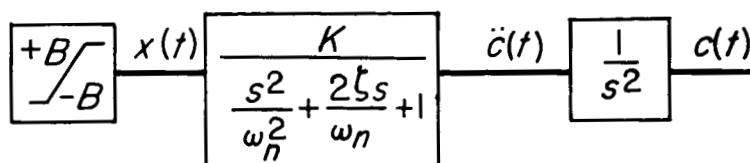


Figure 48.- Block diagram of a type 2 fourth-order plant.

diagram it can readily be seen that with  $x$  at its bounded value,  $\ddot{c}$  will approach a steady-state value of  $KB$  for  $\zeta > 0$ . This example then is practically identical to the previous one. The optimum switching will be as shown in figure 49. It thus can be seen that if we define

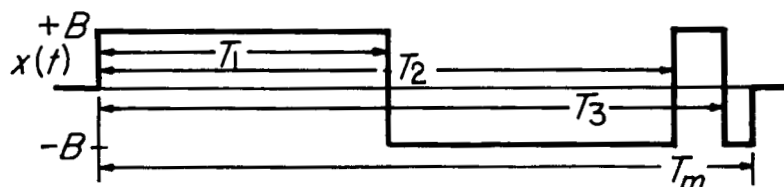


Figure 49.- Optimum motion of the plant input,  $x(t)$ , for a type 2 fourth-order plant.

$(T_3 - T_2)\omega_n = T_1^*$  and  $\omega_n(T_m - T_2) = T_2^*$  then the results of the previous solution given in section 3.6.1 can be used in the asymptotic solution for this example.

The results are valid for  $T_2$  long enough so that  $\ddot{c}$  is very close to the steady-state value (i.e.,  $\ddot{c} \approx 0$ ). Combining equation (110) with equation (111) and using the above definitions of  $T_1^*$  and  $T_2^*$  after certain manipulations gives

$$\omega_n T_1 = \sqrt{\frac{R_0}{KB} \omega_n^2 + 3T_1^{*2} - 2T_1^* T_2^*} \quad (112)$$

$$\omega_n T_m = 2T_1^* + 2 \sqrt{3T_1^{*2} + \frac{R_0}{KB} \omega_n^2 - 2T_1^* T_2^*} \quad (113)$$

Equations (112) and (113) are sufficiently accurate to allow the extension of the curves of figures 46 and 47 to larger values of  $R_0 \omega_n^2 / KB$  for  $\zeta \leq 2$ ;  $T_1^*$  and  $T_2^*$  in equations (112) and (113) are obtained from figure 41. For  $\zeta > 2$  one can obtain an accurate extension of the curves by factoring the second-order equation  $(s^2/\omega_n^2) + (2\zeta s/\omega_n) + 1$  of the denominator of  $G(s)$  into an equation of form  $(s\tau_1 + 1)(s\tau_2 + 1)$ . The smaller of the two time constants is assumed zero and  $G(s)$  is approximated by  $G(s) \approx K/s^2(s\tau + 1)$ . This allows one to use the data for a type 2 third-order system presented in figures 44 and 45.

### 3.10 A Type 3 Third-Order Plant

For this case use of the theorem of reference 4 and previous arguments gives

$$x(t) = B[u(t) - 2u(t-T_1) + 2u(t-T_2) - u(t-T_m)]$$

The solution of the equations which must be satisfied in order that  $E(s)$  be entire are

$$T_1 = \left( \frac{R_0}{2KB} \right)^{1/3} \quad (114)$$

$$T_m = \left( \frac{32R_0}{KB} \right)^{1/3} \quad (115)$$

These results are plotted in figure 50.

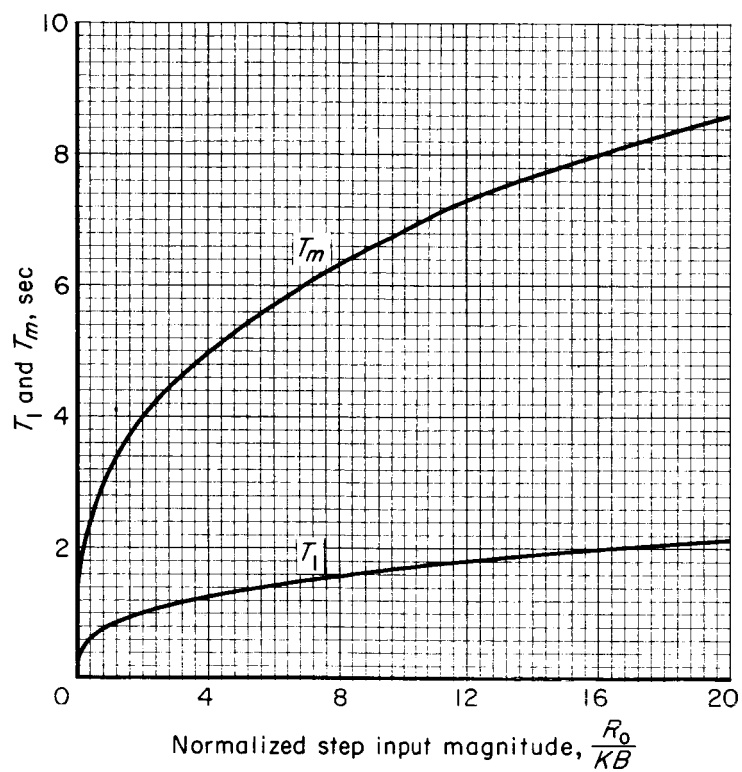


Figure 50.- Optimum switching times for a type 3 third-order plant.

#### IV. EXAMPLES OF SATURATED CONTROL SYSTEMS

##### 4.1 Introduction

It is the purpose of this chapter to apply the methods proposed in chapter II to examples of control systems. The validity of the procedure has already been shown for second-order plants, so consequently we shall use third-order plants. In addition, the examples chosen are for two different types of third-order plants, namely, type 1 and type 2.

For reasons of the author's familiarity with the subject, both examples are aircraft autopilots. As can be found by appropriate linearization of the rigid body equations of motion for an aircraft (ref. 16), a rate-limited control-surface servo in a bank-angle autopilot is equivalent to saturation on the input to a type 2 third-order plant. Similarly, a rate-limited control-surface servo in a normal acceleration autopilot provides a type 1 third-order plant. Control-surface position limiting, which also must exist, will be neglected in this study.

For reasons of simplicity, the aerodynamics used will be identical to those in two previous reports. The aerodynamics for the bank-angle autopilot are the same as those of reference 5 (F-86 at a representative flight condition). The aerodynamics for the normal acceleration autopilot are the same as those of reference 8 (F-100 at a representative flight condition).

The purpose of choosing these examples is to allow some practical significance to be attached to the numerical results. The examples are chosen for illustrative purposes, however, and no claims are made regarding the suitability of these designs for their respective aircraft.

##### 4.2 A Sampled-Data Bank-Angle Autopilot (Feedback Design)<sup>1</sup>

Reference 5 showed a continuous bank-angle autopilot in which a nonlinear error function was designed to compensate for a limit on the control-surface velocity. It was shown there that a linear error gain resulted in an unstable system for large step inputs. The method used to design the nonlinear error function to give a good response for large inputs was essentially the same as the method described in chapter II.

In this section we shall design a sampled-data bank-angle autopilot whose linear behavior is determined by the dominant mode of the continuous system of reference 5. The design will use output velocity feedback for stabilizing purposes. In the next section we shall design an autopilot in which the digital computer is used to obtain the stabilizing quantity.

---

<sup>1</sup>Feedback will hereafter be abbreviated as FB.

These two designs will illustrate two different sampled-data systems and the usefulness of the techniques of chapter II for analyzing both, as well as for synthesizing nonlinear functions for both.

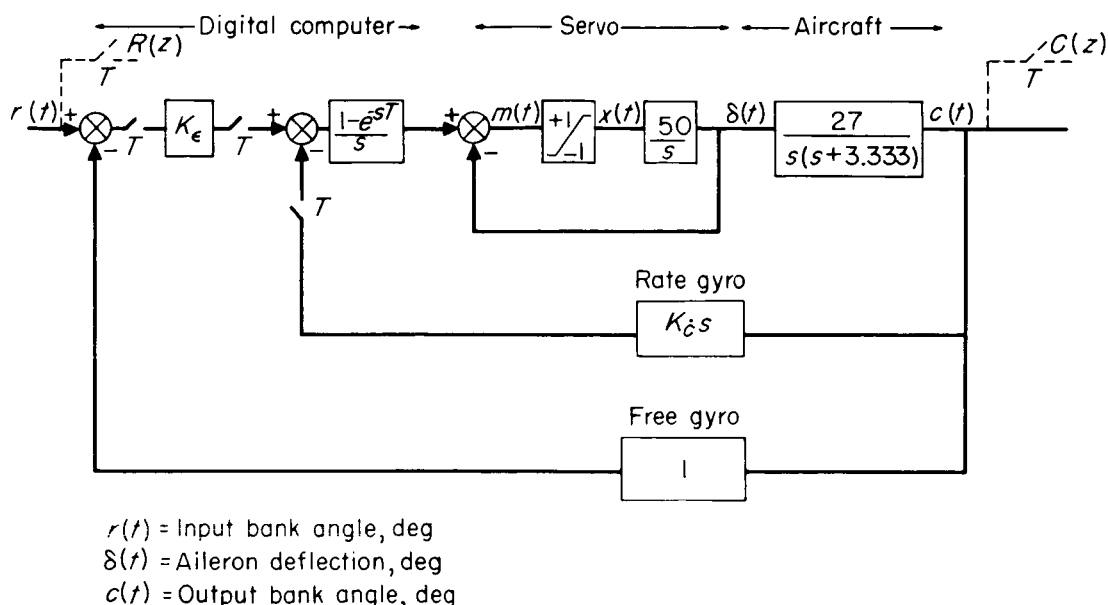


Figure 51.- Block diagram of a sampled-data bank-angle autopilot; FB design.

Consider the block diagram of the autopilot shown in figure 51. The symbols are defined on the figure. The limiter in this case has unity gain and a limit level of  $\pm 1$  which corresponds to a maximum aileron rate,  $\dot{\delta}_{\max}$ , of  $50^\circ$  per second.

This system differs from figure 1(b) since both continuous and sampled feedbacks are used around the limiter. The continuous feedback here is the control-surface deflection. The sampled feedbacks are the sum of the outputs of roll-rate and roll-position gyros.

Prior to considering any nonlinear characteristics of this system, it is necessary to establish a linear design. For this purpose we shall design the sampled-data system to have the same dominant mode as the continuous system given in reference 5. In reference 5 the gains were chosen in order to obtain a good transient response. This results in a transfer function,  $C(s)/R(s)$ , given by equation (116).

$$\frac{C(s)}{R(s)} = \frac{1}{(1 + 0.0271s) \left[ \frac{s^2}{(11.04)^2} + \frac{2(0.744)}{11.04} s + 1 \right]} \quad (116)$$

Equation (116) shows the dominant second-order mode characteristics to be  $\omega_n = 11.04$ ,  $\zeta = 0.744$ .

The next item which must be chosen is the sampling period,  $T$ . Experience has shown that if the sampling frequency is at least 10 times the dominant-mode frequency, no difficulties are involved in designing the sampled-data system. For this reason, the sampling period is chosen as  $T = 0.05$ , which gives a sampling frequency of 20 cycles per second.

One can now transfer the dominant mode from the  $s$  plane to the  $z$  plane and establish positions of desired modes (in the  $z$  plane) of the pulse transfer function,  $C(z)/R(z)$ .

These are, after factoring the second-order equation,

$$z = 0.6186 \pm 0.2391i \quad (117)$$

With reference to figure 51, one can derive the characteristic equation of the pulse transfer function,  $C(z)/R(z)$

$$1 + Z \left[ \left( \frac{1 - e^{-sT}}{s} \right) \left( \frac{1}{1 + 0.02s} \right) \left( \frac{27}{s(s + 3.333)} \right) (K_e + K_c s) \right] \quad (118)$$

Since the system is third order (see fig. 51), this characteristic equation must also be third order because no poles are added by the digital computer pulse transfer function in this example. The desired characteristic equation is obtained by expressing the desired dominate modes of equation (117) in polynomial form and multiplying by a second first-order factor as given in equation (119).

$$(1 - 1.237z^{-1} + 0.4398z^{-2})(c_0 + c_1z^{-1}) \quad (119)$$

Now  $c_0$ ,  $c_1$ ,  $K_e$ , and  $K_c$  are all undetermined coefficients. To find their values, one must carry through the process of equating equal powers of  $z^{-1}$  between equations (118) and (119). The details are not given here but the results are

$$\left. \begin{aligned} K_e &= 2.158 \\ K_c &= 0.3302 \\ c_1/c_0 &= -0.392 \end{aligned} \right\} \quad (120)$$

Only the ratio of  $c_1/c_0$  is specified here since  $c_0$  really affects the gain and has no bearing on choosing the roots of the characteristic equation.

Reference to equation (119) shows all the roots of the characteristic equation to be inside the unit circle in the  $z$  plane. If the magnitude of  $c_1/c_0$  had been greater than unity, one would find that it would be necessary to repeat the process using a higher sampling frequency or some other lower frequency dominant mode.

The linear design is now completed. We shall now use the methods of chapter II and data of chapter III to analyze the system for step inputs.

First, with reference to figure 51, it can be seen that we are dealing with a type 2 third-order plant; that is, the transfer function relating the saturated quantity,  $x(t)$ , to the output,  $c(t)$ , is given by

$$\frac{C(s)}{X(s)} = \frac{(50)(27)}{s^2(s + 3.333)} = \frac{405}{s^2(0.3s + 1)} \quad (121)$$

Application of rule II of chapter II shows that we can expect the response to become more oscillatory as the input step to the system is increased. We do not know whether the system is unstable or not as the limiter gain is reduced and for this purpose a loci of pole positions as a function of limiter gain has been computed. This is shown in figure 52 where it can be seen that the system is unstable for low values of limiter gain.

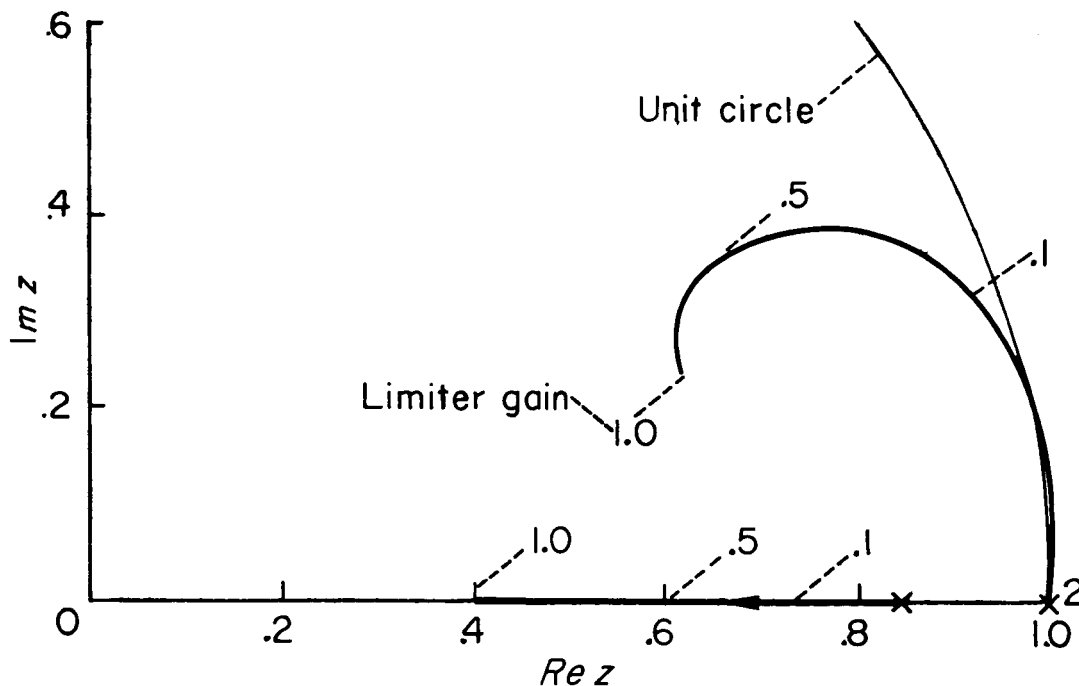


Figure 52.- Pole position loci as a function of the limiter gain; FB design.

A note should be added that one cannot use conventional root-locus procedures to determine the loci of pole positions in the  $z$  plane. This is a result of the continuous feedback around the limiter of figure 51 which causes the zeros as well as the poles to shift as a function of the limiter gain. To obtain the pole position plot it is necessary to compute the roots of the denominator of  $C(z)/R(z)$  which is not a simple computational process.

It is necessary to determine the size of the inputs which cause this oscillatory performance to exist. This will be done using the switch time analysis method explained in chapter II. If the step input magnitude which causes poor performance is out of the range of practical interest, then no nonlinearities are required. If, however, they are within the range of practical interest, we shall have to design a nonlinear function. For this example, it is probable that step inputs from  $0^\circ$  to  $90^\circ$  should be considered as the practical range.

The optimum first reversal time and minimum response time are given for this example in figures 44 and 45 of chapter III. To use these data, it is necessary to obtain the time constants and gain for the plant which are given in equation (121). The limit level,  $B$ , is unity as can be seen by inspection of figure 51. The optimum first reversal time and minimum response time can thus be determined.

The next step is to determine the actual first reversal time as a function of the input step size,  $R_0$ . It may be noted from figure 51 that if  $R_0 > 1/K_\epsilon \approx 0.5^\circ$  and  $\delta(0) = \dot{c}(0) = c(0) = 0$ , saturation will occur. Thus, we shall only be concerned with step inputs greater than approximately  $0.5^\circ$ . What is desired is an expression for  $m(t)$  of figure 51 for a unit step of  $x(t)$ . This expression can be derived directly from figure 51 and is given in equation (122). The symbol,  $n$ , is an integer which is equal to zero at the first sampling instant after the step is applied. The time origin,  $t = 0$ , also starts at this same instant.

$$\begin{aligned}
 m(t) &= K_\epsilon R_0 u(t) - \delta(t) - K_\delta \dot{c}(nT) - K_\epsilon c(nT) \\
 &= K_\epsilon R_0 u(t) - L^{-1} \left( \frac{50}{s^2} \right) - K_\delta L^{-1} \left[ \frac{(50)(27)}{s^2(s+3.333)} \right] \Big|_{t=nT} - K_\epsilon L^{-1} \left[ \frac{(50)(27)}{s^3(s+3.333)} \right] \Big|_{t=nT}
 \end{aligned} \tag{122}$$

After putting in the values for  $K_\delta$ ,  $K_\epsilon$ , and  $T$ , and carrying through the inverse Laplace transforms indicated in equation (122), the result is

$$m(t) = 2.158 R_0 u(t) - 50t - 873.92 \frac{(0.05n)^2}{2} + 128.38(0.05n) - 38.51 + 38.51e^{-0.1667n} \tag{123}$$

The relationship between  $t$  and  $n$  is as follows:

$$\left. \begin{array}{ll} 0 \leq t < 0.05 & n = 0 \\ 0.05 \leq t < 0.1 & n = 1 \\ 0.1 \leq t < 0.15 & n = 2 \\ \text{etc.} \end{array} \right\} \quad (124)$$

The continuous signal of  $m(t)$  which is a result of control-surface deflection feedback makes the first reversal time continuous rather than staircase as was the example carried through in chapter II. For computing purposes, however, it is much simpler to consider only  $m(0.05n)$  and determine the staircase curve relating  $R_0$  to  $T_1$ . The results as will be shown later are not particularly affected by this simplification.

To find  $R_0$  for a particular value of  $n$  (or  $T_1$ ), one sets  $m = -1$  in equation (123) to find the right-hand side of the curve given in figure 53. The left-hand side of the curve for the  $n + 1$  value of  $T_1$  is found by setting  $m = 1$  in equation (123) and finding  $R_0$  to satisfy the equation. Dotted lines are drawn between these two values of  $R_0$  in figure 53. One thus proceeds "walking up the staircase," taking as high a value of  $n$  as is required to cover the range of interest of  $R_0$ .

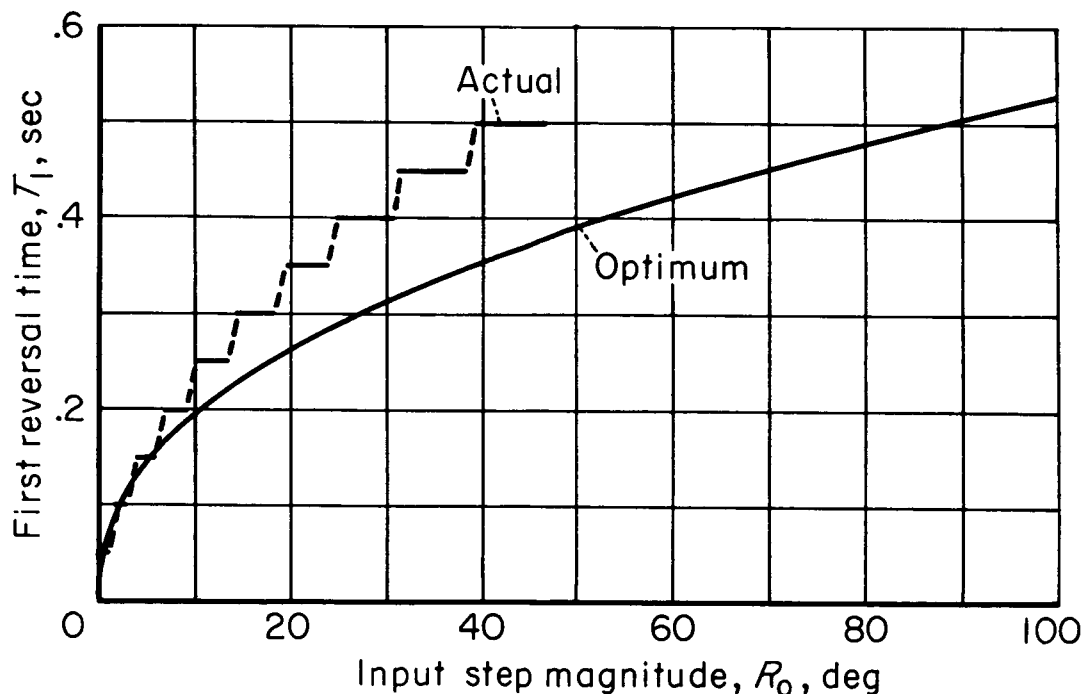


Figure 53.- First reversal times for a sampled-data bank-angle autopilot; FB design.

Inspection of figure 53 shows that overshoot due to limiting can be expected for step inputs greater than about  $5^\circ$ . This hypothesis is verified by the analog computer responses of the system shown in figure 54.

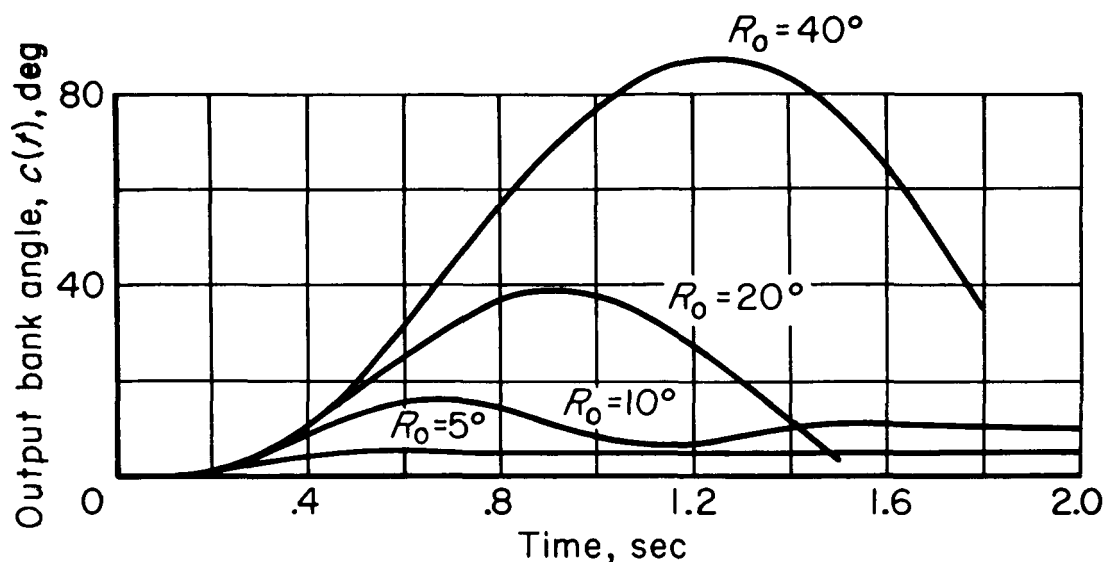


Figure 54.- Step responses of a sampled-data bank-angle autopilot; FB design.

One item of importance which can be seen by comparing figures 53 and 54 is the accuracy with which one can compute the first overshoot using the data of figure 53. For step inputs of  $40^\circ$ ,  $20^\circ$ , and  $10^\circ$ , the curves of figure 53 indicate the overshoot to be  $88^\circ$ ,  $39^\circ$ , and  $17^\circ$ , respectively. The overshoots shown in figure 54 are in good agreement with these values. As was mentioned in chapter II, the first overshoot is obtained by projecting the first reversal time from the actual curve, for a given step input, to the optimum curve.

Perhaps, practically speaking, it is unnecessary to compute response times for this system since its response is so poor one would surely want to design a nonlinear function to improve the characteristics. To give the reader some confidence in the method described in chapter II, however, this computation is compared with the data measured from analog computer results and the minimum curve (obtained from chapter III) in figure 55. The measured data are the time for the error to be within 10 percent of the step input amplitude for errors less than  $10^\circ$  and for the error to be less than  $1^\circ$  for inputs greater than  $10^\circ$ . The calculated curve was obtained (for large inputs) by use of the method explained in chapter II, with the exception that a continuous curve was faired through the middle of the staircase curve given in figure 53. The dotted portion of the curve was computed by taking the value of time when the envelope of the damped

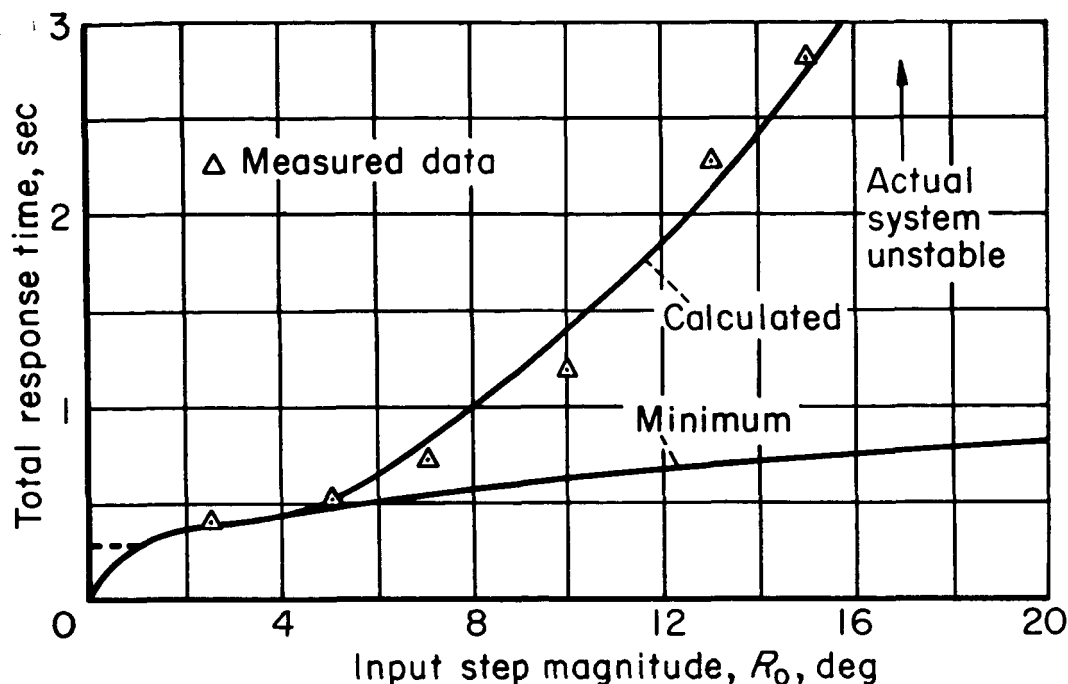


Figure 55.- Calculated, measured, and minimum response times for the sampled-data bank-angle autopilot; FB design.

sine wave (obtained by taking the inverse of eq. (116) for a step input) was 10 percent of the input step magnitude. Although this is a sampled-data system, rather than a continuous system, previous work (ref. 8) has shown that the sampled-data-system response will be very close to the response of the continuous system from which it is derived if the sampling frequency is high compared to the dominant mode frequency.

The calculated curve is seen to be in reasonable agreement with the measured data.

The computation of a nonlinear compensation function follows the method outlined in chapter II. The first step is to obtain a staircase approximation to the optimum first reversal curve. The approximation used here is shown in figure 56. This gives the input as a function of the first reversal time for use in equation (122). One then solves equation (122) for  $K_e \epsilon(T_1)$ .

$$K_e \epsilon(T_1) = K_e [R_0(T_1) - c(T_1)] = \delta(T_1) + K_d \dot{c}(T_1) + m(T_1) \quad (125)$$

In this equation  $m(T_1)$  is taken as zero and  $K_c$  is taken as a constant, 0.3302. One solves for  $K_e \epsilon(T_1)$  for various values of  $T_1$ ;  $R_O(T_1)$  is obtained from the staircase curve of figure 56.

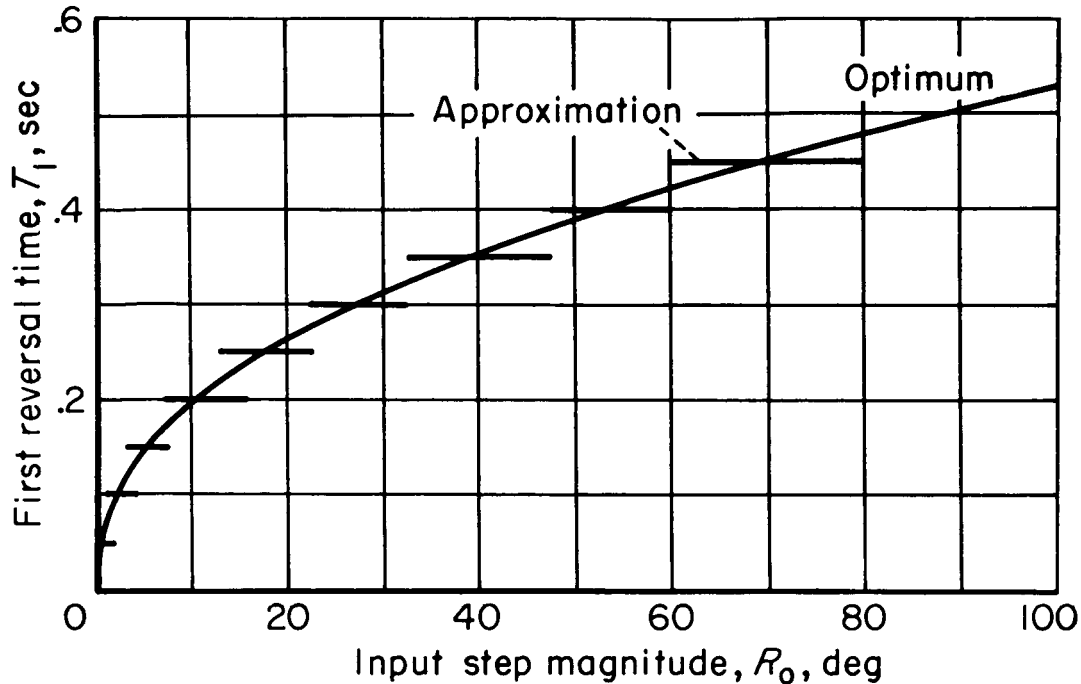


Figure 56.- Staircase approximation to the optimum first reversal curve.

Since

$$\epsilon(T_1) = R_O(T_1) - c(T_1) \quad (126)$$

the results can be plotted as a function of the error. The computed curve is shown in figure 57.

For the modified system, the digital computer operations are

- (1) Take the sampled error signal and from this compute the value of  $K_e(\epsilon)\epsilon$  given in figure 57.
- (2) Subtract  $K_c \dot{c}(nT)$  from the result obtained in step (1).
- (3) Feed the stored result (hold circuit) to the control-surface servo input.
- (4) Go back to step (1) at the next sampling instant.

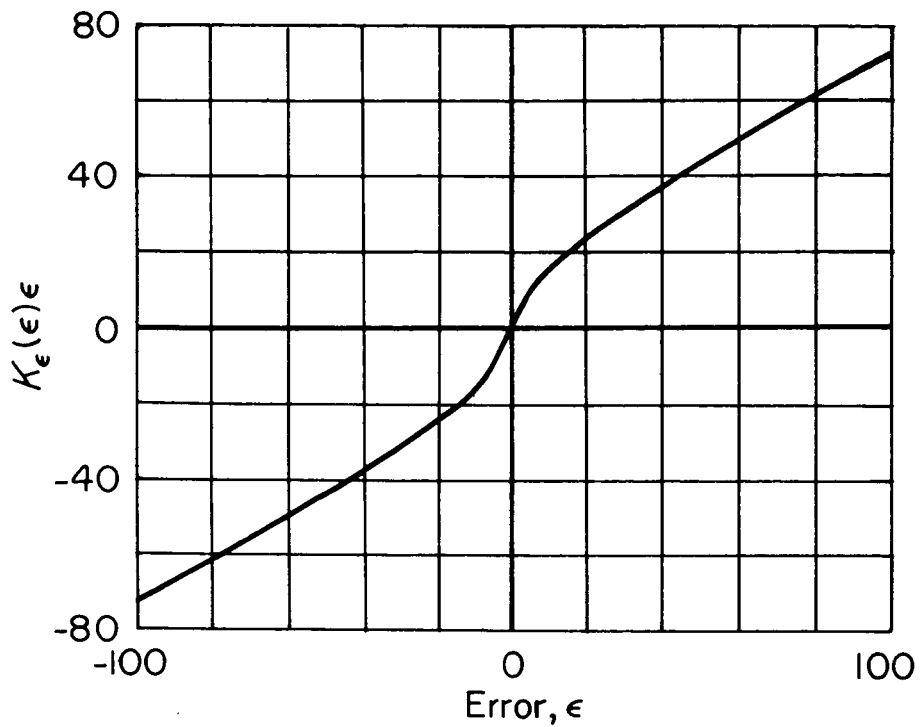


Figure 57.- Nonlinear function used to modify the sampled-data bank-angle autopilot; FB design.

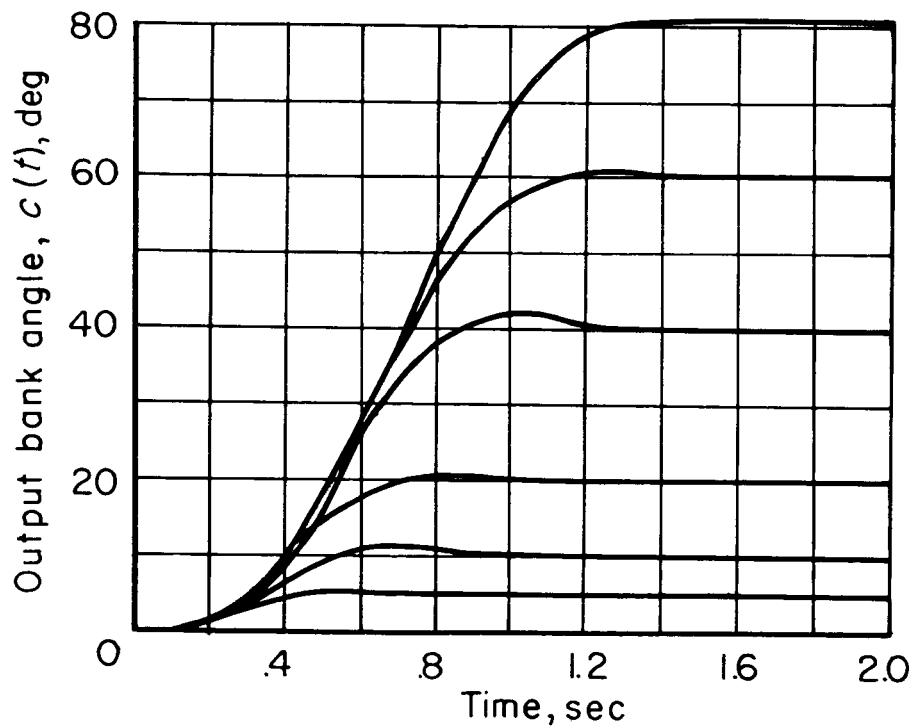


Figure 58.- Step responses of the modified sampled-data bank-angle autopilot; FB design

The results of an analog computer simulation of these operations are shown in figure 58. As can be recognized, the response is very well damped, corresponding closely to the optimum as can be seen by comparing the response times of the step responses of figure 58 with the minimum shown in figure 55.

A note should be added that this system does not obey the limitations imposed in chapter II since there is more than one zero in the expression  $G(s) H(s)$ . Probably because this system is dominant second order for all values of the limiter gain, as can be seen in figure 52, we obtain good results by using only one nonlinear function. No further consideration of this subject is deemed necessary here because of these good results. This will also be the case in the example considered in the next section.

#### 4.3 A Sampled-Data Bank-Angle Autopilot, $D(z)$ Design

The block diagram of this example is shown in figure 59. As can be seen by comparing the figures 59 and 51, this example differs from the previous one by having a more complicated digital computer pulse transfer function which allows one to eliminate the rate-gyro feedback.

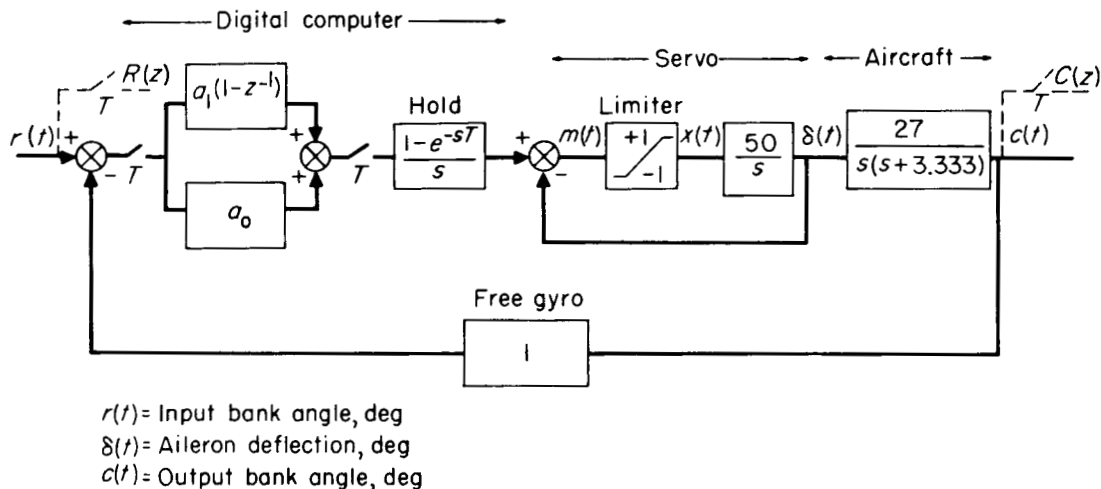


Figure 59.- Block diagram of a sampled-data bank-angle autopilot;  $D(z)$  design.

With this choice of  $D(z)$  and the manner of computation indicated, one can obtain an analogy to error plus error rate which is used so often for stabilizing continuous systems. This is shown as follows:

$$E(z) D(z) = E(z)[a_0 + a_1(1 - z^{-1})] \quad (127)$$

If one recognizes that  $E(z)(1 - z^{-1})/T$  is a two sample approximation of  $\dot{e}(t)$ , then one can say from equation (127) that

$$E(z) D(z) \approx (\text{constant})(\text{error}) + (\text{constant})(\text{error rate}) \quad (128)$$

The various analogies such as this that exist between sampled-data systems and continuous systems designs are usually very helpful in providing an understanding of  $Z$  transform operations.

It is necessary for this example to determine the values of  $a_0$  and  $a_1$  of figure 59 which will give the desired linear characteristics. For this purpose, the design is again obtained using the dominant mode of the system of reference 5. The sampling frequency is also chosen to be identical to the previous example so the desired positions of the dominant mode in the  $z$  plane are given by equation (117).

The mathematical procedure is quite similar to the previous example. One could also use the method explained in references 7 and 8.

One first writes the characteristic equation as follows

$$1 + D(z) Z \left\{ \left( \frac{1 - e^{-sT}}{s} \right) \left( \frac{1}{1 + 0.02s} \right) \left[ \frac{27}{s(s + 3.333)} \right] \right\} = 0 \quad (129)$$

The desired characteristic equation is

$$(1 - 1.237z^{-1} + 0.4398z^{-2})(c_0 + c_1z^{-1} + c_2z^{-2}) = 0 \quad (130)$$

Note that we have now forced the desired characteristic equation to be fourth order. This is simply because  $D(z)$  has one pole and therefore since the plant is third order, the over-all system must be fourth order.

The pulse transfer function  $D(z)$  has two undetermined coefficients and the desired characteristic equation has three. One can equate equal powers of  $z^{-1}$  between equations (129) and (130) to solve for the undetermined coefficients. In this case also only the ratios of  $c_0/c_1$  and  $c_0/c_2$  have an effect on the roots of the characteristic equation and therefore  $c_0$  may be chosen equal to unity. The other coefficients are

$$\left. \begin{array}{ll} a_0 = 1.263 & c_1 = -0.600 \\ a_1 = 4.474 & c_2 = -0.044 \end{array} \right\} \quad (131)$$

One finds the roots of the second-order part of equation (130) given by the coefficients  $c_0$ ,  $c_1$ , and  $c_2$  to make sure the system is stable. These roots are

$$z = 0.666, -0.066 \quad (132)$$

Thus, since all the poles of the pulse transfer function  $C(z)/R(z)$  are well inside the unit circle and in well-damped regions of the  $z$  plane, no change in sampling frequency or dominant-mode characteristic is necessary.

The characteristics of this system for large step inputs remain to be determined. Since this example has the same plant and same dominant-mode characteristics as the previous example, one should expect a great deal of similarity between the results.

The loci of pole positions as a function of limiter gain are shown in figure 60. The arrows denote the direction of increasing limiter gain. As was the case previously, these loci were computed by factoring the denominator of the closed-loop pulse transfer function.

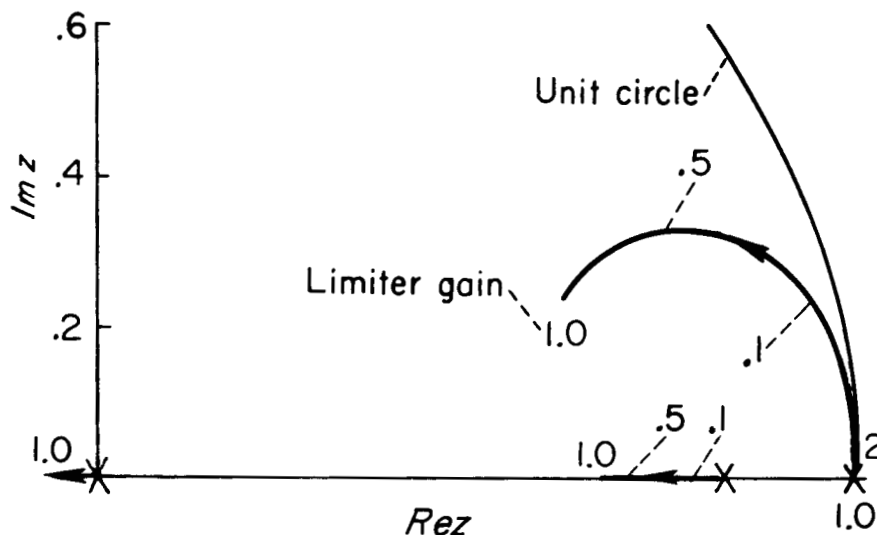


Figure 60.- Pole position loci as a function of the limiter gain; D(z) design.

Figure 60 illustrates this system is unstable for low values of limiter gain and that one should therefore expect the system response to deteriorate with the input step magnitude. Further verification of this fact is demonstrated in the first reversal time curve<sup>2</sup> of figure 61. Here it can be seen that the response should start to deteriorate with

<sup>2</sup>These data are computed in a manner so similar to the previous one that no explanation is considered necessary.

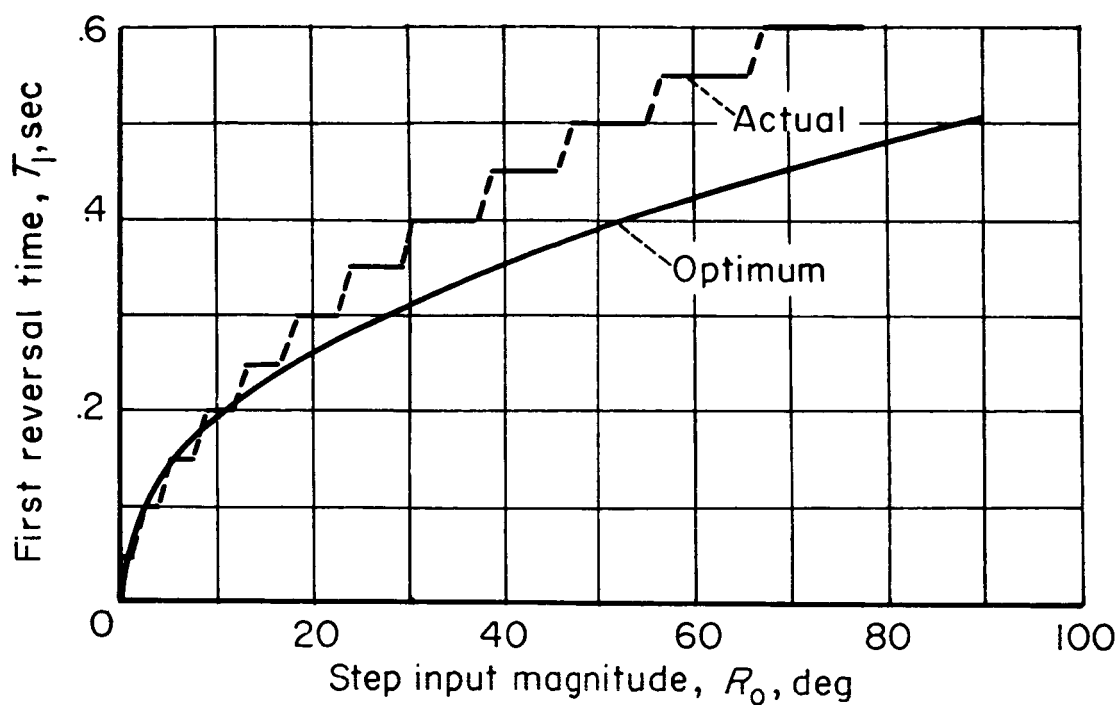


Figure 61.- First reversal times for a sampled-data bank-angle autopilot;  $D(z)$  design.

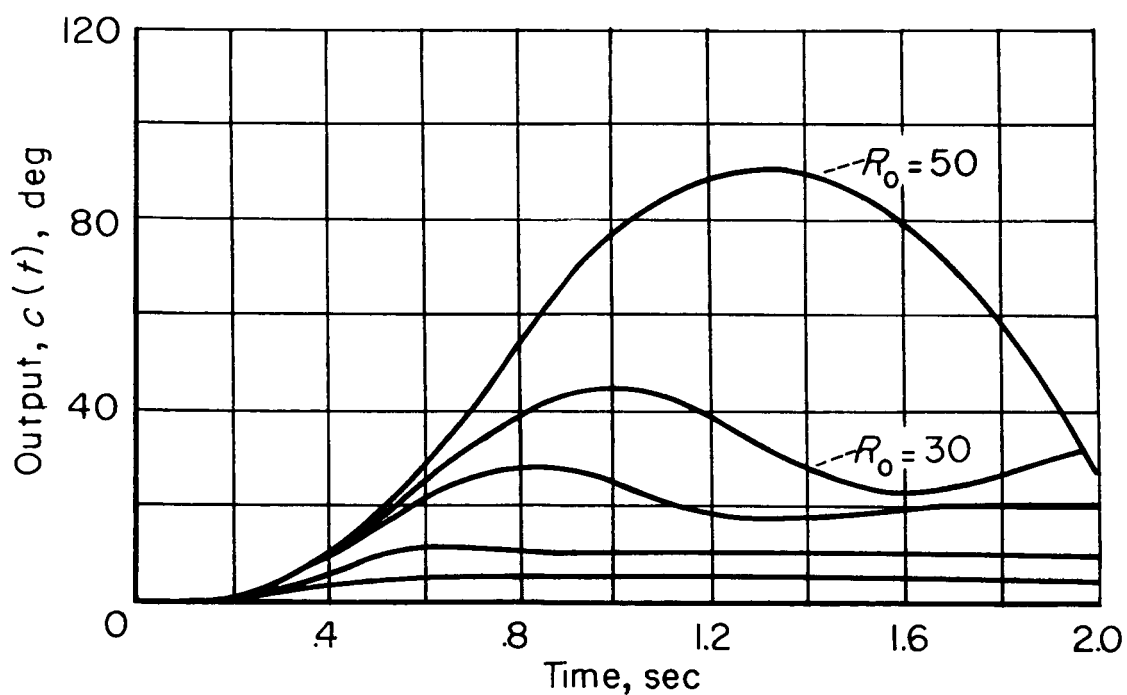


Figure 62.- Step responses of bank-angle autopilot;  $D(z)$  design.

step input magnitudes greater than about 13. This hypothesis is confirmed by the step responses obtained from an analog computer which are presented in figure 62.

As was the case for the previous example, it may be noted that there is a good correspondence between the first overshoot determined from figure 61 and the results given in figure 62.

This particular design is more stable than the previous example. The increase in stability can be noted by comparing figures 61 and 53 as well as 62 and 54. These data show that a larger step is permitted in the present example than in the previous example before the output response starts to deteriorate. The reason for this increase in stability is partially explained by the fact that  $a_0$  for this system is smaller than  $K_e$  for the previous system. It may be noted that these parameters are the "steady state" gain of the digital computer. A second possibility could be associated with the fact that one zero of  $G(z) D(z)$  is "fixed" in the  $z$  plane as the limiter gain is varied for this example; whereas in the previous example, all the zeros of  $Z[GH(s)]$  vary as the limiter gain is varied. It is beyond the scope of this investigation to consider this topic although the general subject of sampled-data systems designed by the dominant mode concept probably requires further study.

The calculated and measured total response times for the present example, along with the minimum are shown in figure 63. The procedure

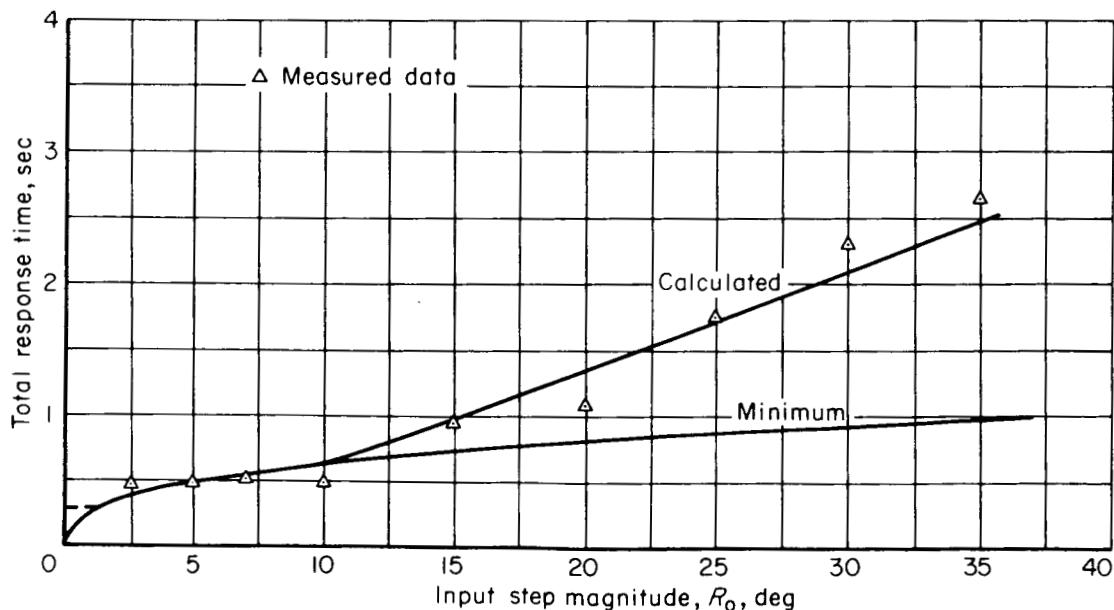


Figure 63.- Calculated, measured, and minimum response times for the sampled-data bank-angle autopilot;  $D(z)$  design.

for calculating the response time was the same as explained for the previous example. The measured response time which was obtained from computer results was defined in the same manner as for the previous example, that is, the time to within 10 percent of the input step magnitude for inputs less than  $10^\circ$  and time to within  $1^\circ$  for inputs greater than  $10^\circ$ . The results between the measured values and computed values show fair agreement. For large inputs, however, the response time is very long. We shall, therefore, design a nonlinear function to compensate for this phenomenon which will provide near optimum response.

To design the nonlinear function, one proceeds in exactly the same manner as was described previously. The computations and details will not be given here since they are straightforward. For this case, it was chosen to make  $a_0$  a function of error. The computed nonlinear function  $a_0(\epsilon)\epsilon$  is shown in figure 64.

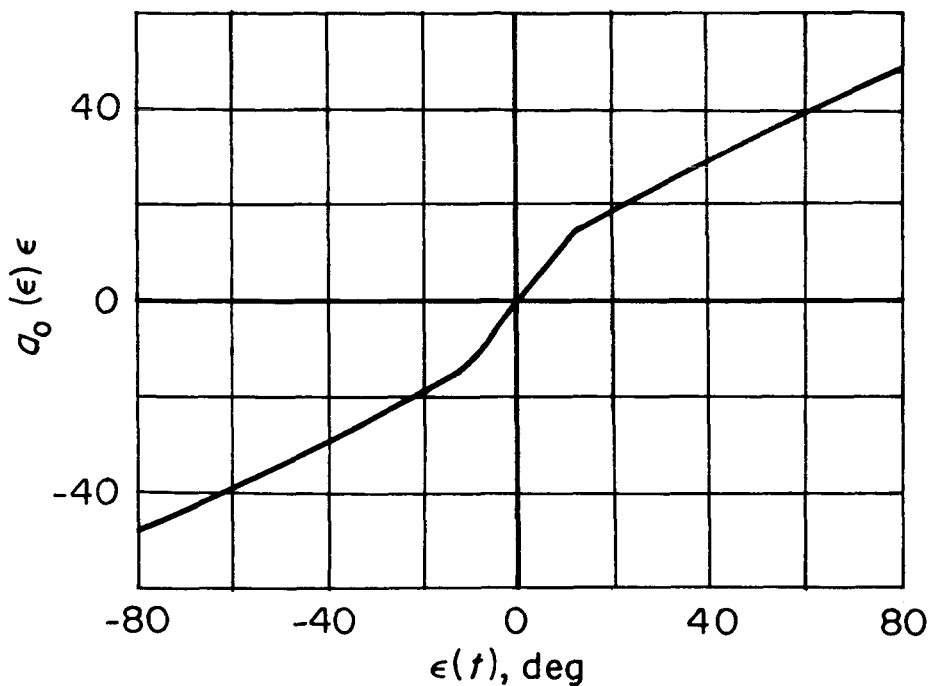


Figure 64.- Nonlinear function used to modify the sampled-data bank-angle autopilot;  $D(z)$  design.

Figure 65 shows the step responses of the system when the nonlinearity of figure 64 is introduced in place of the constant,  $a_0$ . A comparison of figures 62 and 65 shows that the response has been improved tremendously.

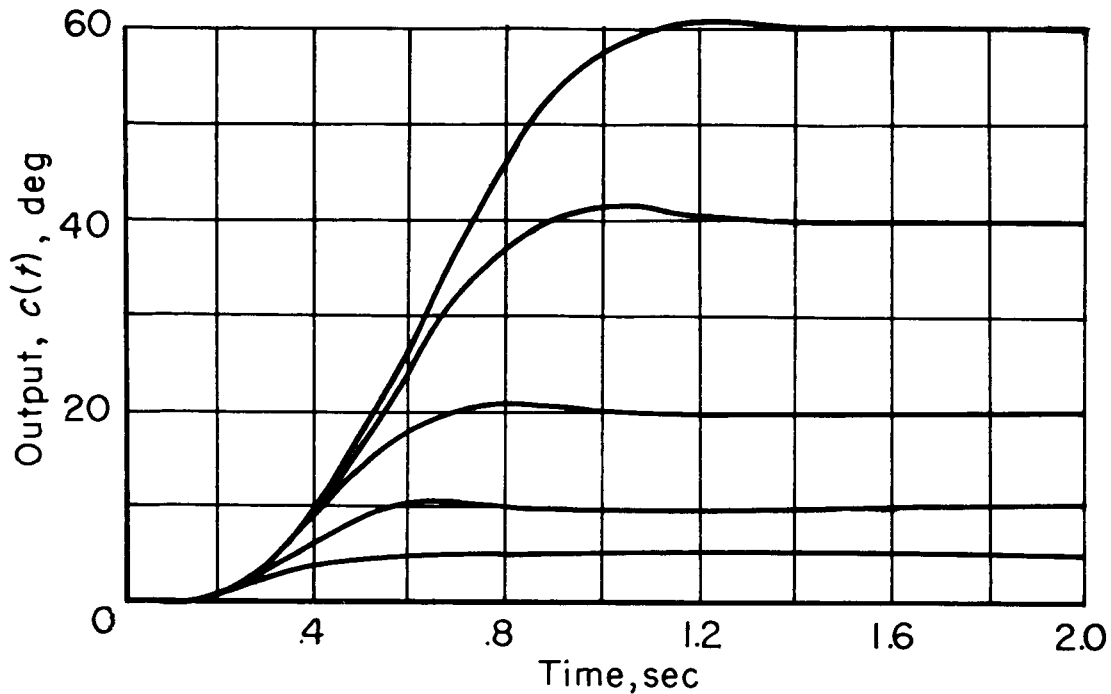


Figure 65.- Step responses of the modified sampled-data bank-angle autopilot;  $D(z)$  design.

#### 4.4 A Continuous Normal Acceleration Autopilot

The two previous examples considered type 2 third-order plants. This example will be for a type 1 third-order plant and will be a continuous system rather than a sampled-data system. The most significant feature of this particular example, as will be shown, is that it is necessary to use a more complicated nonlinear function to obtain satisfactory performance for large step inputs. This allows some verification of the usefulness of some of the ideas presented in section 2.7.

The block diagram of the proposed system and definition of symbols is shown in figure 66. A word of explanation of the figure is necessary. First, the quantity  $w(t)$  is fictitious and has been added for the sole purpose of providing a plant transfer function  $W(s)$  which is one of those given in chapter II. In other words, the design will be to provide good step response between  $r(t)$  and  $w(t)$  and we will take whatever  $c(t)$  we get. Because of the very small second- and first-order coefficients of  $s$  in the transfer function  $C(s)/W(s)$ , however,  $c(t)$  will be fairly close to  $w(t)$ . Second, the input is multiplied by a gain factor  $K_1$  in order to give a steady-state gain of the system equal to unity. This is necessary since an integration in the outer loop does not exist in



The desired transfer function relating  $C(s)/R(s)$  is

$$\frac{C(s)}{R(s)} = \frac{-0.0121s^2 - 0.0079s + 1}{\left[\left(\frac{s}{2\pi}\right)^2 + \frac{1.4}{2\pi}s + 1\right](\tau s + 1)} \quad (134)$$

Note that an unknown first-order factor has been added to the denominator of equation (134) since we are dealing with a third-order control system. Thus, to determine the unknown coefficients  $K_l$ ,  $K_q$ , and  $\tau$ , one equates coefficients of equal powers of  $s$  between the denominators of equations (133) and (134). The coefficient  $K_1$  is then determined by forcing the gain of  $C(s)/R(s)$  to be unity in the steady state.

The results after equating the denominators and solving for the coefficients are

$$\left. \begin{aligned} K_l &= -4.188 \\ K_q &= -0.328 \\ \tau &= 0.03028 \\ K_1 &= 1.66 \end{aligned} \right\} \quad (135)$$

Thus, a linear design has been established. Let us now consider the behavior of the system for large step inputs.

The root loci for limiter gain variations from 0 to 1 are shown in figure 67. Note the change in scale made between -5 and -6 on the abscissa. This is a type 1 plant; however, the locus of the complex pole position indicates that we have designed a system which is almost unstable for a certain range of limiter gain. Furthermore, note that the complex pole is about the same distance away from the origin as the real pole for gain ranges from about 0.1 to 0.25. Since this complex pole is very lightly damped, we should expect the step response for certain ranges of input magnitude to have a lightly damped oscillatory characteristic. The switch time method will be used to determine this range.

As was mentioned previously, no curves of optimum reversal time have been derived for the plant given by the transfer function  $C(s)/X(s)$  of figure 66. We have, however, normalized curves given for  $-W(s)/X(s)$ . We shall therefore use the method for  $w(t)$  rather than  $c(t)$ . The two zeros of the transfer function  $C(s)/W(s)$  are sufficiently far from the origin in the  $s$  plane compared with the poles of  $W(s)/X(s)$  that they should not have too large an influence on the system response.

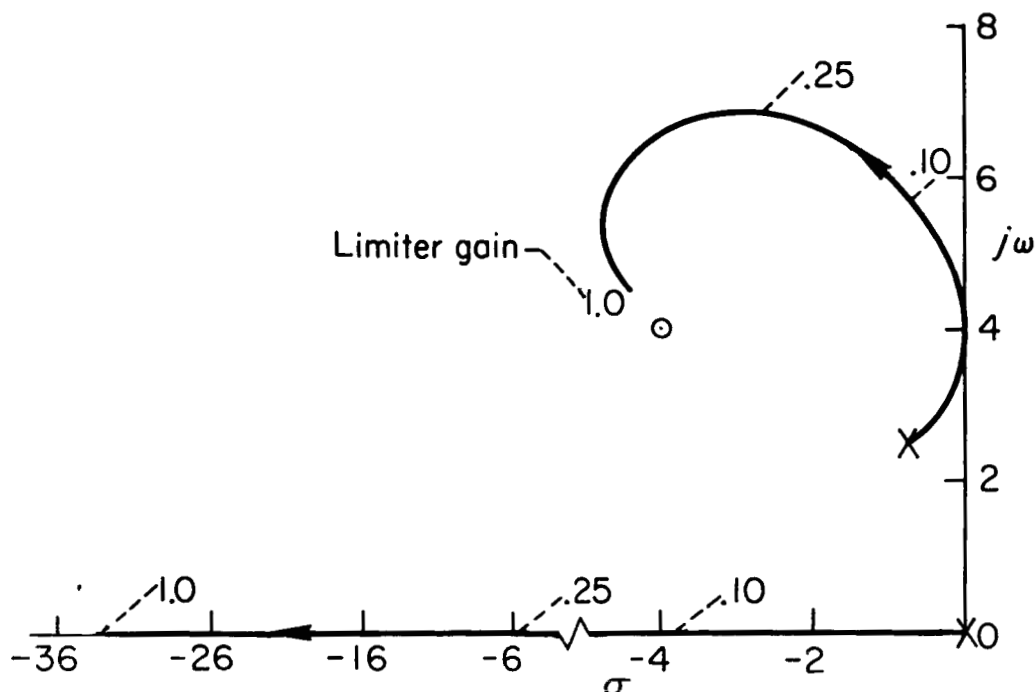


Figure 67.- Root loci of the normal acceleration autopilot as a function of the limiter gain.

For the plant given by  $-W(s)/X(s)$ , reference to figure 66 shows the following:

$$\left. \begin{aligned} \omega_n &= 2.66 \\ \zeta &\approx 0.25 \\ KB &= (0.531)(50)(0.3) = 7.965 \end{aligned} \right\} \quad (136)$$

We are principally interested in the range of  $R_0$  up to a maximum of about 3g; therefore, the maximum value of the abscissa of figure 37, where the normalized first reversal time is given, is

$$\frac{(R_{0\max})\omega_n}{KB} \approx \frac{(3)(2.66)}{7.965} \approx 1.0 \quad (137)$$

Therefore, for reasons of accuracy it is better to use the data given in table II. These data give three points of the optimum first reversal curve as follows

$$\left. \begin{aligned} R_0 &= 0.4417g, & T_1 &= 0.188 \text{ sec} \\ R_0 &= 1.995g, & T_1 &= 0.376 \text{ sec} \\ R_0 &= 4.10g, & T_1 &= 0.564 \text{ sec} \end{aligned} \right\} \quad (138)$$

We now desire to determine the actual first reversal curve. As has been the case previously, we must determine  $m(t)$  of figure 66 for a step of  $r(t)$ . As can be noted from figure 66, if the magnitude of  $R_0$  is greater than  $(0.3/K_1K_L) \approx 0.043g$ , then  $x(t)$  will be saturated. We are only interested in values of  $R_0$  greater than this magnitude. With reference to figure 66

$$m(t) = R_0K_1K_Lu(t) - K_Lc(t) - K_qq(t) - \delta(t) \quad (139)$$

Since  $K_L$  is negative (see eq. (135)),  $m(T_1)$  is equal to  $-0.3$ , for  $R_0$  positive. Thus, for large step magnitudes,  $R_0 > 0.043$ ,

$$m(T_1) = R_0K_1K_L - L^{-1} \left[ \frac{-0.3}{s} \frac{C(s)}{X(s)} K_L + \frac{Q(s)}{X(s)} K_q + \frac{\Delta(s)}{X(s)} \right] \bigg|_{t=T_1} \quad (140)$$

The value of  $m(T_1)$  of equation (140) is taken equal to zero. (See footnote 11, chapter II.

The quantity  $(-0.3/s)$  of equation (140) is the Laplace transform of a negative step of  $x(t)$  of magnitude equal to the limit level. The negative sign must be taken since  $K_L$  is negative and we are assuming  $R_0$  is positive. The transfer functions  $C(s)/X(s)$ ,  $Q(s)/X(s)$ , and  $\Delta(s)/X(s)$  can be determined with reference to figure 66. The coefficients  $K_1$ ,  $K_L$ , and  $K_q$  are given by equation (135).

One can thus carry through the mathematical operations indicated in equation (140) and, by assuming various values of  $T_1$ , solve for the values of  $R_0$  which satisfy the equation.<sup>3</sup>

The results, after carrying through the mathematical operations indicated in equation (140), are compared to the optimum given by equation (138) in figure 68. As can be seen from the figure, the actual curve crosses the optimum for inputs greater than approximately  $1.0g$ . Thus, one can assume that the response will deteriorate if the input step magnitudes are greater than this value. This hypothesis is confirmed by the step responses of the simulated system given in figure 69.

---

<sup>3</sup>It should be pointed out here that for many of these computations, one can make use of the analog computer. For the present case, for example, one could simply simulate the system of figure 66 and put in steps and measure  $T_1$  as a function of the input step magnitude.

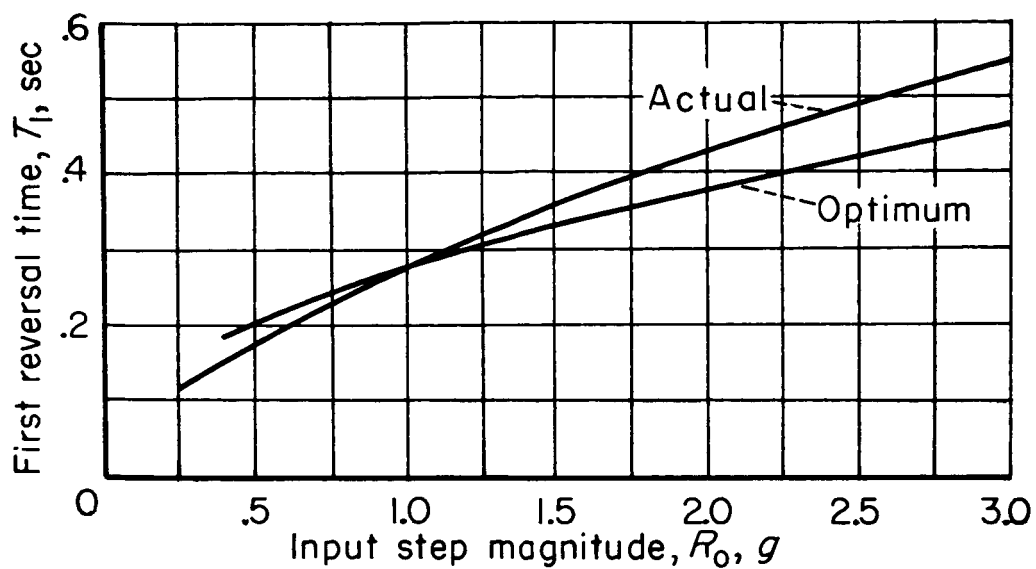


Figure 68.- First reversal times for the normal acceleration autopilot.

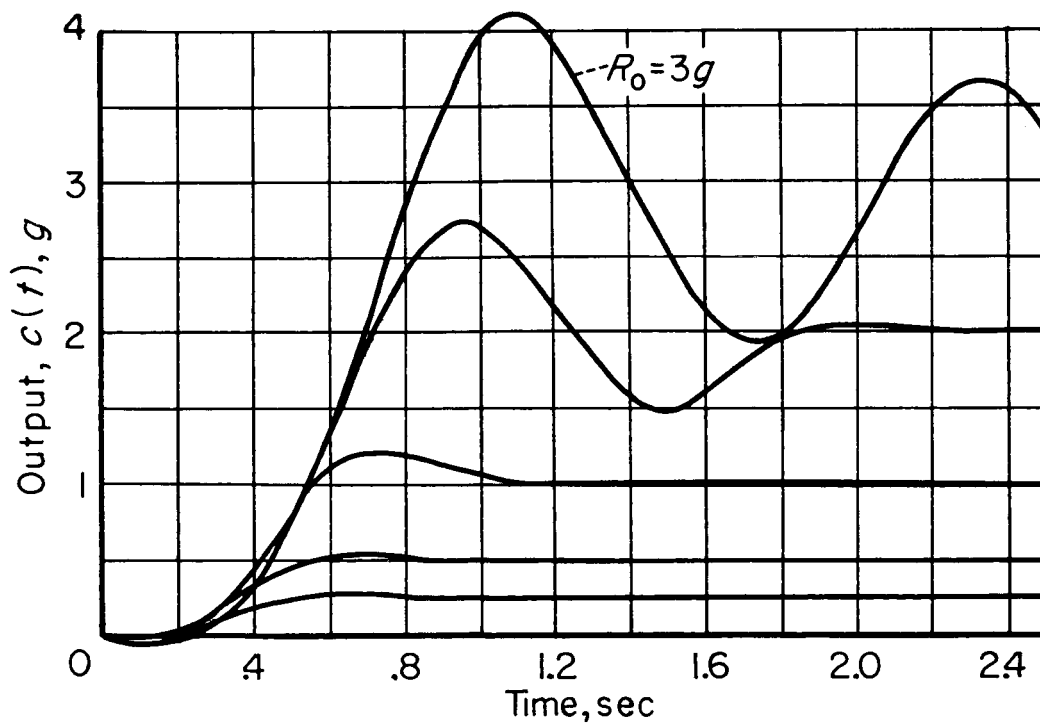


Figure 69.- Step responses of the normal acceleration autopilot.

A note should be added that we have analyzed the system for  $w(t)$  not  $c(t)$ . The small negative part of the response, at the beginning of the transient, is due to the transfer function relating  $C(s)/W(s)$ . The small overshoot for a step of 1.0g magnitude is perhaps a result of this same transfer function, although it more probably is due to the fact that the system has some transition time in going from one limit to the other. Thus, we are really using figure 68 for approximate behavior and the results given by figure 69 show that our original assumption of neglecting the zeros in the transfer function,  $C(s)/X(s)$ , is accurate enough for engineering purposes.

We shall not compute the response time of this system and compare it to the actual since we already know that some form of nonlinearity should be designed. We shall now consider this subject.

Before designing a nonlinear function, one must first consider the possibilities that exist. With reference to figure 66, we see at least two possibilities<sup>4</sup> where a function of a single variable could be used:

(1) Make  $K_L$  a function of  $K_1 r(t) - c(t)$

(2) Make  $K_Q$  a function of  $q$

Neither one of these possibilities requires a multiplier since, for the first possibility, the output of the box labeled  $K_L$  would simply be a function of its input. This is true also for the second case. The first possibility must be ruled out, however, since  $K_1 r(t) - c(t)$  is not zero if  $r(t)$  has a constant value. This means that if  $K_L$  were made to decrease as a function of  $K_1 r(t) - c(t)$ , one would have a system which did not have unity gain in the steady state for constant inputs. Similarly,  $K_Q$ , affects the steady-state gain, however, in a much smaller manner as can be recognized by equation (141).

$$\lim_{s \rightarrow 0} \frac{C(s)}{R(s)} = K_1 \left[ \frac{\frac{-0.531K_L}{1 - (0.531)(2.65)K_Q}}{1 - \frac{0.531K_L}{1 - (0.531)(2.65)K_Q}} \right] \quad (141)$$

If  $K_Q$  is doubled from its normal value for example (see eq. (135)), the steady-state gain reduces from unity to 0.89, whereas, if  $K_L$  is reduced to half its normal value, the gain changes from unity to 0.72. Thus, from these standpoints, a change in  $K_Q$  is more desirable. Furthermore, the steady-state value of  $q$  (see fig. 66) is much smaller than its

---

<sup>4</sup>A block diagram modification would allow at least one other possibility which is described in the footnote 5, chapter IV.

transient value which means that a nonlinear function will have no effect on the steady-state gain if  $q$  is small enough, in the steady state, to be in the linear range (of the nonlinear function) for the practical range of input step magnitudes (i.e., 0 to 3g). With reference to figure 66, if  $c(t)$  is constant at 3g magnitude,  $q$  will be  $3 \times 2.65 = 7.95^\circ$  per second.

To determine the desired nonlinear function, we proceed in the same manner as described previously. First, solve equation (139) for  $K_q q(t)$  for  $t = T_1$

$$K_q q(T_1) = f[q(T_1)] = R_0(T_1)K_1K_2 - m(T_1) - K_2c(T_1) - \delta(T_1) \quad (142)$$

Since  $R_0(T_1)$  will be chosen to be the optimum given in figure 68 and all the other quantities are known at  $T_1$  (since  $x(t) = -0.3u(t)$ ), one can solve equation (142) for  $f(q)$ . The value of  $m(T_1)$  will be taken equal to zero as was done previously. Since

$$q(T_1) = L^{-1} \left\{ \left( \frac{-0.3}{s} \right) \left[ \frac{Q(s)}{X(s)} \right] \right\} \quad (143)$$

we can compute and plot  $q(T_1)$  versus  $f[q(T_1)]$ . The result is shown in figure 70. It can be seen that the nonlinear function has a straight line slope until  $q \approx 7^\circ$  per second. Since the slope is not significantly different for a slightly higher value of  $q$ , we can say that there will be only a small change in steady-state gain for step inputs as high as 3g where the steady-state value of  $q$  is only  $7.95^\circ$  per second, as was previously mentioned.

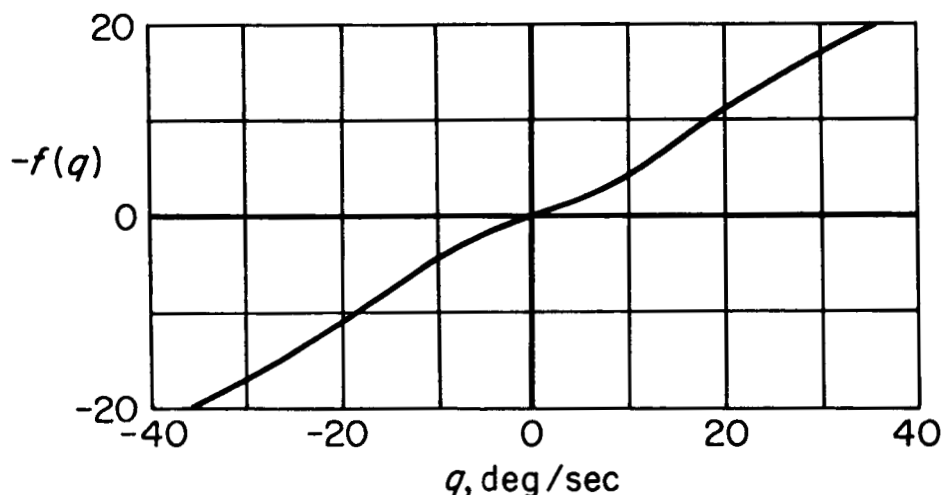


Figure 70.- Nonlinear function used to modify the normal acceleration autopilot.

The step responses of the normal acceleration autopilot, when the nonlinear function was introduced, are shown in figure 71. It can be noted that the system response has not been improved tremendously. Of importance, however, note that the first overshoot is very small. This is simply because we are forcing the first reversal time to be correct, and this should result in very small or zero first overshoot as was mentioned in chapter II.

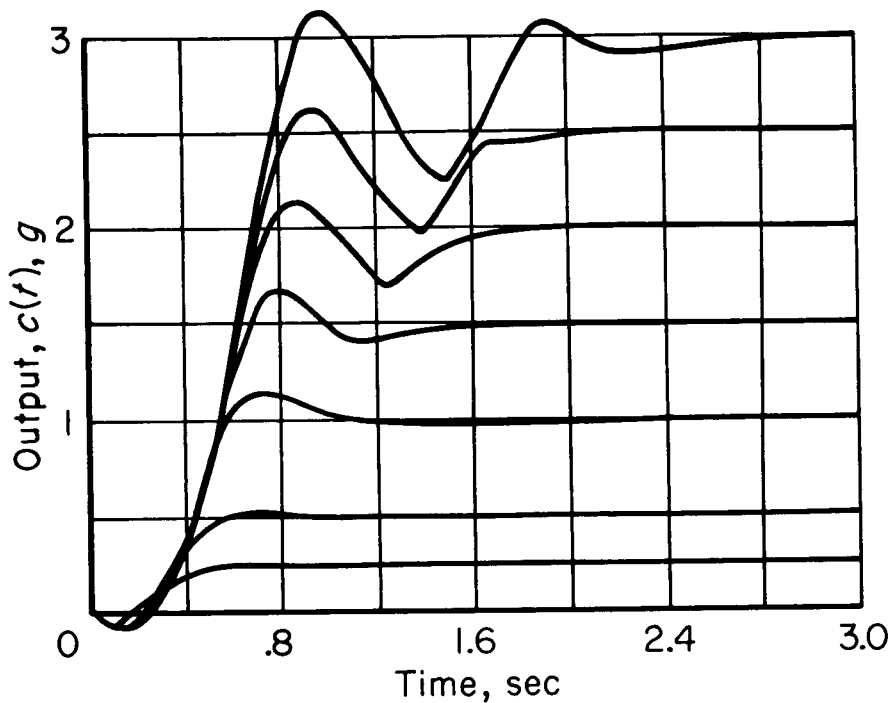


Figure 71.- Step responses of the modified normal acceleration autopilot.

This example offers an opportunity to use some of the ideas suggested in section 2.7 to explain the reasons for the poor responses of figure 71 as well as to do something about them, that is, determine different nonlinear functions which will give good step responses. First, we shall give a root-locus argument that shows why poor responses can exist in this system. Then we will consider what can be done about it.

One first writes the expression for the characteristic equation of  $C(s)/R(s)$  with respect to limiter gain,  $K_L$ . This is

$$1 + 50K_L \left\{ \frac{(0.1413 + 0.00643K_L)s^2 + (0.187 - 2.267K_q + 0.00419K_L)s + (1 - 0.531K_L - 1.407K_q)}{s \left[ \frac{s^2}{(2.66)^2} + \frac{0.498}{2.66}s + 1 \right]} \right\} = 0 \quad (144)$$

Notice that the numerator is second order. Thus, there are two zeros in the expression  $G(s)H(s)$  and, according to the arguments given in chapter II, one should not necessarily expect a single nonlinear function to be sufficient.

Let us plot the loci of zero positions as a function of  $K_q$  in the range given from the slope changes of figure 70 ( $-0.56 \leq K_q \leq -0.328$ ). The loci along with the complex pole loci for a constant  $K_q = -0.328$  are shown in figure 72. The coefficient  $K_L$  is assumed constant at

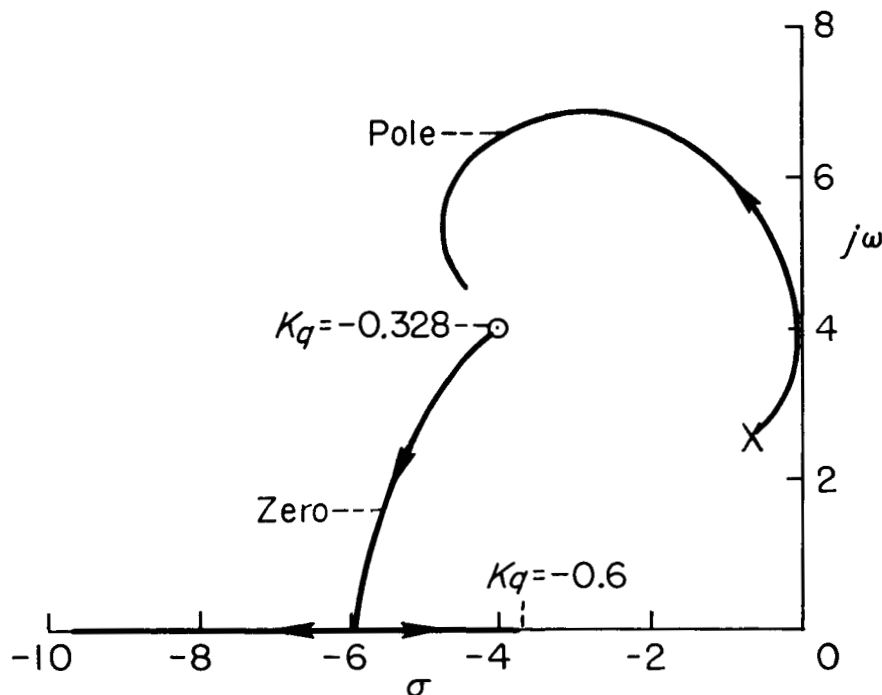


Figure 72.- Loci of zero positions for variable  $K_q$  and locus of complex pole position for  $K_q = -0.328$ .

the value given in equation (135). This shift in zero position as a function of  $q$  does not appear to be desirable. The natural frequency of the zeros stays nearly constant. With experience one can visualize how the complex pole position loci (as a function of limiter gain) would look for each zero position along the zero locus. The conclusion one reaches is that the position of the complex pole loci for low values of limiter gain, say 0.25 to 0.1, will probably always be in a very lightly damped region of the  $s$  plane. These arguments could perhaps be made

less nebulous by a contour plot of pole position for constant values of limiter gain for the zeros shifting in the manner indicated. This has not been done here, since it appears quite reasonable from the above consideration that the zero shift is not desirable and gives a reasonable explanation as to why the step responses of figure 71 were not well damped for large inputs, even though the first reversal time was made to be near optimum.

Consideration will now be given to two more complicated (from the practical standpoint) nonlinear compensation schemes. The first will be to make  $K_l$  a nonlinear function of the error  $\epsilon(t)$  (see fig. 66). This function is more complicated, since a multiplier is required.<sup>5</sup> The second will be to make both  $K_l$  and  $K_q$  nonlinear functions of error,  $\epsilon(t)$ , in such a manner that the natural frequency of the zeros reduces while the damping ratio stays constant.

Consider the problem of making  $K_l$  a nonlinear function of error. We would like to know how the zeros shift as a function of  $K_l$  if  $K_q$  is assumed constant ( $K_q = -0.328$ ). This shift is readily computed from the numerator of the second part of equation (144). The results of these computations are shown in figure 73, along with the complex pole locus for variable limiter gain but a constant  $K_l$  ( $K_l = -4.188$ ). Comparing figures 72 and 73, one can see that this shift in zero position is more desirable than the previous case. The natural frequency of the zeros does decrease somewhat and damping increases so one is demanding less of the system for large values of the error.

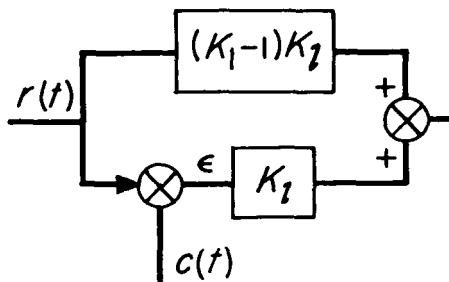
The method of computing the desired nonlinear function of error,  $K_l(\epsilon)$ , is done by making the first reversal time optimum. One rewrites equation (142), this time solved for  $K_l$

$$K_l(\epsilon) = \frac{\delta(T_1) + K_q q(T_1)}{R_o(T_1) K_1 - c(T_1)} \quad (145)$$

The value of  $m(T_1)$  has been taken equal to zero. Since

---

<sup>5</sup>A simple block diagram transformation, which was not recognized until the investigation was completed, would have eliminated the need for a multiplier. This change is shown in the accompanying sketch. The upper box would be made a constant gain and the lower box made a nonlinear function of the error. The results of using this system would undoubtedly be the same as those of the first case considered here.



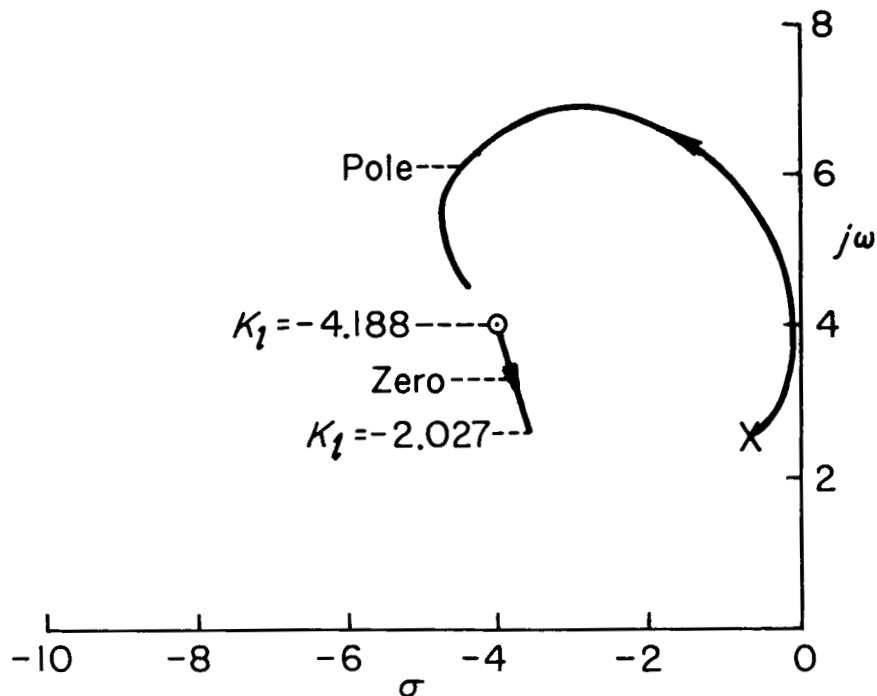


Figure 73.- Locus of zero position for variable  $K_l$  and locus of complex pole position for  $K_l = -4.188$ .

$$e(T_1) = R_0(T_1) - c(T_1) \quad (146)$$

one can compute  $K_l(\epsilon)$  and  $\epsilon$ , the desired nonlinear function. The results of these computations are shown in figure 74.

The step responses for the modified system when the nonlinear function  $K_l(\epsilon)$  was introduced are shown in figure 75. The results show an improvement as the shift in zero positions of figure 73 indicates should be the case. As a matter of fact, the improvement is significant enough so that no further designs need be made. There are probably more complex examples, however, when at least two nonlinear functions are required.

To demonstrate the method of computing two nonlinear functions, we consider a case where both  $K_l$  and  $K_q$  are made nonlinear functions of the error. One should perhaps note that  $K_q$  could be made a function of  $q$ ; however, we will not study this example here, although the method of computing this function is practically the same as for this example.

For this example, we shall force the damping ratio of the zeros to remain constant at a value of 0.703 which is determined from the values of  $K_q$  and  $K_l$  given in equation (135). The equation relating the

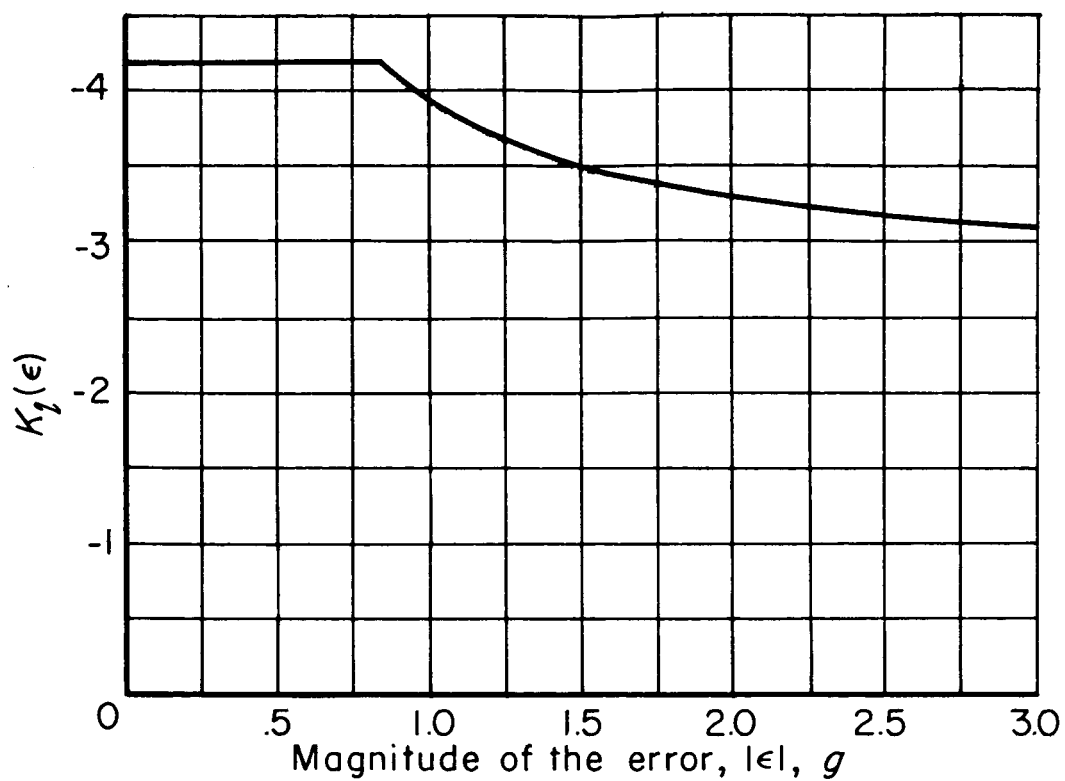


Figure 74.- Nonlinear function of error for normal acceleration autopilot.

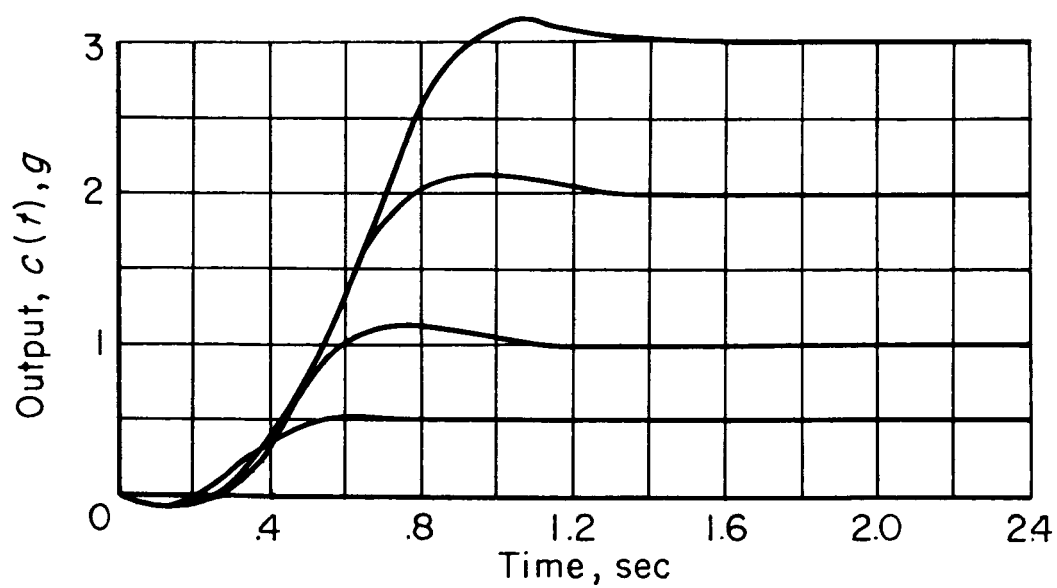


Figure 75.- Step responses of the modified normal acceleration autopilot.

damping ratio,  $\zeta_o$ , and natural frequency,  $\omega_{n_o}$ , of the zeros to  $K_q$  and  $K_l$  is given in equations (147) and (148).

$$\omega_{n_o} = \sqrt{\frac{1-0.531K_l-1.407K_q}{0.1413+0.00643K_l}} \quad (147)$$

$$\zeta_o = \frac{1}{2} \frac{0.187-2.267K_q+0.00419K_l}{\sqrt{(1-0.531K_l-1.407K_q)(0.1413+0.00643K_l)}} \quad (148)$$

Since  $\zeta_o$  of equation (148) is a constant,  $\zeta_o = 0.703$ , we can obtain an equation relating  $K_q$  and  $K_l$  which provides this desired value of  $\zeta_o$ . One can thus put  $\zeta_o = 0.703$  in equation (148) and solve for the relationship between  $K_q$  and  $K_l$ . The resultant quadratic equation is

$$K_q^2 + (-0.0885-0.000218K_l)K_q + (-0.04755+0.02669K_l+0.00132K_l^2) = 0 \quad (149)$$

Note that both  $K_q$  and  $K_l$  must be negative, since the plant has negative gain (see fig. 66). One can assume values of  $K_l$  varying from nominal value  $K_l = -4.188$  to lower values, say  $K_l = -1$ , and solve for  $K_q$ . The results of these computations are plotted in figure 76.

We thus know the desired relationship between  $K_q$  and  $K_l$  which makes the zeros shift with a constant damping ratio. What remains to be determined is how they should shift as a function of the error. This can be accomplished quite readily by forcing them to shift so that the first reversal time is maintained optimum. The method by which this is accomplished is very similar to the one used previously. First, one rewrites equation (142) in the following form:

$$K_l(\epsilon)[R_o(T_1)K_1 - c(T_1)] - K_q(\epsilon)q(T_1) = m(T_1) + \delta(T_1) \quad (150)$$

The value of  $m(T_1)$  is taken equal to zero as has been done previously. For each value of  $T_1$  this equation has the following form

$$K_l(\epsilon)a - K_q(\epsilon)b = c \quad (151)$$

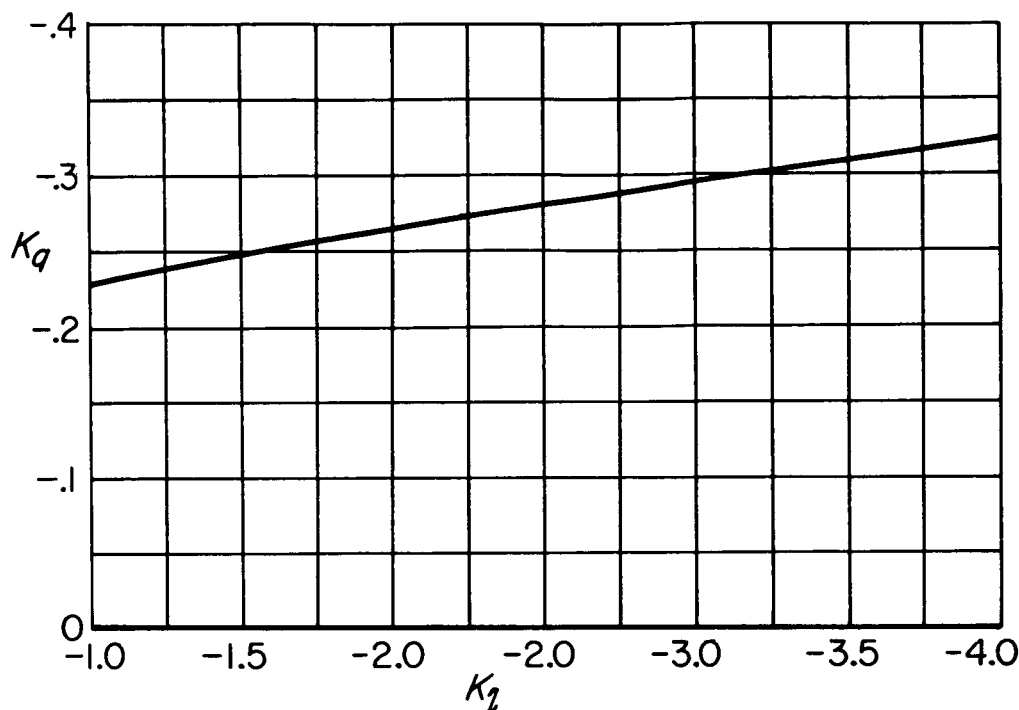


Figure 76.-  $K_q$  versus  $K_1$  for a constant damping ratio of the normal acceleration autopilot.

where  $a$ ,  $b$ , and  $c$  are constants. Equation (151) is a linear equation in  $K_1(\epsilon)$  and  $K_q(\epsilon)$ . It thus can be plotted as a straight line in figure 76. The intersection point between this straight line and the curve of figure 76 is the desired value of  $K_1(\epsilon)$  and  $K_q(\epsilon)$ .

By choosing a number of values of  $T_1$  in equation (150), one can obtain the results plotted in figure 77. Note that both functions decrease as the magnitude of the error increases.

The step responses of the modified system with these nonlinearities introduced are shown in figure 78. As can be noted, there is a very significant improvement in this system response over the example where  $K_q$  was made a function of  $q$ . However, the response is very close to the previous example except that a slight decrease in the overshoot for a  $3g$  step was noted.

The last two examples have demonstrated that the ideas presented in section 2.7 have a real significance for complex problems. Combining root-locus arguments to obtain the desired zero locus (as a nonlinear function of error, for example), and the first reversal time for determining the nonlinear functions, appears to have significance for application to high-order control systems.

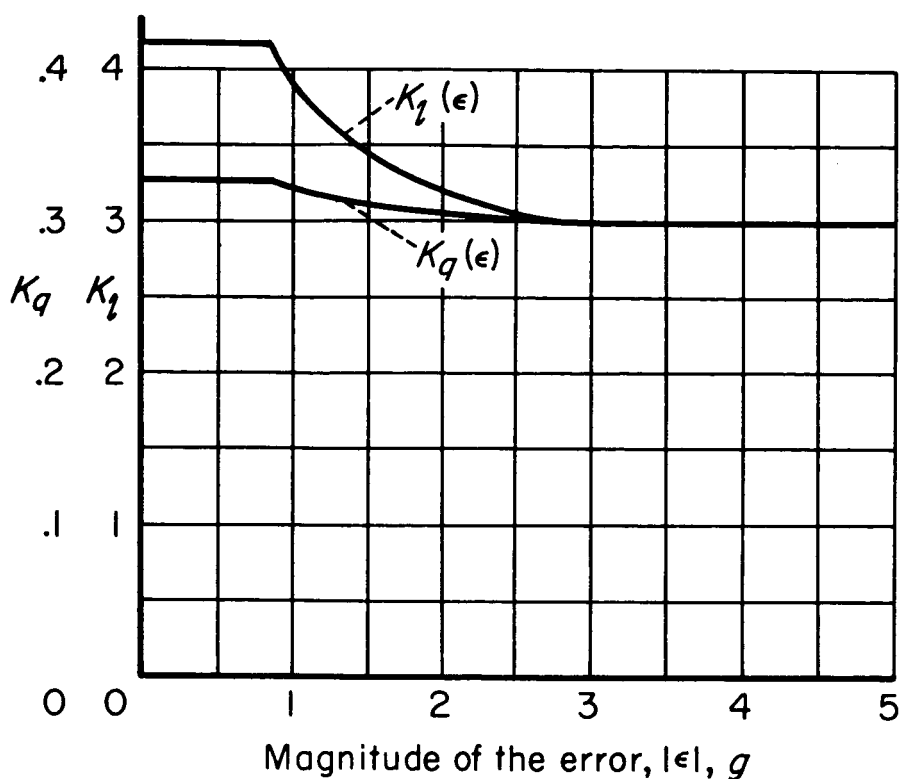


Figure 77.- Nonlinear functions,  $K_q(\epsilon)$  and  $K_l(\epsilon)$ , for use in the normal acceleration autopilot.

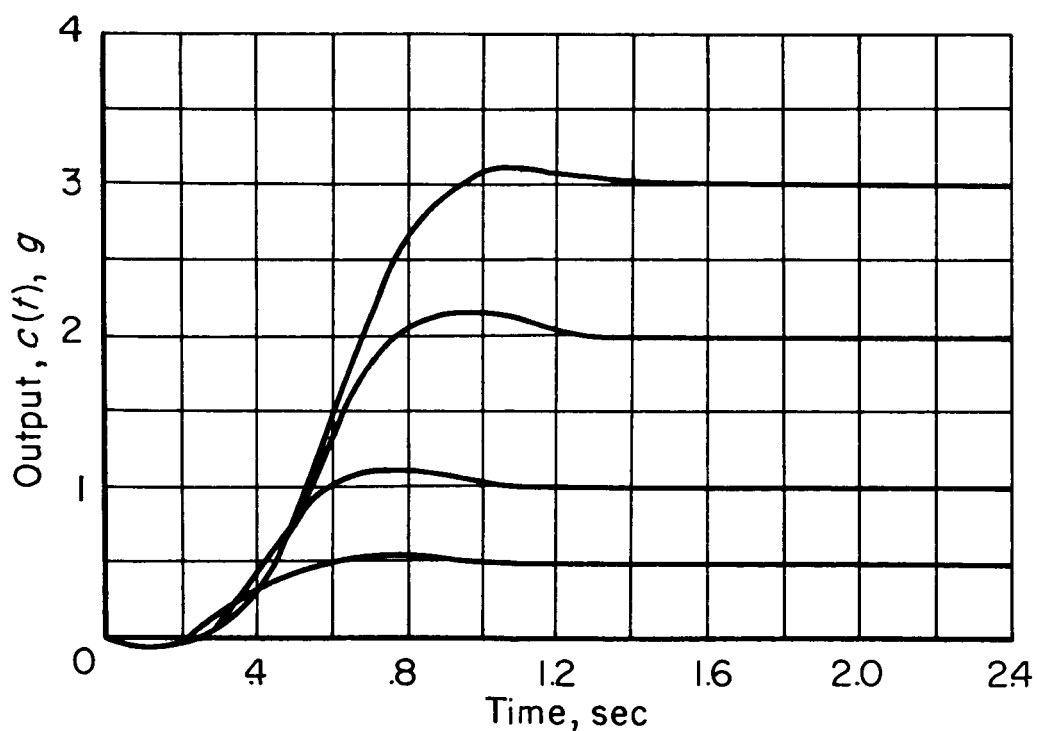


Figure 78.- Step responses of the modified normal acceleration autopilot.

## V. CONCLUSIONS

### 5.1 Summary of Results

The aim of this investigation was to develop methods for the treatment of saturation (or limiting) in feedback control systems. It has been found that if one treats a limiter as an equivalent gain (the gain constant decreases as the magnitude of the input to the limiter increases), then one can draw the root loci as a function of the equivalent limiter gain. These root loci, as has been shown by Kalman (ref. 2), give a qualitative picture of the change in performance as the input to the feedback control system is increased. In particular, it was shown in chapter II, by the use of this root-locus method, that the fundamental characteristics of a saturated control system, for large inputs, depends upon the number of integrations of the plant, that is, the number of poles at  $s = 0$  of the plant transfer function. Thus, the classification of plants according to type, that is, the number of poles at the origin in the  $s$  plane, appears to offer a good way of remembering these fundamental characteristics. In summary, these characteristics are

(1) Type 1 plants are velocity limited and, therefore, the response will become more sluggish as the size of the input is increased.

(2) Type 2 plants are acceleration limited, and their response will become oscillatory as the size of the step input is increased.

(3) Type 3 plants always give control systems which are unstable for low values of equivalent limiter gain, and, therefore, the feedback control system will become unstable for large step inputs.

Of course there are the exceptions to (1) and (2) when the linearly designed feedback control system is unstable or nearly so as the limiter gain is decreased as was shown in the corollaries of the rules presented in chapter II. These exceptions can result in stable limit cycles for type 1 or type 2 plants but unstable limit cycles for type 2 only. The system can be shocked into these limit cycles by large input disturbances.

The most important contribution of this investigation is the application of the switch time method for analysis and synthesis purposes. Although the author and Triplett in reference 5 explored some of the potentialities of the method, its derivation and usefulness were not well understood at that time. One advantage of this method is its simplicity of concept; that is, the simple fact that if the first reversal time is longer than the optimum relay solution, then the step response must overshoot. This simplicity of concept has allowed the use of the method for systems of any order, provided of course that the linear design meets the restrictions imposed in chapter II. The examples shown in chapter IV, where third-order sampled data and continuous autopilots were analysed and synthesized, demonstrate the usefulness of this method.

The switch time method as used for synthesizing nonlinear functions to improve the step response is to the author's knowledge one of the few techniques available for this purpose. In application, it actually provides a switching line which should be on the optimum relay switching surface of the multidimensional (dependent on the order of the plant) phase space. The advantage of the technique, however, is that one does not need to know this switching surface, which for high-order systems is very difficult to determine, in order to apply the technique.

Another advantage of the switch time method is that one works directly with the parameters of the feedback control system and not with parameters of some transformation where, because of the mathematics of the inverse transformation, the determination of the actual system's response, becomes very difficult.

The fact that the Laplace transform of the error time signal must be an entire function, if the error is to be reduced to zero in a finite time, is a valuable technique for determining the optimum response. The disadvantage of the method, however, is that one must, by a priori information, select the general form of the input to the plant. As was shown in chapter III, this selection is aided considerably by simple block diagram transformations and physical reasoning. A partial check of the choice of the general form of the input is obtained if sufficient equations exist to force the error transform to be an entire function.

One of the interesting by-products of this investigation is the fact that one must not force the limited variable to be at its maximum values throughout the transient if one desires the minimum response time for a plant which has zeros in the left half plane. This is a result of the fact that some of the states can be changing in a controlled manner while the error and its derivatives remain zero. This allows one to design a system which is much faster (in some cases) than the system which essentially brings all the states to rest after the transient.

## 5.2 Suggestions for Further Research

The concept of considering root loci as actually shifting as a function of some parameter which was the equivalent limiter gain in this investigation appears to offer one way of analyzing the behavior of certain nonlinear systems. In particular, if one also forces the zeros to shift as a function of some other parameter (error for example), one can obtain a qualitative reason for synthesizing nonlinear systems to behave in some desired fashion. It would, therefore, be desirable to establish theoretically when this type of treatment is permissible. Kalman (ref. 2) made a start in this direction, and further work would be very desirable.

The technique of using the entire function to determine optimum switch times for bang-bang operation (chapter III) may have some usefulness for those interested in determining optimum switching surfaces of high-order plants. This technique can be used, since, regardless of the position in the phase space, the error transform must be an entire function if one has the optimum system.

With regard to the general subject of treatment of high-order systems by phase space techniques it is the opinion of the author that from practical considerations one need not consider the space as infinite in dimension for all the variables. This is hypothesized, since for a large number of systems it is the plant input which drives the system to the positions in the phase space; therefore, if the plant is stable and if the plant input is bounded, certain dimensions of the phase space are bounded. For example, for type 1 plants only one dimension is infinite, since only one integration exists. For type 2 plants only two dimensions are infinite, etc. Thus, if this opinion is accepted, it means that the optimum switching surface is bounded in certain dimensions of the phase space. The fact that it is bounded may, perhaps, offer some simplification in the determination of the optimum switching surface for certain complex plants. These arguments go along with the method proposed by Kalman (ref. 10) for synthesizing nonlinear functions for near optimum response. The general subject of "optimum systems," however, needs much further investigation for high-order systems.

Some further areas of investigation which would make the switch time method of greater use are

- (1) Determine the optimum first reversal times and minimum response time for more plants in which both zeros and unstable poles are included in the plant transfer function.
- (2) Determine, for high-order complex plants, how one should shift the zeros in order to give near optimum response for large inputs. One example has been given in chapter IV; however, further study appears desirable.
- (3) Determine how the nonlinear system designed by the switch time method behaves for inputs other than steps. Some unreported simulation studies have shown that such systems have subharmonic oscillations when driven by large sine wave inputs but that the system cannot be shocked into an unstable mode; however, more experimental and theoretical work would be desirable.

Ames Research Center

National Aeronautics and Space Administration  
Moffett Field, Calif., May 7, 1959

## BIBLIOGRAPHY

1. Higgins, T. J.: Classified Bibliography on Feedback Control Systems, Parts I to VII. Available by writing to the author at the University of Wisconsin.
2. Kalman, R. E.: Physical and Mathematical Mechanisms of Instability in Nonlinear Automatic Control Systems. Trans. A.S.M.E., vol. 79, no. 3, Apr. 1957, pp. 553-563. (Also available as A.S.M.E. Paper 56-IRD-16, 1956)
3. Truxal, John G.: Automatic Feedback Control System Synthesis. McGraw-Hill Book Co., Inc., 1955.
4. Bellman, R., Glicksberg, I., and Gross, O.: On the "Bang-Bang" Control Problem. Quart. Jour. Appl. Math., vol. XIV, no. 1, Apr. 1956, pp. 11-18.
5. Schmidt, Stanley F., and Triplett, William C.: Use of Nonlinearities to Compensate for the Effects of a Rate-Limited Servo on the Response of an Automatically Controlled Aircraft. NACA TN 3387, 1955.
6. Ragazzini, John R., and Franklin, Gene F.: Sampled-Data Control Systems. McGraw-Hill Book Co., Inc., 1958.
7. Schmidt, Stanley F.: Application of Continuous System Design Concepts to the Design of Sampled Data Systems. AIEE Paper 58-1083, 1958.
8. Schmidt, Stanley F., and Harper, Eleanor V.: Sampled-Data Techniques Applied to a Digital Controller for an Altitude Autopilot. NASA MEMO 4-14-59A, 1959.
9. Booton, Richard C., Jr., Mathews, Max V., and Seifert, William W.: Nonlinear Servomechanisms With Random Inputs. M.I.T. Dynamic Analysis and Control Lab. Rep. No. 70, Aug. 20, 1953.
10. Kalman, R. E.: Analysis and Design Principles of Second and Higher Order Saturating Servomechanism. AIEE Paper 55-551. (Also available in Trans. AIEE, vol. 74, pt. 2, no. 21, Nov. 1955, pp. 294-308)
11. Chestnut, Harold, and Mayer, Robert W.: Servomechanisms and Regulating System Design. Vol. I, John Wiley & Sons, Inc., 1951.

12. Flügge-Lotz, Irmgard, and Lindberg, Herbert E.: Studies of Second and Third Order Contactor Control Systems. Tech. Rep. No. 114, Division of Eng. Mech., Stanford Univ., 1958.
13. Guillemin, Ernst A.: The Mathematics of Circuit Analysis. John Wiley & Sons, Inc., 1949.
14. Titchmarsh, E. C.: Introduction to the Theory of Fourier Integrals. Oxford, The Clarendon Press, 1937.
15. Flügge-Lotz, Irmgard, and Ishikawa, Tomo: Investigation of Third Order Contactor Control Systems, Part I. Tech. Rep. No. 116, Division of Eng. Mech., Stanford Univ., 1959.
16. Nelson, F. R., Koerner, W., and Trudel, R. E.: Fundamentals of Design of Piloted Aircraft Flight Control Systems. BuAer Rep. AE-61-4, vol. II, Dynamics of the Airframe, Feb. 1953.